The Role of Programmed Cell Death in Mesenchymal Stem Cell Application in Cell Therapy

Lead Guest Editor: Xiao-Kang Li
Guest Editors: Shao-Wei Li and Wei-Tao Que

The Role of Programmed Cell Death in Mesenchymal Stem Cell Application in Cell Therapy

The Role of Programmed Cell Death in Mesenchymal Stem Cell Application in Cell Therapy

Lead Guest Editor: Xiao-Kang Li
Guest Editors: Shao-Wei Li and Wei-Tao Que

Shuiqiao Yuan ⓘ, China
Dunfang Zhang ⓘ, China
Ludovic Zimmerlin, USA
Ewa K. Zuba-Surma ⓘ, Poland

Contents

Hindawi

Review Article

The Effects of Programmed Cell Death of Mesenchymal Stem Cells on the Development of Liver Fibrosis

Hong-wei Wu,[1] **He-dan Chen,**[2] **Ya-hong Chen,**[3] **Xin-li Mao** ![ORCID],[4] **Yu-yi Feng,**[4] **Shao-wei Li** ![ORCID],[4,5,6] **and Xian-bin Zhou** ![ORCID][4,6]

[1]*Department of Infectious Diseases, Taizhou Enze Medical Center (Group) Enze Hospital, Taizhou, Zhejiang, China*
[2]*Department of Infectious Diseases, Taizhou Hospital of Zhejiang Province Affiliated to Wenzhou Medical University, Linhai, Zhejiang, China*
[3]*Health Management Center, Taizhou Hospital of Zhejiang Province Affiliated to Wenzhou Medical University, Linhai, Zhejiang, China*
[4]*Department of Gastroenterology, Taizhou Hospital of Zhejiang Province Affiliated to Wenzhou Medical University, Linhai, Zhejiang, China*
[5]*Key Laboratory of Minimally Invasive Techniques & Rapid Rehabilitation of Digestive System Tumor of Zhejiang Province, Taizhou Hospital Affiliated to Wenzhou Medical University, Linhai, Zhejiang, China*
[6]*Institute of Digestive Disease, Taizhou Hospital of Zhejiang Province Affiliated to Wenzhou Medical University, Linhai, Zhejiang, China*

Correspondence should be addressed to Shao-wei Li; li_shaowei81@wmu.edu.cn and Xian-bin Zhou; 112093168@qq.com

Mesenchymal stem cells have shown noticeable potential for unlimited self-renewal. They can differentiate into specific somatic cells, integrate into target tissues via cell-cell contact, paracrine effects, exosomes, and other processes and then regulate the target cells and tissues. Studies have demonstrated that transplantation of MSCs could decrease the expression and concentration of collagen in the liver, thereby reducing liver fibrosis. A growing body of evidence indicates that apoptotic MSCs could inhibit harmful immune responses and reduce inflammatory responses more effectively than viable MSCs. Accumulating evidence suggests that mitochondrial transfer from MSCs is a novel strategy for the regeneration of various damaged cells via the rescue of their respiratory activities. This study is aimed at reviewing the functions of MSCs and the related roles of the programmed cell death of MSCs, including autophagy, apoptosis, pyroptosis, and ferroptosis, as well as the regulatory pathogenic mechanisms of MSCs in liver fibrosis. Research has demonstrated that the miR-200B-3p gene is differentially expressed gene between LF and normal liver samples, and that the miR-200B-3p gene expression is positively correlated with the degree of liver fibrosis, suggesting that MSCs could inhibit liver fibrosis through pyroptosis. It was confirmed that circulating monocytes could deliver MSC-derived immunomodulatory molecules to different sites by phagocytosis of apoptotic MSCs, thereby achieving systemic immunosuppression. Accordingly, it was suggested that characterization of the programmed cell death-mediated immunomodulatory signaling pathways in MSCs should be a focus of research.

1. Introduction

Mesenchymal stem cells (MSCs), a group of unique cells, have shown great potential for unlimited self-renewal [1]. They are found in various tissues, including the liver, bone marrow, intestine, connective tissues, spleen, and placenta [2, 3]. MSCs can not only differentiate into mesenchymal cell lines (e.g., osteocytes, chondrocytes, skeletal muscle cells) but also develop into ectodermal and endodermal cells (e.g., hepatocytes and neurons) [4–6]. MSCs are becoming a focus of research in the field of cell therapy due to their unique properties, including easy acquisition, specific recruitment to the

damaged site, and low ethical restrictions [7]. In addition, one feature of MSCs is the lack of costimulatory molecules, including CD80, CD86, and HLA-II, which could result in the failure of MSCs to induce an immune response [8]. To date, stem cell technology has undergone great progress, and it may be used to treat various diseases related to the nerves, lung, heart, and liver [9]. Studies have demonstrated that through cell-cell contact, paracrine effects, and exosomes, MSCs may differentiate into cardiomyocyte-like cells, integrate into host tissue, and enhance resident cell activity [10]. MSC-mediated immunomodulation functions through the synergy of cell contact-dependent mechanisms and soluble factors. Hence, the potential application of MSCs as therapeutic agents for autoimmune and inflammatory diseases was confirmed [11].

Current bottlenecks in the therapeutic use of MSCs include donor-to-donor variability and the need for ex vivo expansion. The phenotype and function of MSCs are affected by the donor's age, body mass index (BMI), lifestyle, and pathophysiological conditions, leading to significant heterogeneity in MSCs isolated from different donors [12, 13]. The extended ex vivo expansion of isolated MSCs can further affect their clonogenicity, proliferative potential, and functionality. The therapeutic potential of MSCs is mainly attributed to two aspects: first, the replacement of the damaged tissue by differentiating into various cell lineages; and second, the regulation of immune responses by the immunomodulatory function. The major mechanism underlying MSC-based therapy is the paracrine function, which secretes various soluble factors to exert immunomodulatory, angiogenic, antiapoptotic, and antioxidative effects [14]. Induced pluripotent stem cell- (iPSC-) derived MSCs can be synthesized using a new cell differentiation and expansion platform that eliminates major issues of supply, scalability, and consistency. The iPSC-based approach has the potential to overcome the fundamental limitations of conventional, donor-derived MSC production processes as it facilitates the synthesis of an effectively limitless number of MSCs from a single blood donation. In addition, the need for excessive culture expansion of differentiated MSCs can be avoided by harnessing the indefinite replication potential of iPSCs [15].

Liver fibrosis (LF), which is regulated by activated hepatic stellate cells (HSCs), is a common cause of various chronic liver diseases. After liver injury, HSCs undergo phenotypic transformation from resting HSCs to myofibroblast-like cells, which may stimulate the expression of α-smooth muscle actin (α-SMA) and promote the synthesis of extracellular matrix (ECM) [16]. Endogenous tissue inhibitors of metalloproteinases (TIMPs) reduce excessive proteolytic ECM degradation by matrix metalloproteinases (MMPs), and an imbalance in the MMPs/TIMPs activity ratio may underlie the pathogenesis of LF. Therefore, the crucial objective of LF treatment is to inhibit the production of ECM and degrade its components. Cytokine transforming growth factor-β (TGF-β) is considered an essential factor in the LF. Once binding with the receptor, TGF-β triggers the activation of a signaling cascade, promoting the proliferation of prefibrotic cells and myofibroblasts. Therefore, the TGF-β pathway is critical for antifibrosis therapy, and the regula-

tory mechanisms have been extensively investigated in different preclinical and clinical trials [17].

The development and homeostasis of multicellular organisms are not only associated with the regulation of cell proliferation but also with the disposal of damaged cells. Programmed cell death can be induced by developmental programs and stress-induced signals, stimulating membrane-bound, and cytosolic proteins that trigger cell death via intricate cascades of transcriptional changes and post-translational protein modifications [18]. To date, mitochondrial transfer from MSCs has demonstrated protective effects on lung injury, bronchial epithelial injury, allergic diseases, damaged cardiomyocytes, alkali-burnt corneal epithelial cells, kidney injury, ischemic damage, neurotoxicity, and spinal cord injury. In addition, several signals were identified, including the release of damaged mitochondria, mitochondrial DNA, and mitochondrial products along with elevated levels of reactive oxygen species, triggering mitochondrial transfer from MSCs to the recipient cells [19, 20].

Therefore, the present study is aimed at assessing the influences of MSCs on LF and their potential clinical value, especially the mechanisms of programmed cell death of MSCs in LF through apoptosis, autophagy, pyroptosis, and ferroptosis. The findings may facilitate the understanding of the programmed cell death of MSCs and suggest a potential therapeutic method for LF.

1.1. Progress of Mesenchymal Stem Cells in LF Treatment.
Animal and clinical studies revealed that MSCs derived from bone marrow or other tissues might be transformed into hepatocyte-like cells cultured in specific conditions in vitro and show the normal metabolic functions of hepatocytes [21–23]. MSCs also contribute to the recovery of liver function to some extent and suppress inflammation in the liver, thereby exhibiting a potential therapeutic effect on LF [24]. Studies have indicated that in LF models, transplantation of MSCs could significantly reduce the expression of collagen and its concentration in the liver, which is associated with the reduced degree of fibrosis [25–28]. Sakaida et al. used fluorescent protein-labeled bone marrow-derived MSCs (BMSCs) to treat mice with LF induced by carbon tetrachloride (CC1$_4$), and the results showed that LF was alleviated in mice that underwent transplantation of MSCs and that their survival rate was significantly improved [29]. A meta-analysis evaluated the efficacy and the safety of BMSCs in decompensated cirrhosis, and it was revealed that, at 8, 16, 24, and 48 weeks after the infusion of MSCs, the albumin level was significantly elevated, and the end-stage liver disease score, alanine aminotransferase level, total bilirubin level, and prothrombin time improved to different degrees with no serious adverse events or complications [30]. Kharaziha et al. conducted a phase I-II clinical trial of autologous BMSCs to treat LF with multiple causes, and it was demonstrated that MSCs could improve liver function [31]. Jang et al. and Suk et al. found that autologous BMSC transplantation safely improved histologic fibrosis and liver function in patients with alcoholic cirrhosis [32, 33]. MSCs suppress the proliferation of HSCs and the α-SMA expression level via cell-to-cell contact, where the Notch signaling pathway

possibly plays a crucial role [34, 35]. It was also confirmed that transplantation of MSCs promoted the activation of MMP-9 and MMP-13, while it weakened the activation of TIMP-1, thereby promoting the degradation of collagen and other ECM proteins in LF [27, 34, 36]. It has also been found that MSCs play an antifibrosis role via extracellular vesicles (EVs) or exosomes. EVs from human umbilical cord-derived MSCs were used to treat mice with LF induced by CCl_4 and were found to slow the progression of LF, alleviate liver inflammation, and reduce collagen deposition. A previous study indicated that this process may be realized through dysfunction of the TGF-β1/SMAD signaling pathway [37]. In a liver injury study, EVs produced by MSCs showed a protective effect on liver cells in drug-induced liver injury models, suggesting that MSCs may partially restore the liver function by upregulating liver cell proliferation [38]. In a thioacetamide- (TAA-) induced rat model of LF, EVs from human embryonic stem cell- (ESC-) derived MSCs could reduce the degree of LF. A gene expression analysis also showed that after rats with LF were treated by MSC-EVs and MSCs, the expression levels of collagenases (e.g., MMP13 and MMP9), anti-inflammatory cytokines (e.g., IL-10 and TGF-β1), and antiapoptotic genes (e.g., BCL-2) were all upregulated, while the expression levels of proapoptotic genes (BAX), proinflammatory cytokines (e.g., TNF-α, IL-2), and the main factors contributing to fibrosis (Collα, α-SMA, and TIMP1) were downregulated. It was suggested that MSC-EVs could regulate the hepatic inflammatory microenvironment through the downregulation of immune cell infiltration and the regulation of both the expression and secretion of inflammatory factors, including anti-inflammatory and proinflammatory factors [3, 39]. Other EVs from various sources of MSCs have shown similar effects on liver protection and regeneration, including BMSCs [40–42], human menstrual blood-derived MSCs [43], adipose-derived MSCs, and human liver-derived MSCs [44, 45] (Figure 1).

1.2. Programmed Cell Death of Mesenchymal Stem Cells

1.2.1. Apoptotic MSCs. For a long time, it was assumed that different functional MSCs were efficacious for disease treatment. However, recent studies have suggested that the survival role of MSCs may be affected, and apoptotic MSCs (apo-MSCs) may also have a protective effect on the inflammatory microenvironment *in vivo* [46–48].

Most intravenously injected MSCs may be trapped in the capillary beds in the lung [49]. However, in the respiratory system, the total number of viable MSCs can rapidly decrease within one day [49]. Almost all captured MSCs are phagocytosed by alveolar macrophages, circulating neutrophils, and monocytes and are then redistributed throughout the system, accumulating primarily in the liver and spleen [11]. Although pulmonary transplantation of MSCs has emerged as a leading clinical intervention, several studies suggested that direct injection into the damaged tissue exhibited outcomes similar to intravenous injection, and the apoptosis of locally transplanted MSCs was reported after 3-5 days. Within one week, nearly all MSCs that were locally transplanted appeared in tissue-specific phagocytes [11]. It was revealed that the immune regulation mediated by MSCs can be achieved through apoptotic, metabolically dysfunctional, or fragmented MSCs. There is also evidence that apo-MSCs can inhibit harmful immune responses and reduce persistent inflammation more effectively than viable MSCs [11]. The dramatic decrease in the number of viable MSCs does not affect the immunosuppressive or therapeutic effects of MSCs, and apo-MSCs can regulate the role of immune cells [11].

Apoptosis plays a pivotal role in the arbitration of cell deletion in tissue homeostasis, embryological development, and immunological functioning [50–52]. Cells undergo a series of morphological changes, including cytoplasmic contraction and nuclear aggregation during the apoptosis of MSCs [50, 53–55]. Subsequently, the activated cysteine protease cleaves Rho-associated protein kinase 1 (ROCK1) to produce a truncated kinase with bioactivity of actin-myosin remodeling and cell contraction [56]. The membrane gradually protrudes, accompanied by blistering and fragmentation, eventually forming apoptotic fragments and apoptotic extracellular vesicles (apo-EVs) [57]. Apo-EVs have been demonstrated to precisely modulate the function of the immune system, such as T cells and macrophages, and improve tissue repair, including the regeneration of skin and protection for blood vessels [58–60]. A growing body of evidence has demonstrated that apo-EVs are key mediators of MSCs, and that the administration of apo-EVs is a promising cell-free therapeutic strategy [47, 61]. Apo-EVs play a regulatory role in a precisely tuned molecular network through phagocytosis or dynamic interaction with recipient cells [61, 62]. Notably, the direct delivery of apo-MSCs and apo-EVs is associated with excessively viable MSCs [63, 64]. Therefore, the transplantation of MSC-derived apo-EVs is expected to treat a number of diseases, including but not limited to osteoporosis, myocardial infarction, colitis, and graft-versus-host disease [54, 61, 64–66].

Galleu et al. utilized activated peripheral blood mononuclear cells (PBMCs) from healthy donors *in vitro* to determine the driving mechanism of apoptosis in MSCs. When PBMCs were activated, early apoptosis of MSCs was induced, which peaked within 4 h and shifted to late apoptosis within 24 h. According to the *in vivo* observations, the activation of caspase 3 in MSCs could only be induced by activated PBMCs, which peaked at 90 min, and this phenomenon was thoroughly eliminated by the pan-caspase inhibitor Z-VAD-FMK [47].

A study also showed that CD56+ NK and CD8+ T cells participated in the apoptosis of MSCs. To characterize the mechanism by which activated cytotoxic cells induce MSC apoptosis, the related factors involved in the activation of caspase 3 were investigated. The inhibition of granase B (GrB) or perforin completely eliminated the ability of activated PBMCs to kill MSCs or activate caspase 3. It was also revealed that CD95 ligands (CD95L or Fas ligands (Fas-L or apoptotic antigen 1 ligand)) were neutralized, while they were not neutralized after suppressing TNF-α or TNF-related apoptosis-inducing ligands [47]. The intrinsic phenomenon of the MSC-cytotoxic cell interaction was detected, and Galleu
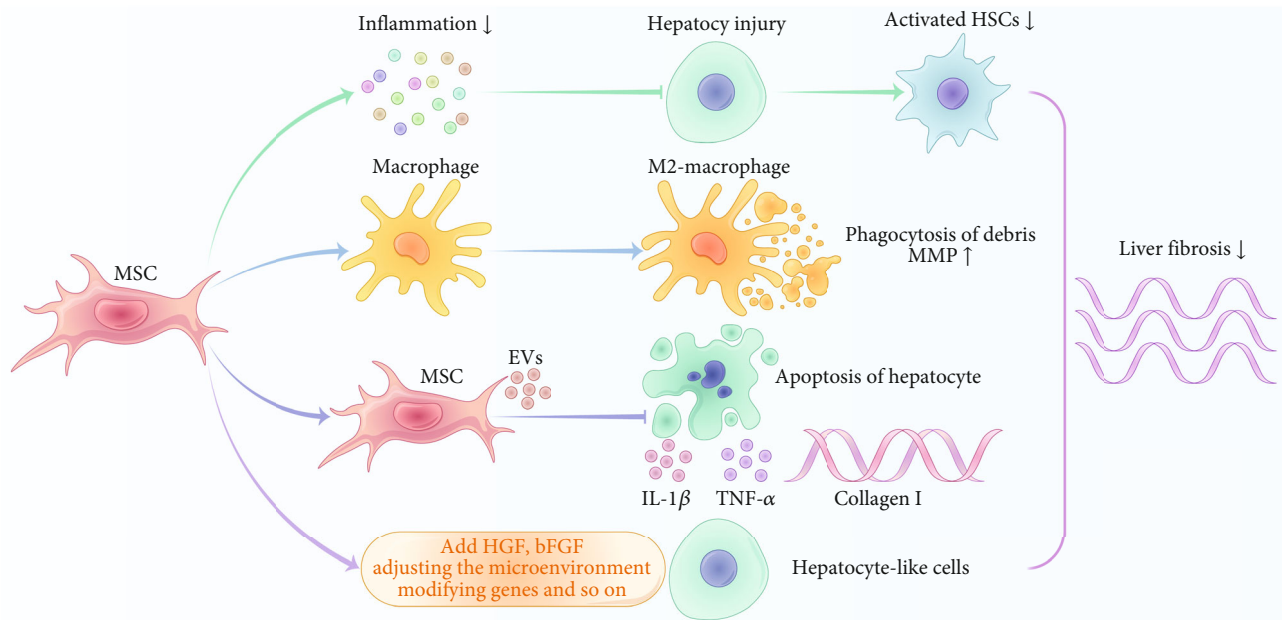
FIGURE 1: Mechanism of MSCs in reducing liver fibrosis. MSCs could increase the expression levels of anti-inflammatory cytokines (interleukin-10 (IL-10) and tumor necrosis factor-α (TNF-α)) and reduce the expression levels of proinflammatory cytokines (IL-6, IL-1A, IL-17, monocyte chemoattractant protein-1 (MCP-1), granulocyte colony-stimulating factor (GCSF), interferon-gamma (IFN-γ), macrophage inflammatory protein-2A (MIP-2A), and granulocyte-macrophage colony-stimulating factor (GMCSF)), thereby reducing hepatocyte injury and inhibiting the activation of hepatic stellate cells. MSCs enhance the generation of anti-inflammatory phenotypes in macrophages (M2 macrophages), phagocytic debris, and increase the production of MMP to reduce the degree of liver fibrosis. MSC-EVs inhibit the production of TNF-α, IL-1β, and collagen-1α, and thus reduce hepatocyte apoptosis and inhibit liver fibrosis. The ability of MSCs to differentiate into hepatocyte-like cells can be improved by adding cytokines and growth factors, regulating the microenvironment, and modifying genes, which could relieve liver fibrosis.

et al. found that apoptosis was unaffected by antihuman leukocyte antigen I (anti-HLA I)- or anti-HLA II-neutralizing antibodies. Activated PBMCs showed no difference in cytotoxic activity against autologous or allogeneic MSCs. Therefore, direct cell contact is important for the immune-suppressive effects of PBMCs to induce apoptosis and block immune synapse formation via the inhibition of polarization in the center of microtubule tissues. The results showed that there is a bystander effect when activated cytotoxic cells kill MSCs without the involvement of immunological synapses [47].

Apoptosis of MSCs increases the ability of MSCs to induce immunosuppressive phenotypes in macrophages, dendritic cells (DCs), and T cells. As apo-MSCs are more readily phagocytic than viable MSCs, CTL-dependent apoptosis of transplanted MSCs is a prerequisite for the MSC-based regulation of the phenotypes and roles of macrophages [67]. Under phagocytosis, apo-MSCs induce monocytes/macrophages to produce immunosuppressive macrophages (M2 macrophages) that promote the production of anti-inflammatory cytokines and growth factors, thereby mitigating inflammatory responses and enhancing the regeneration and recovery of damaged tissues. M2 macrophages suppress T cell proliferation in the liver in a PGE2- and IL-10-dependent manner, inhibit the production of inflammatory factors (IFN-γ and TNF-α) and profibrotic cytokines (TGF-β), and promote the proliferation of regulatory T (Treg) cells, thereby generating an immunosuppressive microenvironment in inflammatory tissues [68].

Notably, apo-MSC-mediated immune regulation is similar to or even superior to mediation by viable MSCs. The immunomodulatory effects of apo-MSCs are more predictable than those of viable MSCs [67].

1.3. Mesenchymal Stem Cell Autophagy and LF. As a cellular degradation pathway, autophagy utilizes lysosomes to get rid of damaged organelles or macromolecules, in which intracellular material circulation and an internal environmental balance can be achieved as amino acids are produced [69]. Based on substrate degradation and transportation methods, autophagy can be divided into three levels: macroautophagy, microautophagy, and chaperone-mediated autophagy [70]. Macroautophagy maintains cellular homeostasis through targeting cytoplasmic contents and organelles into autophagosomes for degradation [71]. In addition to basic homeostasis, autophagy is involved in the pathogenic mechanisms of a number of diseases, including cancer [72], inflammation [73], metabolic diseases [74], neurodegeneration [75], and cardiovascular diseases [76]. A number of studies have explored the functions of autophagy in particular diseases and also developed potential therapeutic strategies [77, 78]. MSC autophagy is critical for limiting inflammation, apoptosis, and oxidative stress in the cells associated with diseases, and it finally promotes treatment using MSCs [79]. It could modulate MSC-regulated immune regulation, suppress inflammation, and enhance anti-inflammation. In a previous study, MSCs were pretreated

with 3-methyladenine (3-MA) and rapamycin to regulate autophagy; then, they were cocultured with CD4+ T cells, and it was found that 3-MA inhibited autophagy in MSCs, which was activated by rapamycin [80]. It was shown that rapamycin could increase the migration of CD4$^+$ T cells, while treatment with 3-MA decreased their migration. Furthermore, MSC autophagy enhanced the migration of CD4$^+$ T cells via CXCL8, promoted the differentiation of Treg cells, and inhibited the differentiation of type 1 T helper (Th1) cells via the secretion of TGF-β1. In addition, Gao et al. suggested that MSC autophagy could modulate the immunosuppression of CD4$^+$ T cells through its influence on TGF-β1 secretion [81]. The homeostasis of CD4+ T cells was considered to be pivotal in hepatitis B virus-related LF [82, 83].

Wang et al. investigated the antifibrosis phenomenon of MSCs in the mouse model of CCl$_4$-induced LF. MSCs were stimulated *in vitro* with fibrosis-related factors (TNF-α, interferon-γ (IFN-γ), and TGF-β1) to mimic the LF microenvironment. The results showed that MSCs responded to the LF microenvironment by upregulating the expression of beclin-1 (Becn1) and exhibiting autophagy *in vitro* and *in vivo*. After Becn1 was knocked out, MSC autophagy was inhibited, which enhanced the antifibrosis effect. The increased antifibrosis potential of MSCs may be attributed to the inhibition of T lymphocyte infiltration, hematopoietic stem cell proliferation, and the production of TGF-β1, IFN-γ, and TNF-α mediated by the paracrine PTGS2/PGE2 pathway [84]. However, tonsil-derived MSCs are differentiated into hepatocellular-like cells and inhibit LF by activating autophagy and downregulating TGF-β [85]. Thus, regulating MSC autophagy is a promising strategy for improving the antifibrosis function of MSCs.

1.4. Mesenchymal Stem Cell Ferroptosis and LF. As a type of iron-dependent programmed cell death, ferroptosis is driven by the intracellular peroxidation of lipids and induced by erastin [86], which is different from necrosis, apoptosis, and autophagy [86–89]. Morphologically, ferroptosis-induced cell death is characterized by mitochondrial contraction, increased membrane density, and mitochondrial crest reduction or disappearance. Ferroptosis does not show the morphology of typical phenotypes of apoptosis (i.e., chromatin aggregation and marginalization), necrosis (i.e., cytoplasm and organelle swelling or plasma membrane rupture), and autophagy (i.e., the formation of double-membrane vesicles) [86, 88–91]. Iron overload could affect ferritin deposition and systemic iron homeostasis [92, 93]. High concentrations of iron were found in the liver and spleen, leading to the aggregation and overproduction of ferritin-containing iron [94]. Ferritin covers light chain and heavy chain, including ferritin light chain (FTL) and ferritin heavy chain (FTH), which may act as a place for intracellular iron storage and play an essential role in the regulation of cell death [81, 95, 96]. The decreased levels of FTH1 and FTL in erastin-induced ferroptosis are correlated with the increased intracellular iron concentrations in MSCs. On the contrary, FTH1/FTL overexpression could alleviate ferroptosis in MSCs [97]. Bridle et al. demonstrated that HSCs express specific receptors for FTH and transferrin [98, 99]. FTH1 activates the expression levels of key profibrosis genes, including

actin alpha-2 (ACTA-2), collagen-1, and bone morphogenetic protein-6 (BMP-6) by interacting with these receptors, which may activate HSCs and induce fibrosis [99, 100]. MSCs may inhibit LF by regulating ferroptosis through FTH1; however, further study is required to elucidate the specific mechanism.

1.5. Mesenchymal Stem Cell Pyroptosis and LF. Pyroptosis (inflammatory necrosis) is a type of inflammatory cell death that is mainly caused by microbial infection, accompanied by the activation of inflammasomes and maturation of pro-inflammatory cytokines. It plays an important role in the pathogenesis of several diseases [101–103]. Pyroptosis can be regulated by gasdermin-D (GSDMD) and caspase-1 [104, 105]. Inflammasomes, such as *NLR family CARD domain-containing protein 4* (NLRC4), absent in melanoma 2 (AIM2), *NLR* family *pyrin domain-containing 1b* (NlRP1b), and NLR family pyrin domain-containing 3 (NLRP3), activate caspase-1 by transforming procaspase1 into Cl-caspase1, and facilitate the formation of IL-18 and IL-1β from their precursors, leading to the mediation of pyroptosis. It was reported that pyroptosis is involved in the development of several inflammatory diseases [106]. Zhang et al. found that ORLNC1 regulates the BMSC pyroptosis induced by chronic myeloid leukemia through the miR-200b-3p/Foxo3 pathway *in vitro* and *in vivo*, and ORLNC1 is not correlated with the expression level of miR-200b-3p, which is critical for MSC pyroptosis [107]. Meanwhile, Ye et al. demonstrated that the miR-200B-3p gene is differentially expressed between LF and normal liver samples, and that its expression is positively correlated with the degree of LF [108], suggesting that MSCs can inhibit LF through pyroptosis, while further research is required (Figure 2).

1.6. Potential Pathways for Programmed Cell Death of Mesenchymal Stem Cells to Treat LF. It is broadly accepted that the indoleamine 2,3-dioxygenase (IDO)/kynurenine pathway is critical for the immunomodulatory properties of apo-MSCs. Apo-MSCs could increase immunosuppressive IDO in both macrophages and DCs [11]. Apo-MSCs injected intraperitoneally were phagocytosed by peritoneal CD11b+macrophages;however, this phenomenon was not observed in the macrophages from the lung or spleen [46]. In contrast, when apo-MSCs were administered intravenously, they were predominantly phagocytosed by CD11b^{high}CD11c^{int}, CD11b^{high}CD11c$^-$, and CD11b$^-$CD11C$^+$ phagocytes in the lung [46]. Importantly, apo-MSCs significantly enhanced the expression of IDO in macrophages and DCs and increased its immunosuppressive properties in an IDO-dependent manner [11].

IDO is a cytoplasmic and heme-containing enzyme that can convert tryptophan to quinolinic acid, which has an immunosuppressive function. The IDO1 enzyme catabolizes the conversion of L-Trp into KYN, which can be consequently processed enzymatically to several metabolites (i.e., KYNA, 3-hydroxykynurenine (3-HK), 3-hydroxyanthranilic acid, and finally to quinolinic and picolinic acids) [18]. The aggregation of 3-HAA, KYNA, QA, and 3-HK induced by IDO directly suppresses the activated T and B cells, resulting in a weakened adaptive immune response. In addition, kynurenine
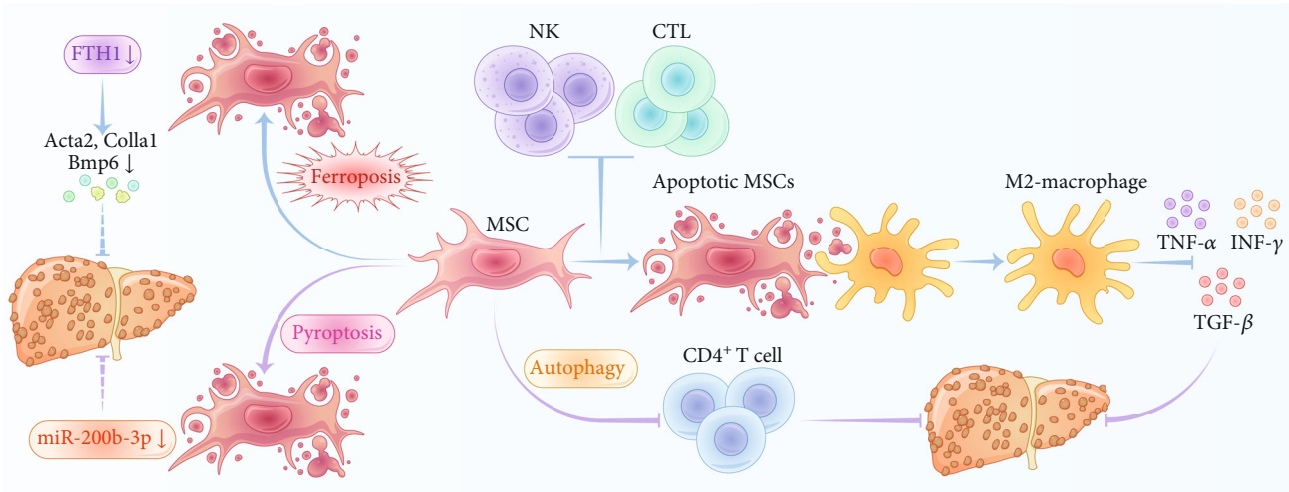
FIGURE 2: Programmed cell death of MSCs attenuates liver fibrosis. Autophagy of MSCs attenuates liver fibrosis through the immunosuppression of CD4+ T cells. NK cells and CTLs initiate apoptosis of MSCs, and apoptotic MSCs promote macrophages to produce an immunosuppressive (M2) phenotype and inhibit the production of TNF-α, TGF-β, and IFN-γ. Ferritin heavy chain-1 (FTH-1) activates the expression of key profibrotic genes, including Col1a1, bone morphogenetic protein-6 (BMP-6), and actin alpha-2 (ACTA-2), which may activate HSCs and induce liver fibrosis. The expression of FTH1 is low in iron-death MSCs, and iron-death MSCs may reduce liver fibrosis through the low expression of FTH1. miR-200b-3p is positively correlated with the degree of liver fibrosis, and the expression of miR-200b-3p decreases in the pyroptosis of MSCs, which may alleviate liver fibrosis.

induces apoptosis of inflammatory cells in a Fas-independent manner by activating caspase-8 and releasing mitochondrial cytochrome C [18].

It is noteworthy that IDO is essential for the crossover between DCs and immunosuppressed Treg cells [18]. DCs promote the production and proliferation of Treg cells by increasing IDO activity, thereby inducing and maintaining immune tolerance. DCs induce the expression of lineage-defining transcription factor FoxP3 in naïve CD4+ T cells in an IDO/kynurenine-dependent manner, resulting in the production of CD4+ FoxP3+ Treg cells, which play an immunosuppressive role [18]. In the initial activation of T cell receptor- (TCR-) mediated resting Treg cells, protein kinase B (PKB/Akt) and mammalian target of rapamycin (mTOR) pathways may disrupt the immunomodulatory function of Treg cells and lead to the activation of a pro-inflammatory phenotype (pre-Tregs), producing more inflammatory cytokines. A limited tryptophan activation could regulate general control nonderepressible 2 (GCN2) kinase, thereby inhibiting Akt/mTOR2 signal transduction [18]. In order to prevent transdifferentiation of CD4+ T cells into Treg cells, DCs induce low tryptophan levels in an IDO/kynurenine-dependent manner and activate GCN2 kinase, thereby inhibiting the activation of the Akt/mTORC2 signaling pathway in Treg cells.

Similarly, the increased activation of GCN2 kinase and IDO in DCs could downregulate the TCR zeta chain of activated CD8+ CTLs, thereby reducing their cytotoxicity [18]. Consistent with these findings, apo-MSCs strengthen the immunosuppressive function and regulation of DCs and macrophages by increasing IDO activity [11]. Galleu et al. demonstrated that apo-MSCs successfully attenuated the macrophage-driven inflammatory response in mouse models by regulating the phagocytic activity and antigene

presenting capabilities of DCs in an IDO/kynurenine-dependent manner [47]. IDO inhibition of apo-MSCs completely attenuated their anti-inflammatory effect, suggesting that IDO/kynurenine would be crucial for the apo-MSC-mediated regulation of phenotypes and the functions of macrophages and DCs [47]. In addition, circulating monocytes could deliver MSC-derived immunomodulatory molecules to different sites by phagocytosis of apo-MSCs, thereby achieving systemic immunosuppression [11]. Zhou et al. [85] administered MSCs to reduce the degree of LF, and they found that IDO inhibited the production of IL-17 by Th17 cells. Apo-MSCs may alleviate LF through the IDO/kynurenine pathway; however, further research is required to confirm this finding.

2. Conclusions

MSCs can ameliorate LF through suppressing the activation of HSCs or inhibiting the inflammatory microenvironment. Programmed cell death of MSCs inhibits harmful immune responses and reduces persistent inflammation more effectively than viable MSCs. Although some studies have provided evidence supporting the potential therapeutic application of MSC programmed cell death, the molecular mechanisms underlying their immunosuppressive regulation should be further clarified. Current bottlenecks in the clinical use of MSCs for therapy include donor-to-donor variability and the need for ex vivo expansion. The phenotype and function of MSCs are affected by the donor's age, BMI, lifestyle, and pathophysiological conditions, leading to significant heterogeneity in MSCs isolated from different donors. The extended ex vivo expansion of isolated MSCs can further affect their clonogenicity, proliferative potential, and functionality. Therefore, the characterization of

programmed cell death-mediated immunomodulatory signaling pathways in MSCs should be a focus of research. In order to improve clinical safety, efficacy, and reliability, additional studies are needed to validate these effects on different stages of LF and explore etiologies.

Abbreviations

MSCs:	Mesenchymal stem cells
PGE2:	Prostaglandin E2
TGF-β:	Transforming growth factor-β
IDO:	Indoleamine 2, 3-dioxygenase
IL-10:	Interleukin-10
IL-1RA:	IL-1 receptor antagonist
HGF:	Hepatic growth factor
NO:	Nitric oxide
HO-1:	Heme oxygenase-1
TNF-α:	Tumor necrosis factor-α
TSG-6:	TNFα-stimulated gene-6
DCs:	Dendritic cells
NK:	Natural killer cells
CTLs:	Cytotoxic T lymphocytes
iPSC:	Induced pluripotent stem cells
HSCs:	Hepatic stellate cells
α-SMA:	α-Smooth muscle actin
TIMPs:	Tissue inhibitors of metalloproteinases
MMPs:	Matrix metalloproteinases
ECM:	Extracellular matrix
LF:	Liver fibrosis
CC1$_4$:	Carbon tetrachloride
BMSCs:	Bone marrow-derived MSCs
EVs:	Extracellular vesicles
ROCK1:	Rho-associated protein kinase 1
apo-EVs:	Apoptotic extracellular vesicles
PBMCs:	Peripheral blood mononuclear cells
anti-HLA I:	Antihuman leukocyte antigen I
apo-MSCs:	Apoptotic mesenchymal stem cells.

Data Availability

The data used to support the findings of this study are included within the article.

Conflicts of Interest

The authors declare no conflicts of interest in association with the present study.

Acknowledgments

References

[1] A. J. Friedenstein, R. K. Chailakhyan, N. V. Latsinik, A. F. Panasyuk, and I. V. Keiliss-Borok, "Stromal cells responsible for transferring the microenvironment of the hemopoietic tissues," *Transplantation*, vol. 17, no. 4, pp. 331–340, 1974.

[2] A. Shariati, R. Nemati, Y. Sadeghipour et al., "Mesenchymal stromal cells (MSCs) for neurodegenerative disease: a promising frontier," *European Journal of Cell Biology*, vol. 99, no. 6, article 151097, 2020.

[3] B. Fazekas, S. Alagesan, L. Watson et al., "Comparison of single and repeated dosing of anti-inflammatory human umbilical cord mesenchymal stromal cells in a mouse model of polymicrobial sepsis," *Stem Cell Reviews and Reports*, vol. 18, no. 4, pp. 1444–1460, 2022.

[4] P. Tropel, N. Platet, J. C. Platel et al., "Functional neuronal differentiation of bone marrow-derived mesenchymal stem cells," *Stem cells*, vol. 24, no. 12, pp. 2868–2876, 2006.

[5] R. A. Rose, A. Keating, and P. H. Backx, "Do mesenchymal stromal cells transdifferentiate into functional cardiomyocytes?," *Circulation research*, vol. 103, no. 9, article e120, 2008.

[6] D. A. Pijnappels, M. J. Schalij, A. A. Ramkisoensing et al., "Forced alignment of mesenchymal stem cells undergoing cardiomyogenic differentiation affects functional integration with cardiomyocyte cultures," *Circulation Research*, vol. 103, no. 2, pp. 167–176, 2008.

[7] K. Le Blanc, L. Tammik, B. Sundberg, S. E. Haynesworth, and O. Ringden, "Mesenchymal stem cells inhibit and stimulate mixed lymphocyte cultures and mitogenic responses independently of the major histocompatibility complex," *Scandinavian Journal of Immunology*, vol. 57, no. 1, pp. 11–20, 2003.

[8] M. Ben Nasr, A. Vergani, J. Avruch et al., "Co-transplantation of autologous MSCs delays islet allograft rejection and generates a local immunoprivileged site," *Acta Diabetologica*, vol. 52, no. 5, pp. 917–927, 2015.

[9] F. Fatima and M. Nawaz, "Stem cell-derived exosomes: roles in stromal remodeling, tumor progression, and cancer immunotherapy," *Chinese Journal of Cancer*, vol. 34, no. 12, pp. 541–553, 2015.

[10] A. Hassanzadeh, H. S. Rahman, A. Markov et al., "Mesenchymal stem/stromal cell-derived exosomes in regenerative medicine and cancer; overview of development, challenges, and opportunities," *Stem Cell Research & Therapy*, vol. 12, no. 1, p. 297, 2021.

[11] A. R. R. Weiss and M. H. Dahlke, "Immunomodulation by mesenchymal stem cells (MSCs): mechanisms of action of living, apoptotic, and dead MSCs," *Frontiers in Immunology*, vol. 10, p. 1191, 2019.

[12] H. J. Yang, K. J. Kim, M. K. Kim et al., "The stem cell potential and multipotency of human adipose tissue-derived stem cells vary by cell donor and are different from those of other types of stem cells," *Cells, Tissues, Organs*, vol. 199, no. 5-6, pp. 373–383, 2015.

[13] L. Shi, Q. Han, Y. Hong et al., "Inhibition of miR-199a-5p rejuvenates aged mesenchymal stem cells derived from patients with idiopathic pulmonary fibrosis and improves their therapeutic efficacy in experimental pulmonary fibrosis," *Stem Cell Research & Therapy*, vol. 12, no. 1, p. 147, 2021.

[14] M. Kang, C. C. Huang, P. Gajendrareddy et al., "Extracellular vesicles from TNFα preconditioned MSCs: effects on

immunomodulation and bone regeneration," *Frontiers in Immunology*, vol. 13, article 878194, 2022.

[15] Q. Lian, Y. Zhang, J. Zhang et al., "Functional mesenchymal stem cells derived from human induced pluripotent stem cells attenuate limb ischemia in mice," *Circulation*, vol. 121, no. 9, pp. 1113–1123, 2010.

[16] Y. W. Eom, K. Y. Shim, and S. K. Baik, "Mesenchymal stem cell therapy for liver fibrosis," *The Korean Journal of Internal Medicine*, vol. 30, no. 5, pp. 580–589, 2015.

[17] M. Gazdic, A. Arsenijevic, B. S. Markovic et al., "Mesenchymal stem cell-dependent modulation of liver diseases," *International Journal of Biological Sciences*, vol. 13, no. 9, pp. 1109–1117, 2017.

[18] A. Acovic, M. Gazdic, N. Jovicic et al., "Role of indoleamine 2,3-dioxygenase in pathology of the gastrointestinal tract," *Therapeutic Advances in Gastroenterology*, vol. 11, p. 175628481881533, 2018.

[19] D. Jiang, F. Gao, Y. Zhang et al., "Mitochondrial transfer of mesenchymal stem cells effectively protects corneal epithelial cells from mitochondrial damage," *Cell Death & Disease*, vol. 7, no. 11, article e2467, 2016.

[20] B. Porubska, D. Vasek, V. Somova et al., "Sertoli cells possess immunomodulatory properties and the ability of mitochondrial transfer similar to mesenchymal stromal cells," *Stem Cell Reviews and Reports*, vol. 17, no. 5, pp. 1905–1916, 2021.

[21] S. N. Shu, L. Wei, J. H. Wang, Y. T. Zhan, H. S. Chen, and Y. Wang, "Hepatic differentiation capability of rat bone marrow-derived mesenchymal stem cells and hematopoietic stem cells," *World journal of gastroenterology: WJG*, vol. 10, no. 19, pp. 2818–2822, 2004.

[22] K. D. Lee, T. K. Kuo, J. Whang-Peng et al., "In vitro hepatic differentiation of human mesenchymal stem cells," *Hepatology*, vol. 40, no. 6, pp. 1275–1284, 2004.

[23] E. Tsolaki and E. Yannaki, "Stem cell-based regenerative opportunities for the liver: state of the art and *beyond*," *Journal of Gastroenterology*, vol. 21, no. 43, pp. 12334–12350, 2015.

[24] H. Qiao, Y. Tong, H. Han et al., "A novel therapeutic regimen for hepatic fibrosis using the combination of mesenchymal stem cells and baicalin," *Die Pharmazie*, vol. 66, no. 1, pp. 37–43, 2011.

[25] G. A. Nasir, S. Mohsin, M. Khan et al., "Mesenchymal stem cells and Interleukin-6 attenuate liver fibrosis in mice," *Journal of Translational Medicine*, vol. 11, no. 1, p. 78, 2013.

[26] V. Rabani, M. Shahsavani, M. Gharavi, A. Piryaei, Z. Azhdari, and H. Baharvand, "Mesenchymal stem cell infusion therapy in a carbon tetrachloride-induced liver fibrosis model affects matrix metalloproteinase expression," *Cell Biology International*, vol. 34, no. 6, pp. 601–605, 2010.

[27] G. Ali, S. Mohsin, M. Khan et al., "Nitric oxide augments mesenchymal stem cell ability to repair liver fibrosis," *Journal of Translational Medicine*, vol. 10, no. 1, p. 75, 2012.

[28] R. L. Pan, P. Wang, L. X. Xiang, and J. Z. Shao, "Delta-like 1 serves as a new target and contributor to liver fibrosis down-regulated by mesenchymal stem cell transplantation," *The Journal of Biological Chemistry*, vol. 286, no. 14, pp. 12340–12348, 2011.

[29] I. Sakaida, S. Terai, N. Yamamoto et al., "Transplantation of bone marrow cells reduces CCl4-induced liver fibrosis in mice," *Hepatology*, vol. 40, no. 6, pp. 1304–1311, 2004.

[30] X. N. Pan, L. Q. Zheng, and X. H. Lai, "Bone marrow-derived mesenchymal stem cell therapy for decompensated liver cirrhosis: a *meta-analysis*," *Journal of Gastroenterology*, vol. 20, no. 38, pp. 14051–14057, 2014.

[31] P. Kharaziha, P. M. Hellstrom, B. Noorinayer et al., "Improvement of liver function in liver cirrhosis patients after autologous mesenchymal stem cell injection: a phase I-II clinical trial," *European Journal of Gastroenterology & Hepatology*, vol. 21, no. 10, pp. 1199–1205, 2009.

[32] Y. O. Jang, Y. J. Kim, S. K. Baik et al., "Histological improvement following administration of autologous bone marrow-derived mesenchymal stem cells for alcoholic cirrhosis: a pilot study," *Liver International*, vol. 34, no. 1, pp. 33–41, 2014.

[33] K. T. Suk, J. H. Yoon, M. Y. Kim et al., "Transplantation with autologous bone marrow-derived mesenchymal stem cells for alcoholic cirrhosis: phase 2 trial," *Hepatology*, vol. 64, no. 6, pp. 2185–2197, 2016.

[34] S. Chen, L. Xu, N. Lin, W. Pan, K. Hu, and R. Xu, "Activation of Notch1 signaling by marrow-derived mesenchymal stem cells through cell-cell contact inhibits proliferation of hepatic stellate cells," *Life Sciences*, vol. 89, no. 25-26, pp. 975–981, 2011.

[35] V. Volarevic, J. Nurkovic, N. Arsenijevic, and M. Stojkovic, "Concise review: therapeutic potential of mesenchymal stem cells for the treatment of acute liver failure and cirrhosis," *Stem Cells*, vol. 32, no. 11, pp. 2818–2823, 2014.

[36] F. Heymann, K. Hamesch, R. Weiskirchen, and F. Tacke, "The concanavalin a model of acute hepatitis in mice," *Laboratory Animals*, vol. 49, 1_suppl, pp. 12–20, 2015.

[37] T. Li, Y. Yan, B. Wang et al., "Exosomes derived from human umbilical cord mesenchymal stem cells alleviate liver fibrosis," *Stem Cells and Development*, vol. 22, no. 6, pp. 845–854, 2013.

[38] C. Y. Tan, R. C. Lai, W. Wong, Y. Y. Dan, S. K. Lim, and H. K. Ho, "Mesenchymal stem cell-derived exosomes promote hepatic regeneration in drug-induced liver injury models," *Stem Cell Research & Therapy*, vol. 5, no. 3, p. 76, 2014.

[39] S. Mardpour, S. N. Hassani, S. Mardpour et al., "Extracellular vesicles derived from human embryonic stem cell-MSCs ameliorate cirrhosis in thioacetamide-induced chronic liver injury," *Journal of Cellular Physiology*, vol. 233, no. 12, pp. 9330–9344, 2018.

[40] H. Haga, I. K. Yan, K. Takahashi, A. Matsuda, and T. Patel, "Extracellular vesicles from bone marrow-derived mesenchymal stem cells improve survival from lethal hepatic failure in mice," *Stem Cells Translational Medicine*, vol. 6, no. 4, pp. 1262–1272, 2017.

[41] A. Damania, D. Jaiman, A. K. Teotia, and A. Kumar, "Mesenchymal stromal cell-derived exosome-rich fractionated secretome confers a hepatoprotective effect in liver injury," *Stem Cell Research & Therapy*, vol. 9, no. 1, p. 31, 2018.

[42] F. Anger, M. Camara, E. Ellinger et al., "Human mesenchymal stromal cell-derived extracellular vesicles improve liver regeneration after ischemia reperfusion injury in mice," *Stem Cells and Development*, vol. 28, no. 21, pp. 1451–1462, 2019.

[43] L. Chen, B. Xiang, X. Wang, and C. Xiang, "Exosomes derived from human menstrual blood-derived stem cells alleviate fulminant hepatic failure," *Stem Cell Research & Therapy*, vol. 8, no. 1, p. 9, 2017.

[44] L. L. Liau, S. Makpol, A. G. N. Azurah, and K. H. Chua, "Human adipose-derived mesenchymal stem cells promote

recovery of injured HepG2 cell line and show sign of early hepatogenic differentiation," *Cytotechnology*, vol. 70, no. 4, pp. 1221–1233, 2018.

[45] M. B. Herrera Sanchez, S. Previdi, S. Bruno et al., "Extracellular vesicles from human liver stem cells restore argininosuccinate synthase deficiency," *Stem Cell Research & Therapy*, vol. 8, no. 1, p. 176, 2017.

[46] S. F. H. de Witte, F. Luk, J. M. Sierra Parraga et al., "Immunomodulation by therapeutic mesenchymal stromal cells (MSC) is triggered through phagocytosis of MSC by monocytic cells," *Stem Cells*, vol. 36, no. 4, pp. 602–615, 2018.

[47] A. Galleu, Y. Riffo-Vasquez, C. Trento et al., "Apoptosis in mesenchymal stromal cells induces in vivo recipient-mediated immunomodulation," *Science translational medicine*, vol. 9, no. 416, p. 9, 2017.

[48] F. Luk, S. F. de Witte, S. S. Korevaar et al., "Inactivated mesenchymal stem cells maintain immunomodulatory capacity," *Stem Cells and Development*, vol. 25, no. 18, pp. 1342–1354, 2016.

[49] C. Huselstein, R. Rahouadj, N. de Isla, D. Bensoussan, J. F. Stoltz, and Y. P. Li, "Mechanobiology of mesenchymal stem cells: which interest for cell-based treatment?," *Bio-medical Materials and Engineering*, vol. 28, no. s1, pp. S47–S56, 2017.

[50] Y. Fuchs and H. Steller, "Live to die another way: modes of programmed cell death and the signals emanating from dying cells," *Nature Reviews Molecular Cell Biology*, vol. 16, no. 6, pp. 329–344, 2015.

[51] M. Doerflinger, Y. Deng, P. Whitney et al., "Flexible usage and interconnectivity of diverse cell death pathways protect against intracellular infection," *Immunity*, vol. 53, no. 3, pp. 533–547.e7, 2020.

[52] Z. Zhang, H. Lin, M. Shi et al., "Human umbilical cord mesenchymal stem cells improve liver function and ascites in decompensated liver cirrhosis patients," *Journal of Gastroenterology and Hepatology*, vol. 27, Suppl 2, pp. 112–120, 2012.

[53] J. F. Kerr, A. H. Wyllie, and A. R. Currie, "Apoptosis: a basic biological phenomenon with wideranging implications in tissue kinetics," *British Journal of Cancer*, vol. 26, no. 4, pp. 239–257, 1972.

[54] R. C. Taylor, S. P. Cullen, and S. J. Martin, "Apoptosis: controlled demolition at the cellular level," *Nature Reviews Molecular Cell Biology*, vol. 9, no. 3, pp. 231–241, 2008.

[55] Y. Zhang, X. Chen, C. Gueydan, and J. Han, "Plasma membrane changes during programmed cell deaths," *Cell Research*, vol. 28, no. 1, pp. 9–21, 2018.

[56] M. L. Coleman, E. A. Sahai, M. Yeo, M. Bosch, A. Dewar, and M. F. Olson, "Membrane blebbing during apoptosis results from caspase-mediated activation of ROCK I," *Nature Cell Biology*, vol. 3, no. 4, pp. 339–345, 2001.

[57] S. Caruso and I. K. H. Poon, "Apoptotic cell-derived extracellular vesicles: more than just debris," *Frontiers in Immunology*, vol. 9, p. 1486, 2018.

[58] H. Chen, S. Kasagi, C. Chia et al., "Extracellular vesicles from apoptotic cells promote TGFβ production in macrophages and suppress experimental colitis," *Scientific Reports*, vol. 9, no. 1, p. 5875, 2019.

[59] A. G. Laing, Y. Riffo-Vasquez, E. Sharif-Paghaleh, G. Lombardi, and P. T. Sharpe, "Immune modulation by apo-

ptotic dental pulp stem cells in vivo," *Immunotherapy*, vol. 10, no. 3, pp. 201–211, 2018.

[60] J. Liu, X. Qiu, Y. Lv et al., "Apoptotic bodies derived from mesenchymal stem cells promote cutaneous wound healing via regulating the functions of macrophages," *Stem Cell Research & Therapy*, vol. 11, no. 1, p. 507, 2020.

[61] H. Liu, S. Liu, X. Qiu et al., "Donor MSCs release apoptotic bodies to improve myocardial infarction via autophagy regulation in recipient cells," *Autophagy*, vol. 16, no. 12, pp. 2140–2155, 2020.

[62] X. Kou, X. Xu, C. Chen et al., "The Fas/Fap-1/Cav-1 complex regulates IL-1RA secretion in mesenchymal stem cells to accelerate wound healing," *Science Translational Medicine*, vol. 10, no. 432, pp. 71–102, 2018.

[63] C. L. Chang, S. Leu, H. C. Sung et al., "Impact of apoptotic adipose-derived mesenchymal stem cells on attenuating organ damage and reducing mortality in rat sepsis syndrome induced by cecal puncture and ligation," *Journal of Translational Medicine*, vol. 10, no. 1, p. 244, 2012.

[64] H. H. Chen, K. C. Lin, C. G. Wallace et al., "Additional benefit of combined therapy with melatonin and apoptotic adipose-derived mesenchymal stem cell against sepsis-induced kidney injury," *Journal of Pineal Research*, vol. 57, no. 1, pp. 16–32, 2014.

[65] D. Liu, X. Kou, C. Chen et al., "Circulating apoptotic bodies maintain mesenchymal stem cell homeostasis and ameliorate osteopenia via transferring multiple cellular factors," *Cell Research*, vol. 28, no. 9, pp. 918–933, 2018.

[66] G. Dou, R. Tian, X. Liu et al., "Chimeric apoptotic bodies functionalized with natural membrane and modular delivery system for inflammation modulation," *Science Advances*, vol. 6, no. 30, p. eaba2987, 2020.

[67] C. R. Harrell and V. Volarevic, "Apoptosis: a friend or foe in mesenchymal stem cell-based immunosuppression," *Advances in Protein Chemistry and Structural Biology*, vol. 126, pp. 39–62, 2021.

[68] C. R. Harrell, N. Jovicic, V. Djonov, N. Arsenijevic, and V. Volarevic, "Mesenchymal stem cell-derived exosomes and other extracellular vesicles as new remedies in the therapy of inflammatory diseases," *Cell*, vol. 8, no. 12, p. 1605, 2019.

[69] A. L. Anding and E. H. Baehrecke, "Cleaning house: selective autophagy of organelles," *Developmental Cell*, vol. 41, no. 1, pp. 10–22, 2017.

[70] K. R. Parzych and D. J. Klionsky, "An overview of autophagy: morphology, mechanism, and regulation," *Antioxidants & Redox Signaling*, vol. 20, no. 3, pp. 460–473, 2014.

[71] L. Galluzzi and D. R. Green, "Autophagy-independent functions of the autophagy machinery," *Cell*, vol. 177, no. 7, pp. 1682–1699, 2019.

[72] C. M. Dower, C. A. Wills, S. M. Frisch, and H. G. Wang, "Mechanisms and context underlying the role of autophagy in cancer metastasis," *Autophagy*, vol. 14, no. 7, pp. 1110–1128, 2018.

[73] Y. Matsuzawa-Ishimoto, S. Hwang, and K. Cadwell, "Autophagy and inflammation," *Annual Review of Immunology*, vol. 36, no. 1, pp. 73–101, 2018.

[74] K. H. Kim and M. S. Lee, "Autophagy—a key player in cellular and body metabolism," *Nature Reviews Endocrinology*, vol. 10, no. 6, pp. 322–337, 2014.

[75] F. M. Menzies, A. Fleming, and D. C. Rubinsztein, "Compromised autophagy and neurodegenerative diseases," *Nature Reviews Neuroscience*, vol. 16, no. 6, pp. 345–357, 2015.

[76] J. M. Bravo-San Pedro, G. Kroemer, and L. Galluzzi, "Autophagy and mitophagy in cardiovascular disease," *Circulation Research*, vol. 120, no. 11, pp. 1812–1824, 2017.

[77] D. C. Rubinsztein, P. Codogno, and B. Levine, "Autophagy modulation as a potential therapeutic target for diverse diseases," *Nature Reviews Drug Discovery*, vol. 11, no. 9, pp. 709–730, 2012.

[78] P. Chen, M. Cescon, and P. Bonaldo, "Autophagy-mediated regulation of macrophages and its applications for cancer," *Autophagy*, vol. 10, no. 2, pp. 192–200, 2014.

[79] S. Ceccariglia, A. Cargnoni, A. R. Silini, and O. Parolini, "Autophagy: a potential key contributor to the therapeutic action of mesenchymal stem cells," *Autophagy*, vol. 16, no. 1, pp. 28–37, 2020.

[80] S. Cen, P. Wang, Z. Xie et al., "Autophagy enhances mesenchymal stem cell-mediated CD4(+) T cell migration and differentiation through CXCL8 and TGF-β1," *Stem Cell Research & Therapy*, vol. 10, no. 1, p. 265, 2019.

[81] M. Gao, P. Monian, Q. Pan, W. Zhang, J. Xiang, and X. Jiang, "Ferroptosis is an autophagic cell death process," *Cell Research*, vol. 26, no. 9, pp. 1021–1032, 2016.

[82] L. S. Cheng, Y. Liu, and W. Jiang, "Restoring homeostasis of CD4(+) T cells in hepatitis-B-virus-related liver fibrosis," *World Journal of Gastroenterology*, vol. 21, no. 38, pp. 10721–10731, 2015.

[83] B. Binder and R. Thimme, "CD4+ T cell responses in human viral infection: lessons from hepatitis C," *The Journal of Clinical Investigation*, vol. 130, no. 2, pp. 595–597, 2020.

[84] H. Y. Wang, C. Li, W. H. Liu et al., "Autophagy inhibition via Becn1 downregulation improves the mesenchymal stem cells antifibrotic potential in experimental liver fibrosis," *Journal of Cellular Physiology*, vol. 235, no. 3, pp. 2722–2737, 2020.

[85] Q. Zhou, Y. Shi, C. Chen, F. Wu, and Z. Chen, "A narrative review of the roles of indoleamine 2,3-dioxygenase and tryptophan-2,3-dioxygenase in liver diseases," *Annals of Translational Medicine*, vol. 9, no. 2, p. 174, 2021.

[86] S. J. Dixon, K. M. Lemberg, M. R. Lamprecht et al., "Ferroptosis: an iron-dependent form of nonapoptotic cell death," *Cell*, vol. 149, no. 5, pp. 1060–1072, 2012.

[87] D. Tang, R. Kang, T. V. Berghe, P. Vandenabeele, and G. Kroemer, "The molecular machinery of regulated cell death," *Cell Research*, vol. 29, no. 5, pp. 347–364, 2019.

[88] Y. Xie, W. Hou, X. Song et al., "Ferroptosis: process and function," *Cell Death and Differentiation*, vol. 23, no. 3, pp. 369–379, 2016.

[89] J. Li, F. Cao, H. L. Yin et al., "Ferroptosis: past, present and future," *Cell Death & Disease*, vol. 11, no. 2, p. 88, 2020.

[90] W. S. Yang and B. R. Stockwell, "Synthetic lethal screening identifies compounds activating iron-dependent, nonapoptotic cell death in oncogenic-RAS-harboring cancer cells," *Chemistry & Biology*, vol. 15, no. 3, pp. 234–245, 2008.

[91] N. Yagoda, M. von Rechenberg, E. Zaganjor et al., "RAS-RAF-MEK-dependent oxidative cell death involving voltage-dependent anion channels," *Nature*, vol. 447, no. 7146, pp. 865–869, 2007.

[92] H. J. Garringer, J. M. Irimia, W. Li et al., "Effect of systemic iron overload and a chelation therapy in a mouse model of the neurodegenerative disease hereditary ferritinopathy," *PLoS One*, vol. 11, no. 8, article e0161341, 2016.

[93] G. Morris, M. Berk, A. F. Carvalho, M. Maes, A. J. Walker, and B. K. Puri, "Why should neuroscientists worry about iron? The emerging role of ferroptosis in the pathophysiology of neuroprogressive diseases," *Behavioural brain research*, vol. 341, pp. 154–175, 2018.

[94] T. Basu, S. Panja, A. K. Shendge, A. Das, and N. Mandal, "A natural antioxidant, tannic acid mitigates iron-overload induced hepatotoxicity in Swiss albino mice through ROS regulation," *Environmental Toxicology*, vol. 33, no. 5, pp. 603–618, 2018.

[95] K. Honarmand Ebrahimi, P. L. Hagedoorn, and W. R. Hagen, "Unity in the biochemistry of the iron-storage proteins ferritin and bacterioferritin," *Chemical Reviews*, vol. 115, no. 1, pp. 295–326, 2015.

[96] T. T. Mai, A. Hamai, A. Hienzsch et al., "Salinomycin kills cancer stem cells by sequestering iron in lysosomes," *Nature Chemistry*, vol. 9, no. 10, pp. 1025–1033, 2017.

[97] J. Liu, Z. Ren, L. Yang et al., "The NSUN5-FTH1/FTL pathway mediates ferroptosis in bone marrow-derived mesenchymal stem cells," *Cell Death Discovery*, vol. 8, no. 1, p. 99, 2022.

[98] K. R. Bridle, D. H. Crawford, and G. A. Ramm, "Identification and characterization of the hepatic stellate cell transferrin receptor," *The American Journal of Pathology*, vol. 162, no. 5, pp. 1661–1667, 2003.

[99] G. A. Ramm, R. S. Britton, R. O'Neill, and B. R. Bacon, "Identification and characterization of a receptor for tissue ferritin on activated rat lipocytes," *The Journal of Clinical Investigation*, vol. 94, no. 1, pp. 9–15, 1994.

[100] M. Burns, S. Muthupalani, Z. Ge et al., "Helicobacter pylori infection induces anemia, depletes serum iron storage, and alters local iron-related and adult brain gene expression in male INS-GAS mice," *PLoS One*, vol. 10, no. 11, article e0142630, 2015.

[101] Q. Pu, C. Gan, R. Li et al., "Atg7 deficiency intensifies inflammasome activation and pyroptosis in pseudomonas sepsis," *Journal of Immunology*, vol. 198, no. 8, pp. 3205–3213, 2017.

[102] A. Pfalzgraff, L. Heinbockel, Q. Su, K. Brandenburg, and G. Weindl, "Synthetic anti-endotoxin peptides inhibit cytoplasmic LPS-mediated responses," *Biochemical Pharmacology*, vol. 140, pp. 64–72, 2017.

[103] R. A. Aglietti and E. C. Dueber, "Recent insights into the molecular mechanisms underlying pyroptosis and gasdermin family functions," *Trends in Immunology*, vol. 38, no. 4, pp. 261–271, 2017.

[104] S. M. Man, R. Karki, and T. D. Kanneganti, "Molecular mechanisms and functions of pyroptosis, inflammatory caspases and inflammasomes in infectious diseases," *Immunological Reviews*, vol. 277, no. 1, pp. 61–75, 2017.

[105] E. A. Miao, I. A. Leaf, P. M. Treuting et al., "Caspase-1-induced pyroptosis is an innate immune effector mechanism against intracellular bacteria," *Nature Immunology*, vol. 11, no. 12, pp. 1136–1142, 2010.

[106] Z. Qiu, Y. He, H. Ming, S. Lei, Y. Leng, and Z. Y. Xia, "Lipopolysaccharide (LPS) aggravates high glucose- and hypoxia/reoxygenation- induced injury through activating ROS-dependent NLRP3 inflammasome-mediated pyroptosis in H9C2 cardiomyocytes," *Journal Diabetes Research*, vol. 2019, article 8151836, pp. 1–12, 2019.

[107] L. Zhang, S. Li, J. Li, and Y. Li, "LncRNA ORLNC1 promotes bone marrow mesenchyml stem cell pyroptosis induced by advanced glycation end production by targeting miR-200b-3p/Foxo3 pathway," *Stem Cell Reviews and Reports*, vol. 17, no. 6, pp. 2262–2275, 2021.

[108] M. Ye, S. Wang, P. Sun, and J. Qie, "Integrated microRNA expression profile reveals dysregulated miR-20a-5p and miR-200a-3p in liver fibrosis," *BioMed Research International*, vol. 2021, Article ID 9583932, 10 pages, 2021.

Research Article

FAIM Enhances the Efficacy of Mesenchymal Stem Cell Transplantation by Inhibiting JNK-Induced c-FLIP Ubiquitination and Degradation

Jinyong Chen [1,2] **Feng Liu,**[1,2] **Wangxing Hu,**[1,2] **Yi Qian,**[1,2] **Dilin Xu,**[1,2] **Chenyang Gao,**[2,3] **Zhiru Zeng,**[2,4] **Si Cheng,**[1,2] **Lan Xie,**[1,2] **Kaixiang Yu,**[1,2] **Gangjie Zhu,**[1,2] **and Xianbao Liu** [1,2]

[1]*Department of Cardiology, The Second Affiliated Hospital, Zhejiang University School of Medicine, Hangzhou 310009, China*
[2]*Cardiovascular Key Laboratory of Zhejiang Province, Hangzhou 310009, China*
[3]*Department of General Intensive Care Unit, The Second Affiliated Hospital, Zhejiang University School of Medicine, Hangzhou 310009, China*
[4]*Department of Rheumatology, The Second Affiliated Hospital, Zhejiang University School of Medicine, Hangzhou 310009, China*

Correspondence should be addressed to Xianbao Liu; liuxb@zju.edu.cn

Background. The poor survival rates of transplanted mesenchymal stem cells (MSCs) in harsh microenvironments impair the efficacy of MSCs transplantation in myocardial infarction (MI). Extrinsic apoptosis pathways play an important role in the apoptosis of transplanted MSCs, and Fas apoptosis inhibitory molecule (FAIM) is involved in regulation of the extrinsic apoptosis pathway. Thus, we aimed to explore whether FAIM augmentation protects MSCs against stress-induced apoptosis and thereby improves the therapeutic efficacy of MSCs. *Methods.* We ligated the left anterior descending coronary artery (LAD) in the mouse heart to generate an MI model and then injected FAIM-overexpressing MSCs (MSCs_{FAIM}) into the peri-infarction area in vivo. Moreover, FAIM-overexpressing MSCs were challenged with oxygen, serum, and glucose deprivation (OGD) in vitro, which mimicked the harsh microenvironment that occurs in cardiac infarction. *Results.* FAIM was markedly downregulated under OGD conditions, and FAIM overexpression protected MSCs against OGD-induced apoptosis. MSCs_{FAIM} transplantation improved cell retention, strengthened angiogenesis, and ameliorated heart function. The antiapoptotic effect of FAIM was mediated by cellular-FLICE inhibitory protein (c-FLIP), and FAIM augmentation improved the protein expression of c-FLIP by reducing ubiquitin–proteasome-dependent c-FLIP degradation. Furthermore, FAIM inhibited the activation of JNK, and treatment with the JNK inhibitor SP600125 abrogated the reduction in c-FLIP protein expression caused by FAIM silencing. *Conclusions.* Overall, these results indicated that FAIM curbed the JNK-mediated, ubiquitination–proteasome-dependent degradation of c-FLIP, thereby improving the survival of transplanted MSCs and enhancing their efficacy in MI. This study may provide a novel approach to strengthen the therapeutic effect of MSC-based therapy.

1. Introduction

Mesenchymal stem cells (MSCs) transplantation has been shown to be safe and beneficial in the treatment of myocardial infarction (MI) due to the low immunogenicity, multidirectional differentiation ability, and robust paracrine effects of these cells [1, 2]. Several studies have revealed that the main factor that impairs the therapeutic efficacy of MSCs transplantation is the poor survival rate of transplanted cells [3], which is caused by cell death induced by a harsh microenvironment and the limited self-renewal rates of MSCs [4]. A previous study reported that Fas-FasL interactions have a significant effect on death receptor (DR) activation in implanted MSCs, and that inhibiting this interaction by recombinant Fas/Fc protein treatment improves cell retention and restores cardiac function [5], suggesting that extrinsic apoptosis pathways play an important role in transplanted MSCs apoptosis and that intervening in these

pathways by genetic modification may be a new strategy to augment the longevity of transplanted MSCs.

Originally identified as an inhibitor of Fas signaling in B-cell receptor-activated lymphocytes [6], Fas apoptosis inhibitory molecule (FAIM) plays an essential role in apoptosis, metabolism, cell growth, and tumorigenesis [7]. Studies have revealed two splice variants of FAIM, and the short variant is ubiquitously expressed in multiple cell types [8–10]. Increasing evidence indicates that FAIM exerts an antiapoptotic effect on thymocytes and hepatocytes by suppressing T-cell receptor (TCR) signaling or DR signaling [11, 12]. FAIM has been implicated in the regulation of heat- and oxidative stress-induced cell death, and FAIM knockout cells exhibit impaired resistance to cell death induced by stress [13]. A recent study reported that FAIM facilitates cell proliferation by suppressing autophagy [14]. We therefore hypothesized that FAIM might be an excellent candidate to promote MSCs survival and optimize the abilities of MSCs in a hostile ischemic environment.

Cellular FLICE inhibitory protein, also known as c-FLIP, is a strong regulator of the extrinsic apoptosis pathway and competitively inhibits the binding of caspase-8 with FADD, thus avoiding the activation of caspase-8 [15, 16]. c-FLIP expression is markedly decreased in thymocytes and hepatocytes in the absence of FAIM [17]. To date, however, the underlying mechanisms linking FAIM to c-FLIP expression remain unclear, necessitating further exploration.

In this study, we discovered that FAIM overexpression promoted MSCs survival and enhanced their therapeutic effect in MI. The potential mechanisms involve reducing the ubiquitination and degradation of c-FLIP mediated by impairing JNK activation. Our results provide new insights and alternative treatment strategies for stem cell transplantation.

2. Materials and Methods

2.1. Cell Culture and Characterization. Mouse bone marrow-derived MSCs were purchased from Procell (Wuhan, China). Cells were cultured in low-glucose DMEM (#C11885500BT, Gibco, CA, USA) supplemented with 10% (v/v) fetal bovine serum (FBS) (#10270-106, Gibco) and 100 U/ml penicillin/streptomycin (PS) (#15140-122, Gibco) in a 5% CO_2 humidified atmosphere at 37°C.

MSCs were characterized by flow cytometry to analyze the expression of membrane markers with a mouse MSCs surface marker assay kit (#MUXMX-09011, Cyagen Biosciences, Suzhou, China). In brief, MSCs were digested with trypsin (Genom Bio., Hangzhou, China) and resuspended in Hank's balanced salt solution (HBSS) (Genom Bio.). Subsequently, the single-cell suspensions were incubated with cell surface marker antibodies at 4°C for 30 min (mesenchymal surface markers: Scr-1, CD29, CD44, and CD90; hematopoietic stem cell marker: CD117; endothelial cell marker: CD31; and isotype-matched control). After being washed with HBSS, the MSCs were incubated with fluorescence-conjugated secondary antibodies for another 30 min. Surface marker expression was analyzed with an LSRFortessa flow cytometer (BD, USA). The MSCs were positive for CD29,

CD44, CD90, and Sca-1 and negative for CD31 and CD117, and the MSCs were fusiform and arranged in a swirled pattern (Supplementary Figure S1(a)-1(b)).

2.2. Lentivirus Infection. Recombinant lentiviruses expressing mouse FAIM-S labeled with GFP and Flag (GFP-FAIM) or mouse c-FLIP labeled with GFP (GFP-FLIP) and empty lentivirus labeled with GFP (GFP-Vec) were provided by GeneChem (Shanghai, China). MSCs were transduced with lentiviruses (MOI = 50) overnight with HitransG A (Gene-Chem, Shanghai, China) after being seeded in flasks. Then, the virus-containing supernatants were replaced with fresh medium for further culture. The infection efficiency was determined by measuring the expression of the target gene and the fluorescence of GFP.

2.3. siRNA Transfection. Small interfering RNA (siRNA) oligonucleotides targeting mouse FAIM (si-FAIM) or mouse c-FLIP (si-FLIP) and scramble siRNA (si-Scr) were synthesized (Tsingke, Hangzhou, China) and transfected into MSCs with RNAiMAX reagent (#13778-150, Invitrogen, CA, USA). Twenty-four hours after transfection, the transfection efficiency was measured by Western blotting. The siRNA sequences are listed in Table 1.

2.4. Cell Apoptosis Model. To simulate the microenvironment of the ischemic myocardium, a glucose/serum-deprived/hypoxia-induced apoptosis model (OGD) and an H_2O_2-induced apoptosis model were established as previously described [18]. For the OGD model, forty-eight hours after lentivirus infection, $MSCs_{Vec}$ (MSCs infected with vector) or $MSCs_{FAIM}$ (MSCs infected with murine FAIM) were washed with PBS and cultured with glucose-free DMEM under hypoxic conditions (0.3% O_2) for an additional 12 h until they were harvested. An H_2O_2-induced apoptosis model was also used in this study. In brief, after transfection with lentivirus, MSCs were challenged with 1 mM H_2O_2 in glucose-free DMEM for 2 h until they were harvested.

2.5. TUNEL Assays. TUNEL assays were carried out using a TUNEL staining kit (#C1090, Beyotime, Shanghai, China). In brief, cells were fixed in 10% formalin and permeabilized with 0.5% Triton X-100, followed by incubation with TUNEL staining reagent at 37°C in the dark for 1 hour. Additionally, nuclei were stained with Hoechst 33258 (#H3569, Thermo Fisher, CA, USA). Fluorescence images were acquired, and the apoptotic rates were calculated as the percentages of TUNEL-positive cells.

2.6. Annexin V/Propidium Iodide (PI) Staining. Annexin V/PI staining was carried out using an Annexin V-APC/PI apoptosis kit (#70-AP107, Liankebio, Hangzhou, China). Briefly, the culture medium was collected, and cells were digested with trypsin. The two components were then mixed and centrifuged. Then, the supernatant was discarded, and 1× binding buffer was added to resuspend the MSCs. The single-cell suspensions were incubated with an Annexin V-APC and PI mixture for 15 min at room temperature and then quantified with an LSRFortessa flow cytometer. The

TABLE 1: siRNA sequences.

siRNA name		Sequence ($5' ->3'$)
si-FAIM	Sense	GGAUUAUCCAUACCCUCAUTT
	Antisense	AUGAGGGUAUGGAUAAUCCTT
si-c-FLIP	Sense	CAAGUAUGGCCCAACAUCATT
	Antisense	UGAUGUUGGGCCAUACUUGTT
si-scramble	Sense	UUCUCCGAACGUGUCACGUTT
	Antisense	ACGUGACACGUUCGGAGAATT

TABLE 2: qRT–PCR primer sequences.

Target gene	Primer name	Sequence ($5' ->3'$)
β-actin	Forward primer	GGTGGGAATGGGTCAGAAGG
	Reverse primer	GTACATGGCTGGGGTGTTGA
FAIM	Forward primer	ATGGGACCACATCAGGCAAG
	Reverse primer	TCCAGCGTGTACTCGTATGC
c-FLIP	Forward primer	ACACAGGCAGAGGCAAGATA
	Reverse primer	TGGCTCTTTACTTCGCCCATT

apoptosis rate was calculated as the sum of the percentages of Annexin V$^+$/PI$^-$ cells and Annexin V$^+$/PI$^+$ cells.

2.7. RNA Analysis. Total RNA was isolated using TRIzol reagent (#15596-018, Invitrogen) and reverse-transcribed into cDNA with PrimeScript RT Master Mix (#RR036A, TaKaRa, Beijing, China). For qRT–PCR, cDNA was amplified using TB Green Premix Ex Taq™ (#RR420A, TaKaRa) on a LightCycler 480 system (Roche, USA). The mRNA expression levels were determined using the $2^{-\Delta Ct}$ method, and the results were normalized to β-actin. The primer sequences used for qRT–PCR are listed in Table 2.

2.8. Western Blotting. Whole-cell lysate was isolated using RIPA buffer (#P0013B, Beyotime) supplemented with a 1× protease and phosphatase inhibitor cocktail mixture (#78442, Thermo Fisher), and the total protein concentration was quantified with a BCA assay kit (#FD200, Fude Biological, Hangzhou, China). Proteins were separated by SDS–PAGE and then transferred onto PVDF membranes. After blocking with 5% skim milk (#LP0031B, Thermo Fisher), the membranes were incubated overnight at 4°C with the specific primary antibodies listed in Table 3, followed by HRP-linked secondary antibody incubation. Finally, the proteins were detected by an Amersham ImageQuant 800 Western blot imaging system using ECL Western blotting substrate (#FD8020, Fude Biological). The images were quantified using ImageQuant TL 8.2 analysis software, and the protein expression levels were normalized to the housekeeping protein GAPDH or β-actin.

2.9. Mouse MI Model and MSCs Transplantation. Animal breeding, maintenance, and procedures were performed in accordance with the Guide for the Care and Use of Laboratory Animals published by the NIH and approved by the Animal Use Committee of Zhejiang University.

A mouse MI model was established in 10- to 12-week-old male C57BL/6 J mice (23-26 g, Hangzhou Medical College Animal Research Center, Hangzhou, China) by left anterior descending coronary artery (LAD) ligation. Then, MSCs$_{FAIM}$ or MSCs$_{Vec}$ ($1.5 \times 10^{\wedge}5$ cells in 20 μl of DMEM per mouse) were immediately transplanted into the border zone of the ischemic area by intramyocardial injection. Control mice were injected with an equivalent volume of DMEM.

2.10. Echocardiography. Transthoracic echocardiography was performed to evaluate cardiac function on days 0, 3, 7, 14, and 28 after MI surgery. Mice were anesthetized with 2% isoflurane in 95% O_2. Serial B-mode and M-mode images were obtained using a Vevo® 2100 ultrasound system (Visual Sonics, Canada), followed by cardiac function analysis using Vevo® LAB software (version 3.1.0).

2.11. Sirius Red Staining. Mice were euthanized by cervical dislocation after being injected with sodium pentobarbital. The hearts were harvested, fixed with 10% formalin, embedded in paraffin, and subsequently sectioned into 3 μm slices. The slices were stained with Sirius Red (#SBJ-0294, SenBeiJia Biological, Nanjing, China). The images were quantitatively analyzed using ImageJ software (NIH, USA). The infarct size was calculated as follows: infarct size = [(endocardial + epicardial circumference of the infarct area)/(endocardial + epicardial circumference)] × 100%.

2.12. Immunofluorescence Staining. OCT-embedded hearts were sectioned in a cryostat at a thickness of 7 μm. The slices were fixed with 10% formalin for 10 min, permeabilized with 0.5% Triton X-100 for 15 min, and blocked with 3% BSA (#B265993, Aladdin, Shanghai, China) for 30 min. Subsequently, overnight incubation was performed with the specific primary antibodies listed in Table 4, followed by incubation with Alexa Fluor-conjugated secondary antibody. Nuclei were stained with DAPI mounting medium (#H-1200-10, Vector, CA, USA).

2.13. Tube Formation Assays. Tube formation assays were conducted to evaluate the angiogenic potential of MSCs in response to different treatments. Human umbilical vein endothelial cells (HUVECs) were digested, counted, and resuspended in different conditioned media. Then, single-cell suspensions of the HUVECs were seeded into 96-well plates (1.2×10^4 cells per well) coated with 50 μl of solidified Matrigel (#354230, Corning, MA, USA) and cultured for 6 h under standard conditions. Images were captured with Leica DM IL LED microscopes, and the branch points and capillary lengths were quantified with ImageJ software using the angiogenesis analyzer plugin.

2.14. Cycloheximide (CHX) Chase Assay. To evaluate protein stability, MSCs were treated with 10 μg/ml CHX (#S7418, Selleck) to arrest c-FLIP protein biosynthesis under hypoxic conditions for 0 h, 3 h, and 6 h. After the MSCs were harvested, c-FLIP protein expression was assessed by Western blotting.

TABLE 3: Antibodies used for immunoblotting.

Antibody	Species	Dilution	Catalog no.	Company
Anti-β-actin	Mouse	1/5000	#KC-5A08	KangCheng biotech
Anti-GAPDH	Mouse	1/5000	#KC-5G5	KangCheng biotech
Anti-FAIM	Rabbit	1/1000	#PA5-29200	Thermo fisher
Anti-cleaved caspase-3	Rabbit	1/1000	#9661	CST
Anti-cleaved caspase-8	Rabbit	1/1000	#8592	CST
Anti-cleaved caspase-9	Rabbit	1/1000	#9509	CST
Anti-FLIP (D5J1E)	Rabbit	1/1000	#56343	CST
Anti-SAPK/JNK	Rabbit	1/1000	#9252	CST
Anti-phospho-SAPK/JNK	Rabbit	1/1000	#4668	CST
HRP-linked anti-ubiquitin	Mouse	1/1000	#14049	CST
HRP-linked anti-mouse	Horse	1/3000	#7076	CST
HRP-linked anti-rabbit	Goat	1/3000	#7074	CST
HRP-linked anti-rabbit (light-chain specific)	Mouse	1/3000	#93702	CST

TABLE 4: Antibodies used for immunofluorescence.

Antibody	Species	Dilution	Catalog no.	Company
Anti-GFP	Rabbit	1/200	#ab290	Abcam
Anti-CD31	Rat	1/300	#550274	BD
Anti-α-SMA	Rabbit	1/200	#19245	CST
Anti-cTnI	Goat	1/300	#ab56357	Abcam
Anti-Rabbit-488	Donkey	1/300	#ab150073	Abcam
Anti-Goat-555	Donkey	1/300	#ab150134	Abcam
Anti-Rat-488	Donkey	1/300	#ab150153	Abcam

2.15. Protein Degradation and Ubiquitination Assays. To examine protein degradation, MG132 (10 μM, #HY-13259, MCE, Shanghai, China) and chloroquine (CQ, 50 nM, #HY-17589A, MCE) were used to inhibit the ubiquitin–proteasome and autophagy pathways, respectively. Cells were incubated with MG132 or CQ for the indicated times before being harvested, and c-FLIP protein expression was assessed by Western blotting.

For the ubiquitination assay, MSCs were treated with 10 μM MG132 under hypoxic conditions for 6 h before being harvested for immunoprecipitation. The lysates were incubated with anti-FLIP antibodies (#56343, CST, MA, USA) or normal rabbit IgG (#2729, CST), bound to magnetic protein A beads (Bio-Rad), washed thoroughly, and eluted by boiling in 2× loading buffer, followed by Western blotting to examine the level of ubiquitin bound to the c-FLIP protein.

2.16. Immunoprecipitation. Immunoprecipitation was performed as previously described [19]. Briefly, MSCs were lysed with NP-40 cell lysis buffer (#P0013F, Beyotime) supplemented with a 1× protease phosphatase inhibitor cocktail mixture, 10 mM N-ethylmaleimide (NEM) (# HY-D0843, MCE), and 1 mM EDTA. In total, 10% of the lysates was kept as input, and the remaining samples were used for immunoprecipitation. Rabbit monoclonal anti-FLIP antibodies (1 : 100, #56343, CST) or normal rabbit IgG was incu-

bated with magnetic protein A beads (#1614013, Bio-Rad) for 1 h at room temperature. The supernatant was discarded, and the bead–antibody complexes were washed with lysis buffer 3 times. Then, the bead–antibody complexes were incubated overnight at 4°C with the cell lysates mentioned above. The bead–antibody–protein immunocomplexes were washed 3 times with lysis buffer and then boiled in loading buffer with SDS at 98°C for 5 min to elute the proteins from the beads. Immunoblotting was performed to analyze the ubiquitin levels.

2.17. Statistical Analysis. Representative experiments were repeated at least three times, and the results are depicted as the mean ± standard deviation (SD). Statistical differences between two sets of data were analyzed by Student's t test, and multiple groups were compared using one-way ANOVA with Tukey's posttest. All statistical analyses and graphing were performed with GraphPad Prism 8 software. Differences for which $P < 0.05$ were considered statistically significant.

3. Results

3.1. FAIM Promoted the Survival of MSCs In Vitro and In Vivo. FAIM expression was found to be upregulated in SRT1720-pretreated MSCs, and FAIM knockdown abolished the protective effects of SRT1720 on MSCs in our previous study [20]. Thus, we speculated that FAIM may have an important effect on the apoptosis of transplanted MSCs. To explore this hypothesis, two cell apoptosis models were used in vitro to mimic ischemia or ROS generation in the MI microenvironment: the OGD model and the H_2O_2 model (Supplementary Figure S2). As shown in Figures 1(a) and 1(b), the mRNA and protein levels of FAIM were robustly decreased in the OGD model. The same reduction in FAIM protein expression was observed in response to H_2O_2 exposure (Supplementary Figure S3(a)). Thus, a FAIM overexpression experiment was carried out to determine the antiapoptotic effect of FAIM in the OGD model (Supplementary Figure S4(a)-4(b)), and the cell apoptosis rate was evaluated
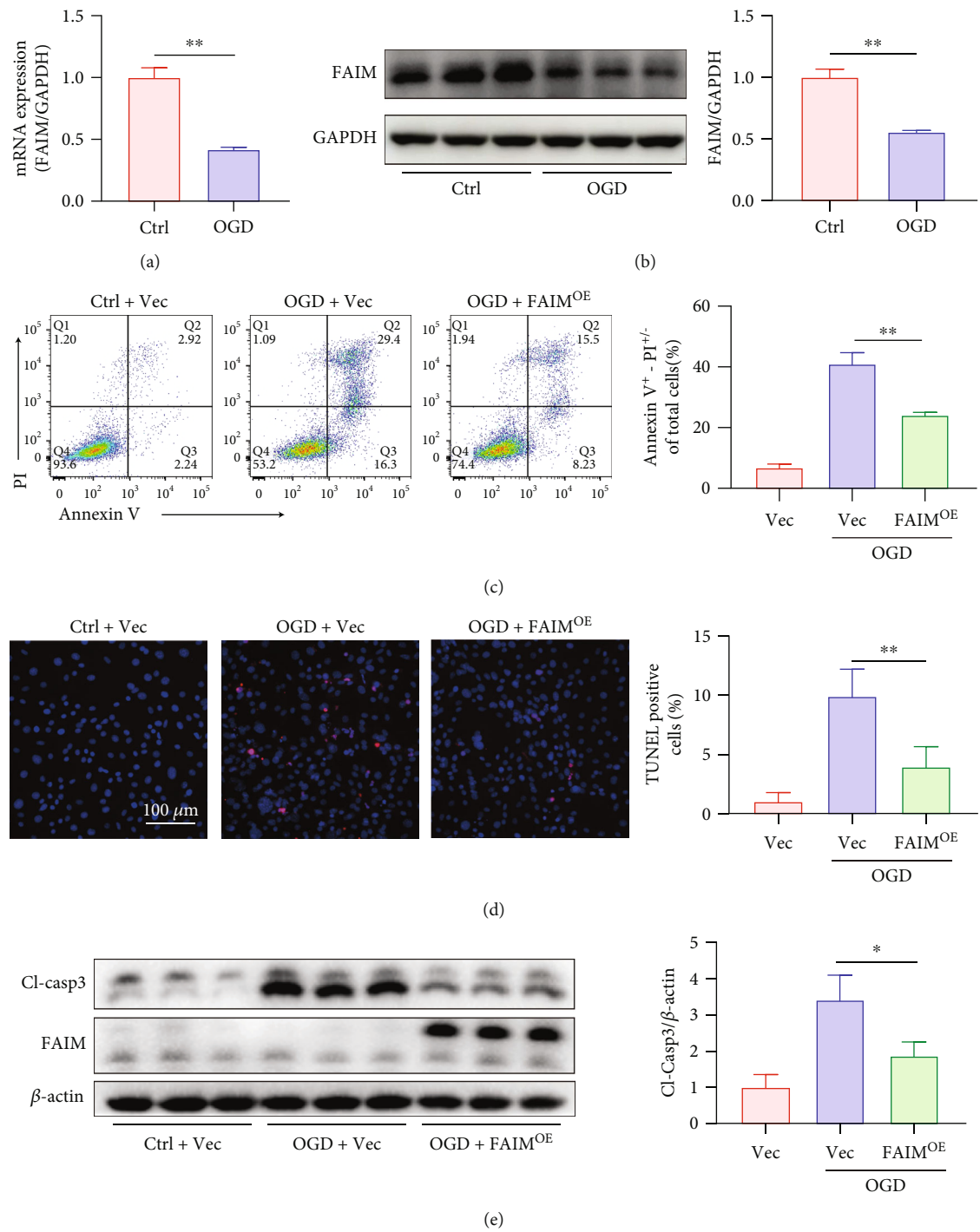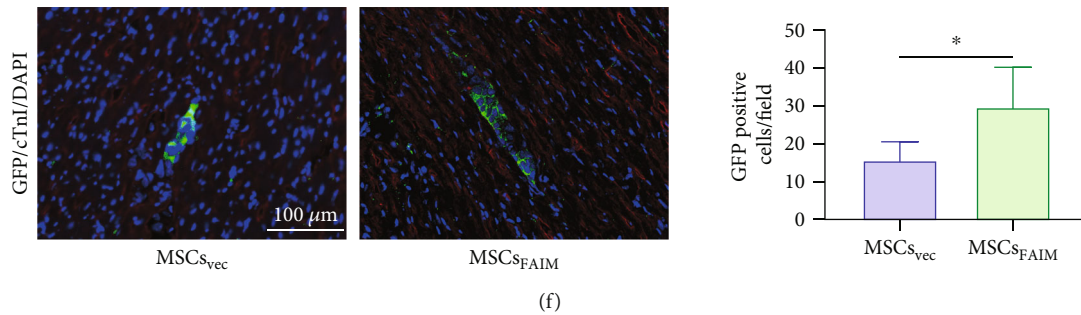
(a)

(b)

(c)

(d)

(e)

Figure 1: Continued.

(f)

FIGURE 1: FAIM protected MSCs against apoptosis in vitro and in vivo. (a) MSCs were cultured for 12 h under OGD conditions or normoxic conditions, and the mRNA level of FAIM was determined by qPCR and normalized to GAPDH. (b) Immunoblot analysis and densitometric quantification of FAIM protein levels under OGD conditions or normoxic conditions. GAPDH served as a loading control. (c) Annexin V-APC/PI staining was performed, and flow cytometry was used to determine the apoptosis rate. The apoptosis rate was calculated as the sum of the percentages of Annexin V$^+$/PI$^-$ cells and Annexin V$^+$/PI$^+$ cells. (d) TUNEL staining after FAIM overexpression followed by OGD stimulation for 12 h (scale bar = 100 μm). Quantitative results are shown on the right. Six visual fields were randomly chosen for each well; the apoptotic index was determined as the percentage of TUNEL-positive nuclei. (e) Cleaved caspase 3 protein expression after FAIM overexpression or vector infection followed by OGD stimulation. The results of densitometric quantitation are shown on the right. (f) Representative images showing GFP immunofluorescence (IF) staining 3 days after LAD ligation followed by MSC transplantation. GFP appears in green, cardiac troponin I (cTnI) in red, and nuclei in blue. (scale bar = 100 μm). Quantitative results are shown on the right ($n = 6$ for the MSCs$_{Vec}$ group and MSCs$_{FAIM}$ group). Data are shown as the mean ± SD. * denotes $P < 0.05$, **$P < 0.01$.

by an Annexin V-APC/PI assay. The FAIM^{OE} group showed a robust decrease in the percentage of apoptotic cells (Annexin V-positive) under OGD conditions compared with that of the vector group (Figure 1(c)), and this result was further supported by TUNEL staining (Figure 1(d)). Furthermore, the protein expression of cleaved caspase-3, the critical executioner of apoptosis, was examined by Western blotting. We found that FAIM overexpression significantly attenuated the activation of caspase-3 (Figure 1(e)). To explore the antiapoptotic effect of FAIM on MSCs in vivo, MSCs were marked with GFP and injected into the peri-infarct region immediately after LAD ligation. The MSCs retention rate was assessed by fluorescence microscopy 3 days after engraftment (Supplementary Figure S2). The immunofluorescence results showed that while no significant differences were observed between the two groups of cells (Supplementary Figure S4(a)), more FAIM-overexpressing MSCs (MSCs$_{FAIM}$) than MSCs infected with vector (MSCs$_{Vec}$) remained in the target tissue (Figure 1(f)). These results strongly suggested that FAIM inhibited caspase-3-dependent apoptosis under hypoxic conditions in vitro and in vivo.

3.2. FAIM-Overexpressing MSCs Improved Cardiac Function and Reduced Infarct Size.

To evaluate the effect of FAIM overexpression on the improvement in the therapeutic effect of MSCs, MSCs$_{Vec}$ and MSCs$_{FAIM}$ were transplanted into the peri-ischemic area immediately after MI model construction, and an equivalent volume of DMEM was injected into the ischemic hearts in the control group. Transthoracic echocardiography was conducted on days 3, 7, 14, and 28 after cell transplantation to evaluate cardiac function, and Sirius Red staining was conducted 28 days after MI to examine the fibrotic area (Supplementary Figure S2). The echocardiography data revealed that compared with the DMEM and MSCs$_{Vec}$ groups, cardiac function after MI was significantly improved in the MSCs$_{FAIM}$ group ($n = 6$ for the sham group, $n = 7$ for the DMEM and MSCs$_{Vec}$ groups, and

$n = 8$ for the MSCs$_{FAIM}$ group) (Figures 2(a)–2(c)). Histological analysis also confirmed these results, and a considerable reduction in infarct scarring was observed in the MSCs$_{FAIM}$ group on day 28 after cell transplantation by Sirius Red staining (Figures 2(d)–2(e)).

Accumulating evidence indicates that the effects of MSCs are principally attributed to their abundant paracrine functions, which result in angiogenesis [21]. Thus, we hypothesized that the increased retention of MSCs$_{FAIM}$ would increase angiogenesis. To validate this hypothesis, the capillary density and microvasculature in the peri-infarct area were measured. Compared with those in the DMEM group and MSCs$_{Vec}$ group, increased numbers of endothelial cells (CD31-positive) and vascular smooth muscle cells (α-SMA-positive) was observed in the MSCs$_{FAIM}$ group 28 days after MSCs engraftment (Figures 2(f)–2(i)). Furthermore, an in vitro tube formation assay was conducted to evaluate the proangiogenic capacity of conditioned medium from MSCs. The supernatants of MSCs$_{Vec}$ and MSCs$_{FAIM}$ cultured under normoxic conditions and hypoxic conditions were used to culture HUVECs. No clear differences were observed between the MSCs$_{FAIM}$ group and the MSCs$_{Vec}$ group under normoxic conditions; however, culture with the supernatants of hypoxia-treated MSCs$_{Vec}$ led to a significant decrease in angiogenesis, and FAIM overexpression rescued this reduction (Supplementary Figure S6). Taken together, these results suggested that MSCs$_{FAIM}$ more effectively promoted angiogenesis, improved cardiac function, and limited the fibrotic area than did the MSCs$_{Vec}$.

3.3. FAIM Regulates the Expression of c-FLIP in MSCs under OGD Conditions.

The extrinsic apoptosis pathway, which is mediated by DRs, and the intrinsic apoptosis pathway, which is mediated by mitochondria, are the two main pathways through which apoptosis is induced. Caspase-8 and caspase-9 are the initiating caspases in these two pathways [22]. Several studies have demonstrated that FAIM strongly
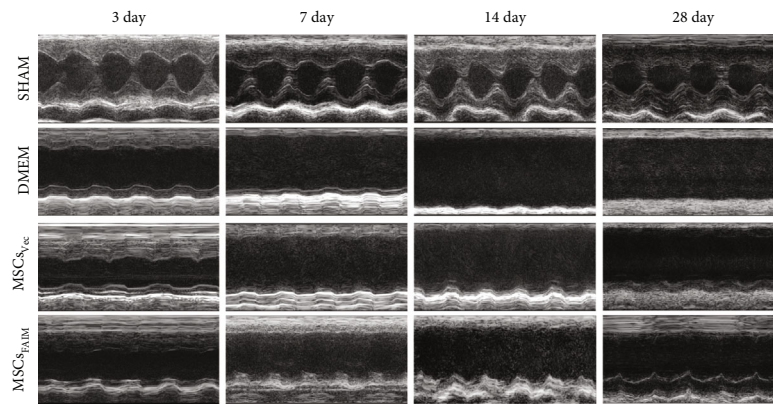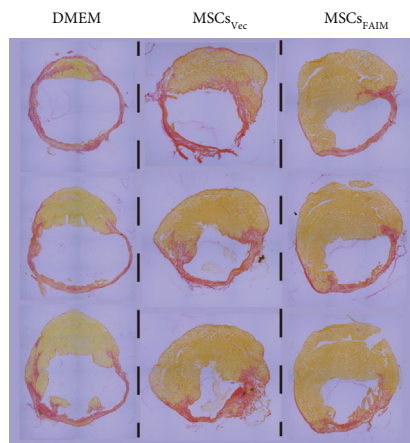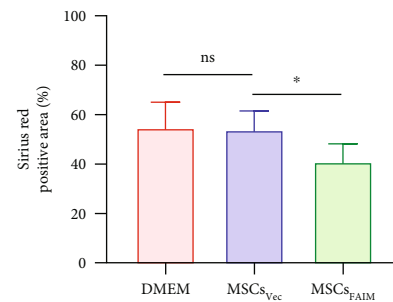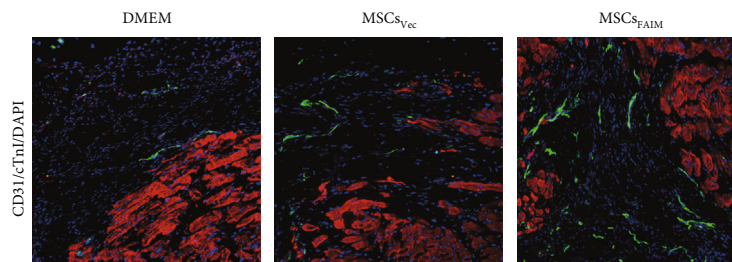
(a)
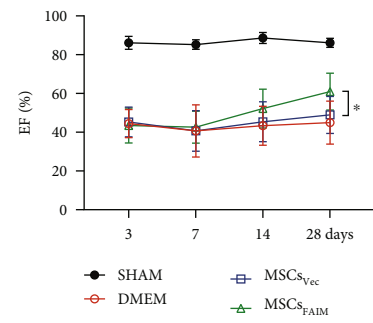
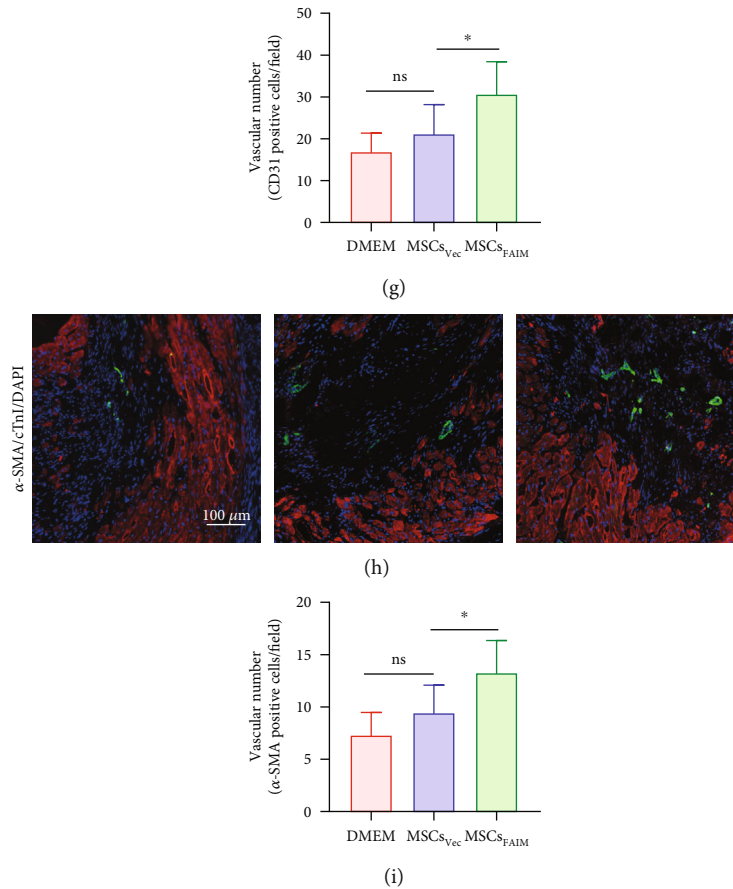

(b)
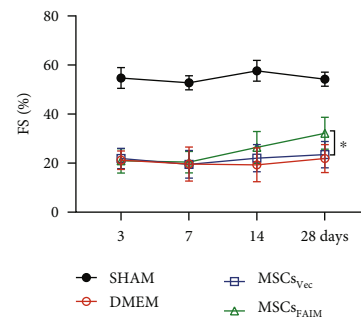
(c)

(d)

(e)

(f)

Figure 2: Continued.

(g)

(h)

(i)

Figure 2: MSCs$_{FAIM}$ improved cardiac function and reduced infarction size. (a) Representative echocardiographic images of the left ventricle in M-mode on days 3, 7, 14, and 28 after LAD ligation followed by MSCs engraftment. (b) Ejection fraction (EF) and (c) fractional shortening (FS) were quantified ($n = 6$ for the sham group, $n = 7$ for the DMEM and MSCs$_{Vec}$ groups, and $n = 8$ for the MSCs$_{FAIM}$ group). (d) Representative Sirius Red staining of ischemic hearts 28 days after MI. (e) Scar size was calculated as the sum of the ratio of the endocardial plus epicardial scar length relative to the total circumference ($n = 7$ for the DMEM and MSCs$_{Vec}$ groups and $n = 8$ for the MSCs$_{FAIM}$ group). (f–g) Representative images showing CD31 immunofluorescence staining in the peri-ischemic area 28 days after MI. CD31 appears in green, cardiac troponin I (cTnI) in red, and nuclei in blue (scale bar = 100 μm). Quantitative results are shown on the right ($n = 7$ for the DMEM and MSCs$_{Vec}$ groups and $n = 8$ for the MSCs$_{FAIM}$ group). (h–i) Representative images showing α-SMA IF staining. α-SMA appears in green; scale bar = 100 μm. Quantitative results are shown on the right ($n = 7$ for the DMEM and MSCs$_{Vec}$ groups and $n = 8$ for the MSCs$_{FAIM}$ group). Vessels in the peri-ischemic area were counted in 5 randomly chosen fields. The data are shown as the mean ± SD. Ns indicates not significant; * denotes $P < 0.05$.

inhibits DR signaling and Fas-mediated apoptosis [12]; however, the specific role of FAIM in hypoxia-induced apoptosis is poorly understood. Thus, the protein expression of cleaved caspase-8 and cleaved caspase-9 was determined. As expected, FAIM overexpression reduced the cleavage of caspase-8 but had no significant effect on caspase-9 activation (Figures 3(a) and 3(b)). c-FLIP regulates the activation of caspase-8, and FAIM-deficient hepatocytes exhibit decreased c-FLIP protein expression [17]. Therefore, to test whether c-FLIP is involved in hypoxia-induced apoptosis, and whether FAIM can regulate c-FLIP expression, the protein expression level of c-FLIP was examined after the knockdown or overexpression of FAIM and culture under hypoxic conditions by Western blotting. c-FLIP protein expression was notably decreased in the context of hypoxia, and FAIM overexpression blocked this reduction (Figures 3(c) and 3(d)). Not surprisingly, c-FLIP expression notably declined after FAIM knockdown (Figures 3(e) and 3(f)).

3.4. c-FLIP Is Required for the Antiapoptotic Effect of FAIM under OGD Conditions.

The relationship between c-FLIP and FAIM was further confirmed. MSCs overexpressing c-FLIP (MSCs$_{FLIP}$) were generated by lentivirus infection, whereas MSCs infected with empty lentivirus labeled with GFP (GFP-Vec) served as the negative control (MSCs$_{Vec}$). The efficiency of c-FLIP overexpression was detected by Western blotting (Supplementary Figure S4(d)). FAIM was silenced by siRNA in both MSCs$_{Vec}$ and MSCs$_{FLIP}$, which was followed by OGD exposure. Upon FAIM silencing, c-FLIP overexpression reduced the percentage of apoptotic MSCs, as shown by Annexin V/PI staining and TUNEL assays (Figures 4(a)–4(d)). Western blotting further confirmed that the protein levels of cleaved caspase-3 were significantly decreased by c-FLIP overexpression (Figures 4(e) and 4(f)). Furthermore, MSCs$_{FAIM}$ were transfected with either siRNA specific for c-FLIP (si-FLIP) or scrambled siRNA (si-Scr), followed by OGD challenge. Under OGD conditions, c-FLIP
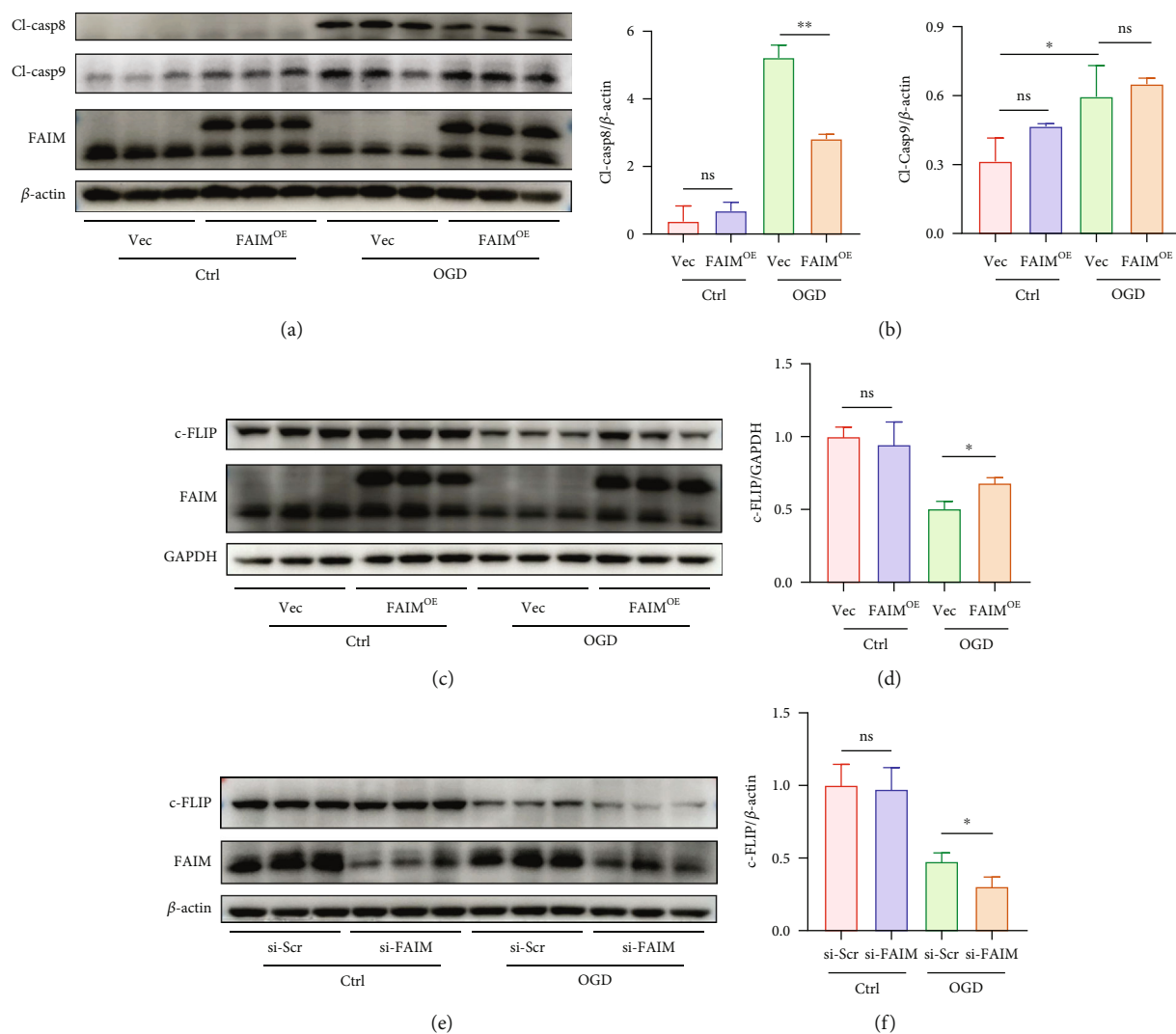
(a)

(b)

(c)

(d)

(e)

(f)

FIGURE 3: FAIM regulated the expression of c-FLIP in MSCs under OGD conditions. (a–b) Immunoblots and densitometric quantitation of cleaved caspase-8 and cleaved caspase-9 protein levels in MSCs$_{Vec}$ and MSCs$_{FAIM}$ under OGD conditions. (c–d) Immunoblots and densitometric quantitation of c-FLIP protein levels in MSCs$_{Vec}$ and MSCs$_{FAIM}$ under OGD conditions. (e–f) c-FLIP protein levels after siRNA-mediated knockdown of FAIM or scrambled siRNA administration followed by OGD stimulation for 12 h. The results of densitometric quantification are shown on the right. The data are shown as the mean ± SD. Ns indicates not significant; * denotes $P <$ 0.05, $^{**}P < 0.01$.

silencing significantly elevated the percentage of Annexin V-positive MSCs$_{FAIM}$ (Figures 4(g) and 4(h)) and the protein expression of cleaved caspase-3 (Figures 4(k) and 4(l)), and the results were also confirmed by TUNEL staining (Figures 4(i) and 4(j)). These results indicated that the antiapoptotic effect of FAIM under OGD conditions was at least partially dependent on c-FLIP.

3.5. FAIM Stabilizes c-FLIP Protein in MSCs by Inhibiting Its Ubiquitination.
To determine the underlying mechanisms, we examined the mRNA level of c-FLIP and found that FAIM overexpression did not alter the transcript expression of c-FLIP (Figure 5(a)). To reveal whether FAIM posttranscriptionally regulates the expression of c-FLIP, a CHX chase assay was performed to test the change in protein stability of c-FLIP in response to FAIM knockdown and overexpression. We found that FAIM overexpression

significantly inhibited the decrease in c-FLIP protein expression (Figure 5(b)), but FAIM knockdown facilitated a reduction in c-FLIP expression in MSCs (Figure 5(c)). These data suggested that the degradation of c-FLIP could be impaired by FAIM.

Autophagy and proteasome-dependent proteolysis are the two main ways by which protein degradation is regulated. Consequently, hypoxia-challenged MSCs were treated with CQ to inhibit the autophagy–lysosome pathway and MG132 to impede the proteasome-dependent pathway. In comparison with that in response to DMSO, the expression of c-FLIP was strongly restored by MG132 but barely affected by CQ (Figure 5(d)). Collectively, these data showed that FAIM upregulates c-FLIP protein expression largely by inhibiting its proteasome-dependent degradation. To further investigate the ubiquitination of c-FLIP, we treated OGD-challenged MSCs with MG132 to arrest the degradation of
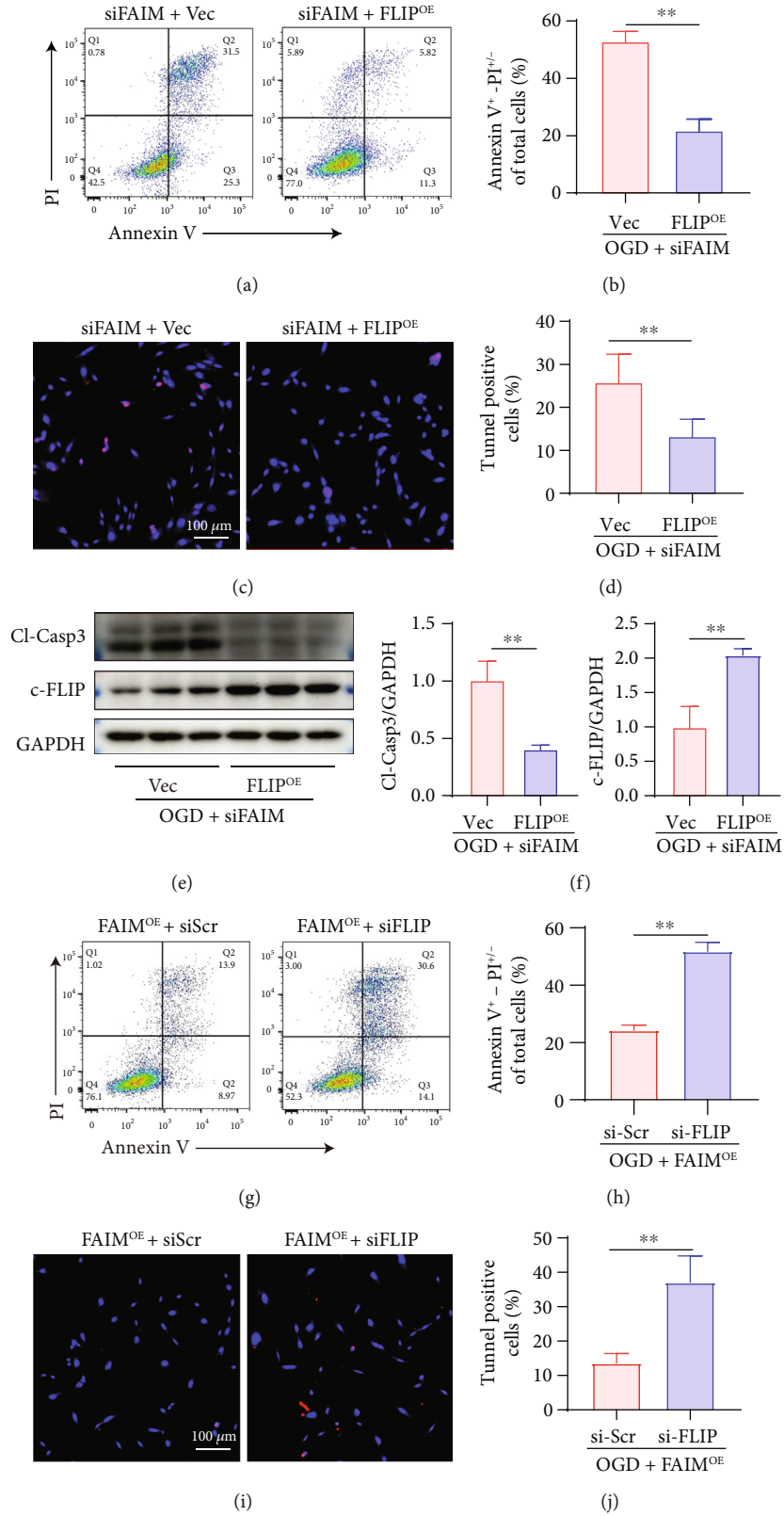
(a)

(b)

(c)

(d)

(e)

(f)

(g)

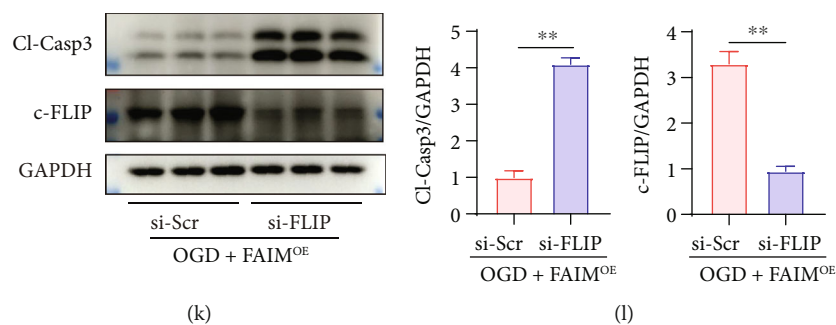(h)

(i)

(j)

FIGURE 4: Continued.

(k)

(l)

Figure 4: c-FLIP is required for the antiapoptotic effect of FAIM. $MSCs_{Vec}$ and $MSCs_{FLIP}$ were transfected with si-FAIM and exposed to OGD. (a–b) Annexin V-APC/PI staining was performed, and flow cytometry was used to determine the apoptosis rate. (c–d) TUNEL staining of $MSCs_{Vec}$ and $MSCs_{FLIP}$ after FAIM knockdown followed by OGD treatment for 12 h. (e–f) Cleaved caspase 3 protein expression was detected by Western blotting. (g–h) Annexin V-APC/PI staining of $MSCs_{FAIM}$ transfected with si-FLIP or si-Scr under OGD conditions. (i–j) TUNEL staining of $MSCs_{FAIM}$ after FLIP knockdown or control treatment followed by OGD treatment for 12 h. (k–l) Cleaved caspase 3 protein expression was measured by Western blotting. The data are shown as the mean ± SD. Ns indicates not significant; ** denotes $P < 0.01$.

c-FLIP without affecting its ubiquitination 6 h before harvesting for analysis. We found that c-FLIP was ubiquitinated under hypoxic conditions, and FAIM overexpression markedly decreased the ubiquitination level of c-FLIP (Figure 5(e)). This result complements our previous finding showing that FAIM modulates c-FLIP expression by inhibiting its ubiquitination–proteasome-dependent proteolysis.

3.6. FAIM Reduces c-FLIP Degradation by Blocking JNK Activation. Phosphorylated JNK has been reported to be upregulated during apoptosis [23] and has also been reported to participate in the degradation of c-FLIP [24]. We hypothesized that the JNK pathway is involved in hypoxia-induced apoptosis, and that FAIM attenuates the degradation of c-FLIP by inhibiting the phosphorylation of JNK. To validate this hypothesis, phosphorylated JNK was assessed by Western blotting. As expected, we found that JNK phosphorylation was strongly inhibited by FAIM in hypoxic MSCs (Figures 6(a) and 6(b)), and FAIM silencing increased this phosphorylation (Figures 6(c) and 6(d)). We further treated FAIM-deficient MSCs with SP600125, a specific JNK inhibitor, and verify its impact on c-FLIP protein expression. We found that SP600125 upregulated c-FLIP protein expression (Figures 6(e) and 6(f)), verifying that FAIM inhibits c-FLIP degradation mainly by blocking JNK activation.

Taken together, our results provide evidence that FAIM inhibits MSC apoptosis by inhibiting the ubiquitination-dependent degradation of c-FLIP, which is mediated by JNK inactivation, thereby improving the efficacy of MSC transplantation (Figure 7).

4. Discussion

In this study, we showed that FAIM was downregulated in MSCs under ischemia-like conditions, including hypoxia and oxidative stress, in vitro. Consequently, we overexpressed FAIM in MSCs and found that FAIM augmentation protected MSCs from apoptosis in a harsh microenvironment. Similarly, we observed improved MSCs survival in a

mouse MI model. Furthermore, improvements in cardiac function and a reduced infarction size were detected in the $MSCs_{FAIM}$ group 28 days after transplantation, accompanied by increased angiogenesis, suggesting that FAIM augmentation improved the efficacy of MSCs transplantation in a mouse MI model. Mechanistically, our findings demonstrated that the antiapoptotic effect of FAIM is largely dependent on c-FLIP, which suppresses the activation of caspase-8. Next, we found that FAIM had no effect on c-FLIP transcription but altered the protein degradation of c-FLIP. Further experiments demonstrated that FAIM protects c-FLIP from ubiquitination–proteasome-dependent degradation, which is mediated by impaired JNK phosphorylation. These data provide a novel approach to improve the effects of stem cells engraftment on cardiovascular indications.

MI poses a grave threat to the health of elderly individuals, and the loss of cardiomyocytes after MI is the most important cause of poor prognosis [25]. Therefore, remuscularization of the heart is the major focus in this field, and countless efforts have been made to find solutions, including promoting the regeneration of cardiomyocytes, transplanting induced pluripotent stem cell (iPSC)-derived cardiomyocytes, exogenous engrafting of stem cells or their derived exosomes, and the application of novel functional materials such as engineered heart tissues and hydrogels [26–29]. It has been demonstrated that within one week of birth, the hearts of neonatal mice exhibit regenerative activity, and subsequent studies showed that regenerative activity also occurred in neonatal pigs [30, 31]. Exploring the mechanism of cardiomyocyte regeneration and implementing treatments have become important research directions. A recent study reported that cardiac-specific knockout of PTEN facilitated the proliferation and renewal of cardiomyocytes [32]. Moreover, Salvador-siRNA delivered by adeno-associated virus 9 promoted the proliferation of cardiomyocytes after ischemia and reperfusion injury by inhibiting the Hippo pathway, which repressed cardiomyocyte proliferation after MI [33]. However, these studies are still in their early stages, and it could take decades to achieve
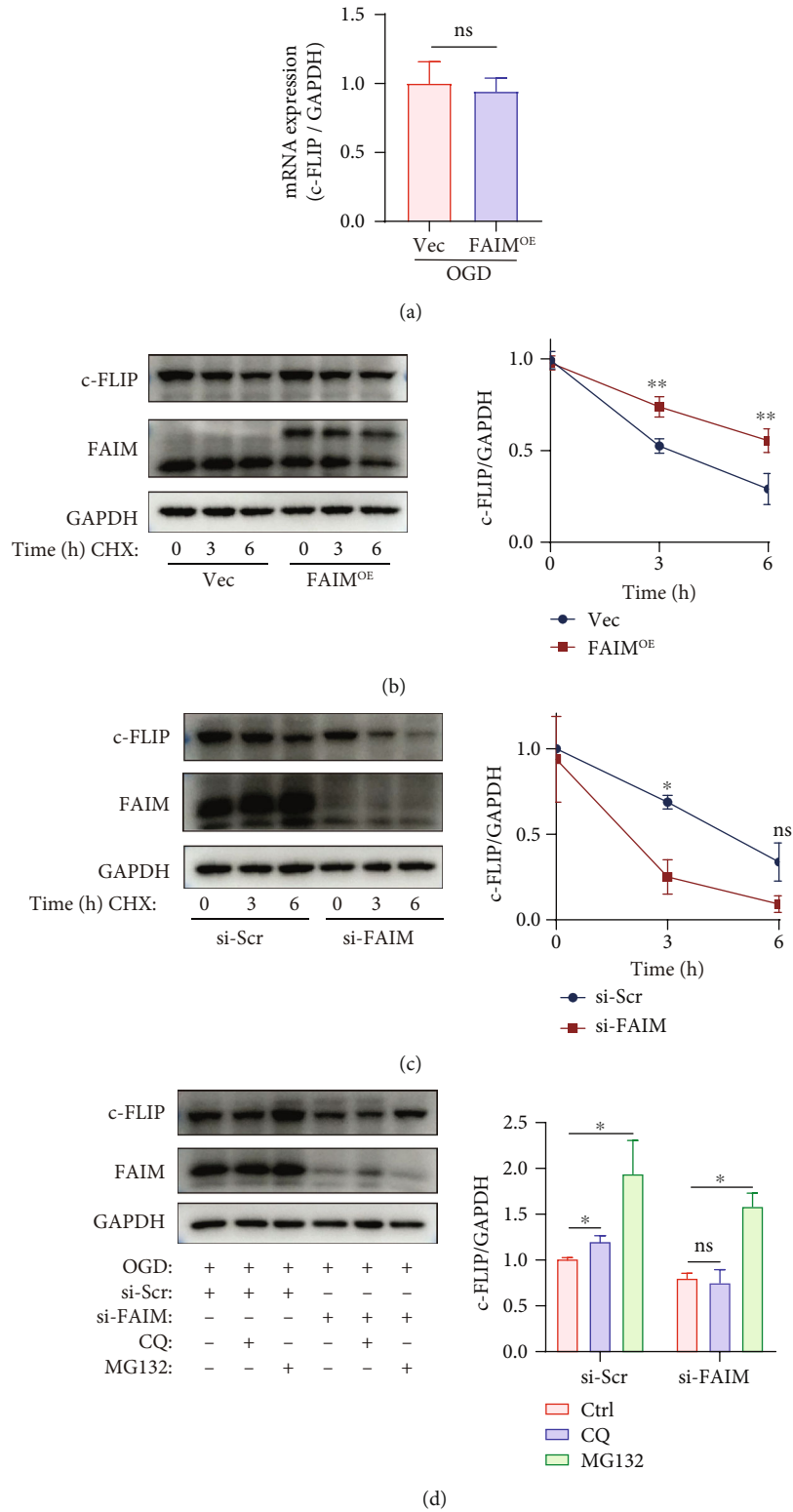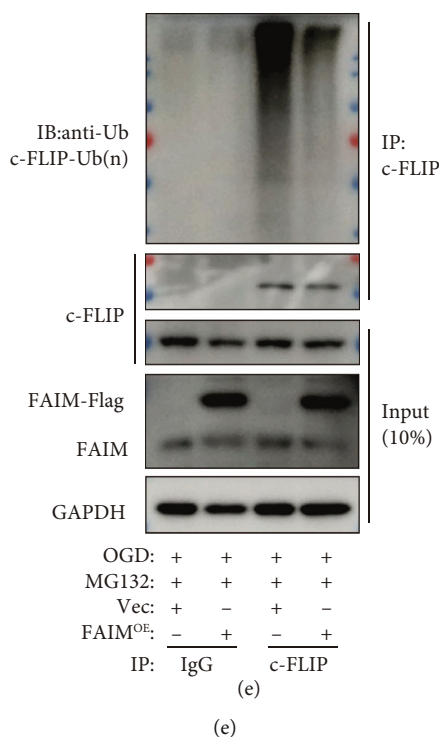
(a)

(b)

(c)

(d)

FIGURE 5: Continued.

(e)

(e)

Figure 5: FAIM stabilizes the c-FLIP protein in MSCs by inhibiting its ubiquitination. (a) mRNA expression of c-FLIP in MSCs$_{Vec}$ and MSCs$_{FAIM}$ challenged with OGD. (b) Representative immunoblots showing c-FLIP protein expression in MSCs$_{Vec}$ and MSCs$_{FAIM}$ treated with $10\,\mu M$ CHX for the indicated times under OGD conditions. The results of densitometric quantitation are shown on the right, and the line chart shows c-FLIP protein levels (normalized to GAPDH) as a percentage of the c-FLIP protein expression of MSCs$_{Vec}$ at $0\,h$ ($n = 3$). (c) Representative immunoblots showing c-FLIP protein levels in MSCs$_{si-scr}$ and MSCs$_{si-FAIM}$ treated with $10\,\mu M$ CHX for the indicated times under OGD conditions. The results of densitometric quantitation are shown on the right ($n = 3$). (d) Representative Western blotting results showing c-FLIP protein expression after siRNA-mediated knockdown of FAIM or scrambled siRNA administration followed by treatment with chloroquine (CQ, $50\,nM$) or MG132 ($10\,\mu M$) under OGD conditions. The results of densitometric quantitation are shown below ($n = 3$). (e) MSCs$_{Vec}$ and MSCs$_{FAIM}$ were treated with MG132 ($10\,\mu M$) under OGD conditions for $6\,h$. Whole-cell lysates were immunoprecipitated with anti-FLIP antibodies, followed by immunoblotting with anti-ubiquitin antibodies. The input (10% of the total) was analyzed by Western blotting using anti-FLIP and anti-FAIM antibodies. The data are shown as the mean $\pm$ SD. Ns indicates not significant; * denotes $P < 0.05$; $^{**}P < 0.01$.

clinical translational applications. In addition, engineering materials have provided some new ideas for the treatment of MI [34]. Patches were used to provide mechanical support to improve outcomes in the early days after MI, and subsequent studies reported the development of patches equipped with anti-inflammatory activity, but they could not compensate for the loss of cardiomyocytes [29]. However, the unique physical and electrical properties of the heart make it difficult for simple bioengineering materials to be of great use, and those engineering materials are often functionalized through synergistic application with stem cells or iPSC-derived cardiomyocytes [35, 36]. Taken together, these results highlight the importance of cell-based therapies for MI treatment.

Tremendous improvements in cell-based therapies for MI have been made in recent decades, and these therapies aim to produce a sufficient number of cardiomyocytes to compensate for the loss of viable cardiomyocytes after MI [37]. A variety of cells are used in the treatment of MI, such as human iPSCs (hiPSCs), human embryonic stem cells (hESCs), and the widely used hMSCs [27, 38]. Generating cardiomyocytes from hiPSCs are no longer difficult [39],

and this strategy has been applied in porcine MI models [40, 41]. However, there are still many challenges before iPSC-derived cardiomyocytes move to early trials, such as arrhythmias that can result from the injection of cardiomyocytes, the long-term immunosuppressant therapy required due to allogeneic-derived iPSCs, and the purity of the large number of iPSC-derived cardiomyocytes during induced proliferation and differentiation [26]. MSCs are ideal candidates for large-scale application in the clinical treatment of MI. Recent studies have shown that the therapeutic effects of MSCs are mainly exerted through their robust paracrine effects [21, 42], which promote the proliferation and migration of endothelial cells and ultimately improve cardiac angiogenesis and left ventricular function [43]. However, the harsh microenvironment formed by conditions including ischemia, hypoxia, oxidative stress, and inflammation causes massive cell death. A large proportion of engrafted stem cells were reported to perish within $24\,h$ after transplantation [44, 45], making strategies that prolong MSCs lifespan an attractive way to improve the efficacy of MSCs [46]. Our previous study showed that pretreatment with SRT1720 improved the efficacy of MSCs in rodent and
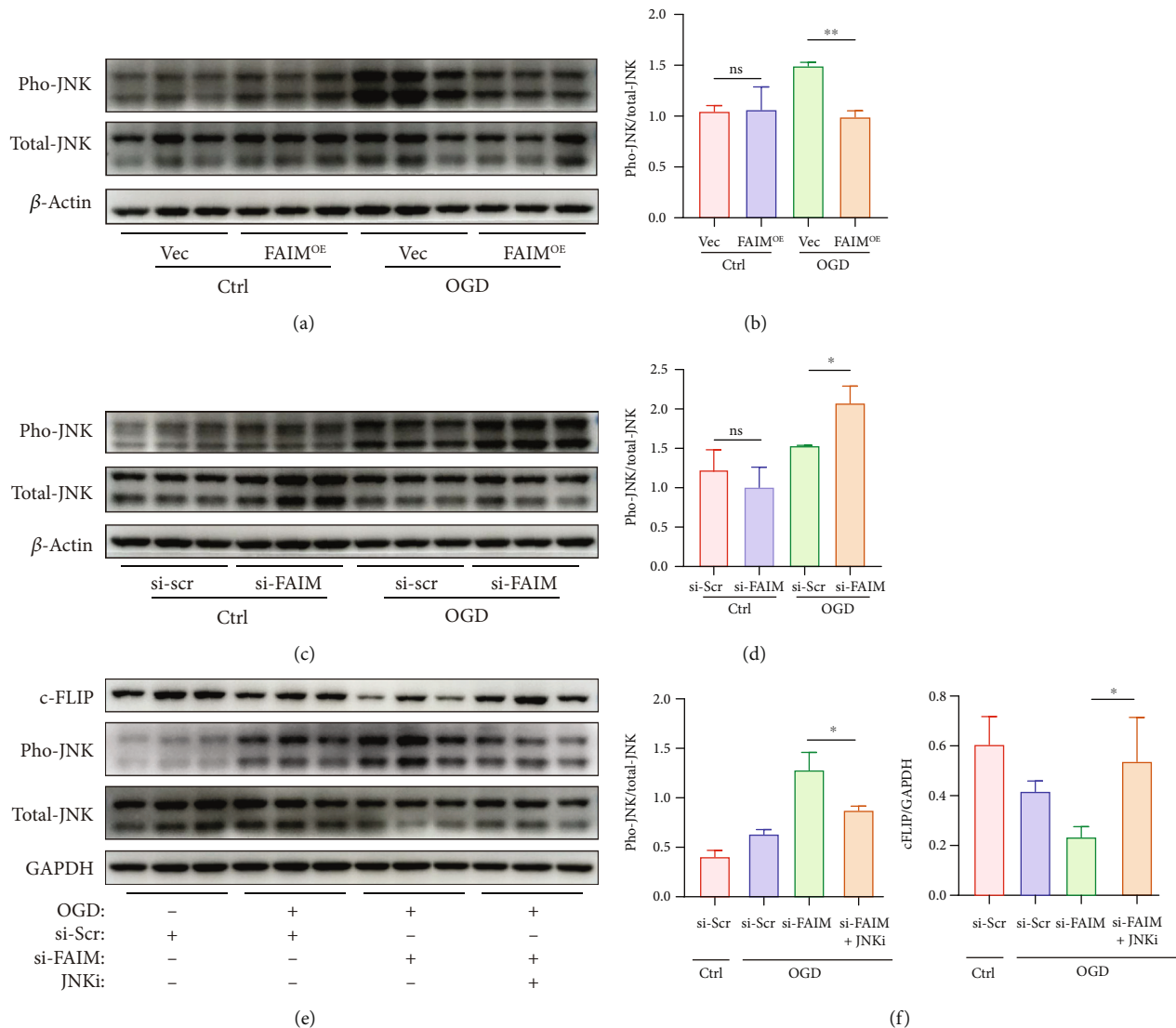
FIGURE 6: FAIM reduces c-FLIP degradation by blocking JNK activation. (a–b) Immunoblots and densitometric quantitation of phosphorylated JNK and total JNK protein expression in MSCs$_{Vec}$ and MSCs$_{FAIM}$ under OGD conditions. (c–d) Western blotting and densitometric quantitation of phosphorylated JNK and total JNK protein expression in MSCs$_{si-scr}$ and MSCs$_{si-FAIM}$ under OGD conditions. (e–f) Phosphorylated JNK, total JNK, and c-FLIP protein expression after siRNA-mediated knockdown of FAIM or scrambled siRNA administration followed by treatment with SP600125 (a JNK inhibitor, $10\,\mu$M) or DMSO under OGD conditions. The data are shown as the mean ± SD. Ns indicates not significant; * denotes $P < 0.05$; ** $P < 0.01$.

nonhuman primate MI models by prolonging MSCs survival [20, 47]. Consistent with these findings, our results showed that FAIM augmentation improved implanted MSCs survival and ultimately promoted neovascularization and ameliorated cardiac function.

Two splicing variants of FAIM have been described; the longer variant, FAIM-L, which is exclusively expressed in neural tissue, and the ubiquitously expressed shorter variant, known as FAIM-S [10]. FAIM-L exerts antiapoptotic effects by suppressing TCR signaling or DR signaling [11, 12]. However, to the best of our knowledge, this is the first study to reveal the protective effect of FAIM-L against apoptosis induced by hypoxia. Previous studies reported that c-FLIP expression was perturbed in FAIM-depleted cells [17]. Con-

sistent with these findings, our results showed that the survival effect of FAIM was mainly achieved by restoring c-FLIP expression. However, to date, the effects of FAIM on c-FLIP expression are not fully understood. FAIM has been reported to exert its biological effects by reducing ubiquitination; FAIM was found to reduce the ubiquitination and degradation of XIAP via direct interaction [48], FAIM knockout led to the presentation of ubiquitinated aggregates in the retina [49], and FAIM protects glutaminase C from ubiquitination and induces cancer cell proliferation in lung adenocarcinoma [14]. Here, we found that FAIM could maintain c-FLIP stabilization under hypoxic conditions by protecting c-FLIP from ubiquitination and degradation, thus protecting MSCs from apoptosis.
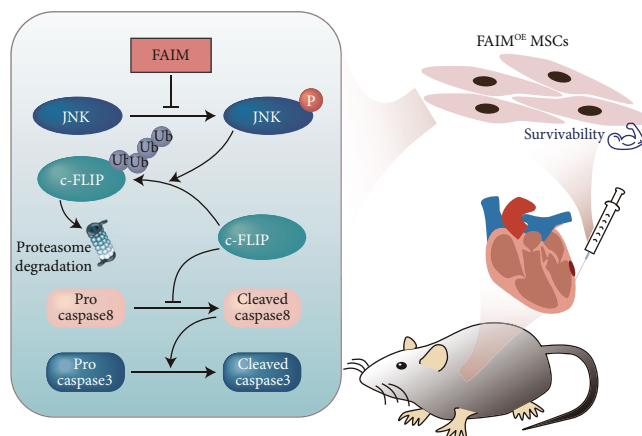
Figure 7: Graphical abstract: Schematic diagram of the proposed mechanism; schematic diagram of the proposed mechanisms by which FAIM impairs the JNK-mediated, ubiquitination–proteasome-dependent degradation of c-FLIP, thereby effectively promoting MSC survival and ultimately ameliorating cardiac function and improving the prognosis of MI in vivo.

c-FLIP, a strong regulator of caspase-8 activation due to the pseudocaspase domain at its C-terminus [50], participates in various cell death pathways, including apoptosis, necroptosis, and autophagy [51, 52]. Recent studies have shown that c-FLIP prevents cells from undergoing apoptosis by impairing p53-mediated PUMA upregulation and caspase-8 activation [53]. However, the functions of c-FLIP are contradictory and depend on its abundance in the death-inducing signaling complex (DISC) [15], which is assembled from Fas, FADD, procaspase 8, and c-FLIP [54]. Low concentrations of c-FLIP in the DISC can cause the formation of a procaspase-8/c-FLIP heterodimer and promote caspase-8 activation [55]. On the other hand, c-FLIP at a high concentration competitively suppresses the assembly of procaspase-8 into the DISC and thus reduces the activation of caspase-8 [56]. In the present study, we demonstrated that high protein expression of c-FLIP inhibited the activation of caspase-8; however, the caspase-8 activation status under low c-FLIP expression levels was not examined because we could not confirm whether the cleavage of procaspase-8 caused by the decrease in c-FLIP protein expression was due to a decrease in inhibition or an increase in activation. Regardless, this does not affect our conclusion that FAIM overexpression reduces MSCs apoptosis by ameliorating the decreased expression of c-FLIP under OGD conditions. In addition, accumulating evidence suggests that c-FLIP is a short-lived protein whose half-life is approximately 3 h [24]. Some studies have shown that the degradation of c-FLIP occurs mainly through the ubiquitin–proteasome pathway [57], and JNK activity may be a critical regulator of c-FLIP protein stability [24]. In agreement with previous findings, we revealed that the protein stability of c-FLIP is closely related to the presence of FAIM, and subsequent experiments showed that FAIM regulates c-FLIP protein stability by impairing JNK phosphorylation, which expands the current knowledge of the protein stability of c-FLIP.

There are some limitations of this study. First, our experimental setting could not completely mimic true clinical conditions. MSCs were injected into the peri-infarct zones immediately after LAD ligation, which is unrealistic in the real world. Second, unbiased analysis was not utilized in this study, and mass spectrometry-based proteomics analysis may be a more accurate way to determine the most predominant protein that regulates the antiapoptotic effects of FAIM in our model. Third, the mechanism by which FAIM regulates JNK activation was not explored in this work.

5. Conclusion

In conclusion, our study demonstrated that FAIM augmentation could effectively promote MSCs survival in vivo and ultimately ameliorate cardiac function and improve the prognosis of MI, providing a novel approach to improve the efficacy of MSC-based therapy.

Abbreviations

MSCs: Mesenchymal stem cells
OGD: Oxygen, serum, and glucose deprivation
MI: Myocardial infarction.
LAD: Left anterior descending coronary artery
FAIM: Fas apoptosis inhibitory molecule
c-FLIP: Cellular-FLICE inhibitory protein
$MSCs_{Vec}$: MSCs infected with vector
$MSCs_{FAIM}$: MSCs infected with FAIM
$MSCs_{FLIP}$: MSCs infected with c-FLIP
FADD: Fas-associated via death domain
DR: Death receptor
CHX: Cycloheximide.

Data Availability

The datasets used and/or analyzed to support the findings of this study are included within the article and supplementary information files.

Ethical Approval

All animal experiment protocols were approved by the Medical Ethics Committee of the Second Affiliated Hospital, Zhejiang University School of Medicine, Hangzhou, China.

Conflicts of Interest

The authors declare that there are no conflicts of interest regarding the publication of this paper.

Authors' Contributions

X.L. conceived the idea, designed the study, and revised the manuscript. J.C. and F.L. performed most of the experiments and drafted the manuscript. W.H., Y.Q., D.X. and C.G. analyzed and interpreted the data. Z.Z., G.Z., S.C. and K.Y. conducted the animal surgery and echocardiography. L.X. contributed to the immunoprecipitation assay and drawn the schematic diagram. All authors read and approved the final manuscript.

Acknowledgments

Supplementary Materials

Supplementary Figure S1: characterization of mesenchymal stem cells (MSCs). Supplementary Figure S2: schematic of the in vitro and in vivo experiments. Supplementary Figure S3: FAIM protected MSCs against H_2O_2-induced apoptosis in vitro. Supplementary Figure S4: identification of FAIM overexpression lentivirus and FAIM siRNA. Supplementary Figure S5: FAIM knockdown facilitated MSCs apoptosis. Supplementary Figure S6: FAIM overexpression reversed the decrease in the proangiogenic capacity of conditioned medium from MSCs induced by OGD. (Supplementary Materials)

References

[1] M. R. Rosen, R. J. Myerburg, D. P. Francis, G. D. Cole, and E. Marbán, "Translating stem cell research to cardiac disease therapies: pitfalls and prospects for improvement," *Journal of the American College of Cardiology*, vol. 64, no. 9, pp. 922–937, 2014.

[2] I. K. Ko and B. S. Kim, "Mesenchymal stem cells for treatment of myocardial infarction," *International Journal of Stem Cells*, vol. 1, no. 1, pp. 49–54, 2008.

[3] C. Toma, M. F. Pittenger, K. S. Cahill, B. J. Byrne, and P. D. Kessler, "Human mesenchymal stem cells differentiate to a cardiomyocyte phenotype in the adult murine heart," *Circulation*, vol. 105, no. 1, pp. 93–98, 2002.

[4] A. Elsasser, K. Suzuki, S. Lorenz-Meyer, C. Bode, and J. Schaper, "The role of apoptosis in myocardial ischemia: a critical appraisal," *Basic Research in Cardiology*, vol. 96, no. 3, pp. 219–226, 2001.

[5] O. Ham, S. Y. Lee, B. W. Song et al., "Modulation of Fas-Fas ligand interaction rehabilitates hypoxia-induced apoptosis of mesenchymal stem cells in ischemic myocardium niche," *Cell Transplantation*, vol. 24, no. 7, pp. 1329–1341, 2015.

[6] T. J. Schneider, G. M. Fischer, T. J. Donohoe, T. P. Colarusso, and T. L. Rothstein, "A novel gene coding for a Fas apoptosis inhibitory molecule (FAIM) isolated from inducibly Fas-resistant B lymphocytes," *The Journal of Experimental Medicine*, vol. 189, no. 6, pp. 949–956, 1999.

[7] J. Huo, S. Xu, and K. P. Lam, "FAIM: an antagonist of Fas-killing and beyond," *Cells*, vol. 8, no. 6, p. 541, 2019.

[8] C. Sole, X. Dolcet, M. F. Segura et al., "The death receptor antagonist FAIM promotes neurite outgrowth by a mechanism that depends on ERK and NF-κB signaling," *The Journal of Cell Biology*, vol. 167, no. 3, pp. 479–492, 2004.

[9] E. Coccia, I. Calleja-Yague, L. Planells-Ferrer et al., "Identification and characterization of new isoforms of human fas apoptotic inhibitory molecule (FAIM)," *PLoS One*, vol. 12, no. 10, article e0185327, 2017.

[10] X. Zhong, T. J. Schneider, D. S. Cabral, T. J. Donohoe, and T. L. Rothstein, "An alternatively spliced long form of Fas apoptosis inhibitory molecule (*FAIM*) with tissue-specific expression in the brain," *Molecular Immunology*, vol. 38, no. 1, pp. 65–72, 2001.

[11] J. Huo, S. Xu, and K. P. Lam, "Fas apoptosis inhibitory molecule regulates T cell receptor-mediated apoptosis of thymocytes by modulating Akt activation and Nur77 expression," *The Journal of Biological Chemistry*, vol. 285, no. 16, pp. 11827–11835, 2010.

[12] M. F. Segura, C. Sole, M. Pascual et al., "The long form of Fas apoptotic inhibitory molecule is expressed specifically in neurons and protects them against death receptor-triggered apoptosis," *The Journal of Neuroscience*, vol. 27, no. 42, pp. 11228–11241, 2007.

[13] H. Kaku and T. L. Rothstein, "FAIM is a non-redundant defender of cellular viability in the face of heat and oxidative stress and interferes with accumulation of stress-induced protein aggregates," *Frontiers in Molecular Biosciences*, vol. 7, p. 32, 2020.

[14] T. Han, P. Wang, Y. Wang et al., "AIM regulates autophagy through glutaminolysis in lung adenocarcinoma," *Autophagy*, vol. 18, no. 6, pp. 1416–1432, 2022.

[15] N. V. Ivanisenko, K. Seyrek, L. K. Hillert-Richter et al., "Regulation of extrinsic apoptotic signaling by c-FLIP: towards targeting cancer networks," *Trends Cancer*, vol. 8, no. 3, pp. 190–209, 2022.

[16] L. Humphreys, M. Espona-Fiedler, and D. B. Longley, "FLIP as a therapeutic target in cancer," *The FEBS Journal*, vol. 285, no. 22, pp. 4104–4123, 2018.

[17] J. Huo, S. Xu, K. Guo, Q. Zeng, and K. P. Lam, "Genetic deletion of *FAIM* reveals its role in modulating c-FLIP expression during CD95-mediated apoptosis of lymphocytes and hepatocytes," *Cell Death & Differentiation*, vol. 16, no. 7, pp. 1062–1070, 2009.

[18] K. Yu, Z. Zeng, S. Cheng et al., "TPP1 enhances the therapeutic effects of transplanted aged mesenchymal stem cells in infarcted hearts via the MRE11/AKT pathway," *Frontiers in Cell and Development Biology*, vol. 8, article 588023, 2020.

[19] F. Yang, R. Wu, Z. Jiang et al., "Leptin increases mitochondrial OPA1 via GSK3-mediated OMA1 ubiquitination to enhance therapeutic effects of mesenchymal stem cell transplantation," *Cell Death & Disease*, vol. 9, no. 5, p. 556, 2018.

[20] X. Liu, D. Hu, Z. Zeng et al., "SRT1720 promotes survival of aged human mesenchymal stem cells via FAIM: a pharmacological strategy to improve stem cell-based therapy for rat

myocardial infarction," *Cell Death & Disease*, vol. 8, no. 4, article e2731, 2017.

[21] M. Z. Ratajczak, M. Kucia, T. Jadczyk et al., "Pivotal role of paracrine effects in stem cell therapies in regenerative medicine: can we translate stem cell-secreted paracrine factors and microvesicles into better therapeutic strategies?," *Leukemia*, vol. 26, no. 6, pp. 1166–1173, 2012.

[22] B. A. Carneiro and W. S. El-Deiry, "Targeting apoptosis in cancer therapy," *Nature Reviews Clinical Oncology*, vol. 17, no. 7, pp. 395–417, 2020.

[23] Y. Fuchs and H. Steller, "Programmed cell death in animal development and disease," *Cell*, vol. 147, no. 4, pp. 742–758, 2011.

[24] R. P. Wilkie-Grantham, S. Matsuzawa, and J. C. Reed, "Novel phosphorylation and ubiquitination sites regulate reactive oxygen species-dependent degradation of anti-apoptotic c-FLIP protein," *The Journal of Biological Chemistry*, vol. 288, no. 18, pp. 12777–12790, 2013.

[25] C. W. Tsao, A. W. Aday, Z. I. Almarzooq et al., "Heart disease and stroke statistics-2022 update: a report from the American Heart Association," *Circulation*, vol. 145, no. 8, pp. e153–e639, 2022.

[26] J. Zhang, R. Bolli, D. J. Garry et al., "Basic and translational research in cardiac repair and regeneration:," *Journal of the American College of Cardiology*, vol. 78, no. 21, pp. 2092–2105, 2021.

[27] Y. W. Liu, B. Chen, X. Yang et al., "Human embryonic stem cell-derived cardiomyocytes restore function in infarcted hearts of non-human primates," *Nature Biotechnology*, vol. 36, no. 7, pp. 597–605, 2018.

[28] J. H. Jung, G. Ikeda, Y. Tada et al., "mi R-106a-363 cluster in extracellular vesicles promotes endogenous myocardial repair via Notch 3 pathway in ischemic heart injury," *Research in Cardiology*, vol. 116, no. 1, p. 19, 2021.

[29] Y. Yao, A. Li, S. Wang et al., "Multifunctional elastomer cardiac patches for preventing left ventricle remodeling after myocardial infarction *in vivo*," *Biomaterials*, vol. 282, article 121382, 2022.

[30] E. R. Porrello, A. I. Mahmoud, E. Simpson et al., "Transient regenerative potential of the neonatal mouse heart," *Science*, vol. 331, no. 6020, pp. 1078–1080, 2011.

[31] W. Zhu, E. Zhang, M. Zhao et al., "Regenerative potential of neonatal porcine hearts," *Circulation*, vol. 138, no. 24, pp. 2809–2816, 2018.

[32] T. Liang, F. Gao, J. Jiang et al., "Loss of phosphatase and tensin homolog promotes cardiomyocyte proliferation and cardiac repair after myocardial infarction," *Circulation*, vol. 142, no. 22, pp. 2196–2199, 2020.

[33] S. Liu, K. Li, L. Wagner Florencio et al., "Gene therapy knockdown of Hippo signaling induces cardiomyocyte renewal in pigs after myocardial infarction," *Science Translational Medicine*, vol. 13, no. 600, 2021.

[34] V. Sharma, S. K. Dash, K. Govarthanan et al., "Recent Advances in cardiac tissue engineering for the management of myocardium infarction," *Cells*, vol. 10, no. 10, p. 2538, 2021.

[35] L. Wang, Y. Liu, G. Ye et al., "Injectable and conductive cardiac patches repair infarcted myocardium in rats and minipigs," *Nature Biomedical Engineering*, vol. 5, no. 10, pp. 1157–1173, 2021.

[36] S. Hinderer, E. Brauchle, and K. Schenke-Layland, "Generation and assessment of functional biomaterial scaffolds for applications in cardiovascular tissue engineering and regenerative medicine," *Advanced Healthcare Materials*, vol. 4, no. 16, pp. 2326–2341, 2015.

[37] P. Menasche, "Cell therapy trials for heart regeneration – lessons learned and future directions," *Nature Reviews Cardiology*, vol. 15, no. 11, pp. 659–671, 2018.

[38] E. Marban, "A mechanistic roadmap for the clinical application of cardiac cell therapies," *Nature Biomedical Engineering*, vol. 2, no. 6, pp. 353–361, 2018.

[39] H. Kempf, C. Kropp, R. Olmer, U. Martin, and R. Zweigerdt, "Cardiac differentiation of human pluripotent stem cells in scalable suspension culture," *Nature Protocols*, vol. 10, no. 9, pp. 1345–1361, 2015.

[40] L. Gao, Z. R. Gregorich, W. Zhu et al., "Large cardiac muscle patches engineered from human induced-pluripotent stem cell-derived cardiac cells improve recovery from myocardial infarction in swine," *Circulation*, vol. 137, no. 16, pp. 1712–1730, 2018.

[41] M. Zhao, Y. Nakada, Y. Wei et al., "Cyclin D2 overexpression enhances the efficacy of human induced pluripotent stem cell-derived cardiomyocytes for myocardial repair in a swine model of myocardial infarction," *Circulation*, vol. 144, no. 3, pp. 210–228, 2021.

[42] K. Zhu, Q. Wu, C. Ni et al., "Lack of remuscularization following transplantation of human embryonic stem cell-derived cardiovascular progenitor cells in infarcted nonhuman primates," *Circulation Research*, vol. 122, no. 7, pp. 958–969, 2018.

[43] J. Ma, Y. Zhao, L. Sun et al., "Exosomes derived from Akt-modified human umbilical cord mesenchymal stem cells improve cardiac regeneration and promote angiogenesis via activating platelet-derived growth factor D," *Stem Cells Translational Medicine*, vol. 6, no. 1, pp. 51–59, 2017.

[44] J. V. Terrovitis, R. R. Smith, and E. Marban, "Assessment and optimization of cell engraftment after transplantation into the heart," *Circulation Research*, vol. 106, no. 3, pp. 479–494, 2010.

[45] M. Mohammadzadeh, R. Halabian, A. Gharehbaghian et al., "Nrf-2 overexpression in mesenchymal stem cells reduces oxidative stress-induced apoptosis and cytotoxicity," *Cell Stress & Chaperones*, vol. 17, no. 5, pp. 553–565, 2012.

[46] L. Li, X. Chen, W. E. Wang, and C. Zeng, "How to improve the survival of transplanted mesenchymal stem cell in ischemic heart?," *Stem Cells International*, vol. 2016, Article ID 9682757, 14 pages, 2016.

[47] Z. Zeng, K. Yu, W. Hu et al., "SRT1720 pretreatment promotes mitochondrial biogenesis of aged human mesenchymal stem cells and improves their engraftment in postinfarct nonhuman primate hearts," *Stem Cells and Development*, vol. 30, no. 7, pp. 386–398, 2021.

[48] E. Coccia, L. Planells-Ferrer, R. Badillos-Rodriguez et al., "SIVA-1 regulates apoptosis and synaptic function by modulating XIAP interaction with the death receptor antagonist FAIM-L," *Cell Death & Disease*, vol. 11, no. 2, p. 82, 2020.

[49] A. Sires, M. Turch-Anguera, P. Bogdanov et al., "*FAIM* knockout leads to gliosis and late-onset neurodegeneration of photoreceptors in the mouse retina," *Journal of Neuroscience Research*, vol. 99, no. 12, pp. 3103–3120, 2021.

[50] M. Djerbi, T. Darreh-Shori, B. Zhivotovsky, and A. Grandien, "Characterization of the human FLICE-inhibitory protein locus and comparison of the anti-apoptotic activity of four different flip isoforms," *Scandinavian Journal of Immunology*, vol. 54, no. 1-2, pp. 180–189, 2001.

[51] C. Plaza-Sirvent, M. Schuster, Y. Neumann et al., "c-FLIP expression in foxp3-expressing cells is essential for survival of regulatory T cells and prevention of autoimmunity," *Cell Reports*, vol. 18, no. 1, pp. 12–22, 2017.

[52] A. R. Safa, "c-FLIP, a master anti-apoptotic regulator," *Experimental Oncology*, vol. 34, no. 3, pp. 176–184, 2012.

[53] A. Lees, A. J. McIntyre, N. T. Crawford et al., "The pseudo-caspase FLIP(L) regulates cell fate following p53 activation," *Proceedings of the National Academy of Sciences of the United States of America*, vol. 117, no. 30, pp. 17808–17819, 2020.

[54] F. C. Kischkel, S. Hellbardt, I. Behrmann et al., "Cytotoxicity-dependent APO-1 (Fas/CD95)-associated proteins form a death-inducing signaling complex (DISC) with the receptor," *The EMBO Journal*, vol. 14, no. 22, pp. 5579–5588, 1995.

[55] C. Pop, A. Oberst, M. Drag et al., "FLIPL induces caspase 8 activity in the absence of interdomain caspase 8 cleavage and alters substrate specificity," *The Biochemical Journal*, vol. 433, no. 3, pp. 447–457, 2011.

[56] I. N. Lavrik, "Systems biology of death receptor networks: live and let die," *Cell Death & Disease*, vol. 5, no. 5, article e1259, 2014.

[57] A. Kaunisto, V. Kochin, T. Asaoka et al., "PKC-mediated phosphorylation regulates c-FLIP ubiquitylation and stability," *Cell Death and Differentiation*, vol. 16, no. 9, pp. 1215–1226, 2009.

Hindawi

Research Article

Erythropoietin Activates Autophagy to Regulate Apoptosis and Angiogenesis of Periodontal Ligament Stem Cells via the Akt/ERK1/2/BAD Signaling Pathway under Inflammatory Microenvironment

Denghao Huang,[1,2] **Jie Lei,**[1,2] **Xingrui Li,**[1,2] **Zhonghao Jiang,**[1] **Maoxuan Luo,**[1] **and Yao Xiao** [1,3,4]

[1]*Luzhou Key Laboratory of Orofacial Reconstruction and Regeneration, The Affiliated Stomatology Hospital of Southwest Medical University & Institute of Stomatology, Southwest Medical University, Luzhou, China*
[2]*Cell Biology Technology Platform, Public Experiment Technology Center of Southwest Medical University, Luzhou, China*
[3]*Department of Chengbei Outpatient, The Affiliated Stomatology Hospital of Southwest Medical University, Luzhou, China*
[4]*Department of Orthodontics, The Affiliated Stomatology Hospital of Southwest Medical University, Luzhou, China*

Correspondence should be addressed to Yao Xiao; orthoxiaoyao@outlook.com

Background. Angiogenic tissue engineering is a vital problem waiting to be settled for periodontal regeneration. Erythropoietin, a multieffect cytokine, has been reported as a protective factor for cell fate. According to our previous study, erythropoietin has a significantly angiogenic effect on periodontal ligament stem cells. To further explore its potential effects and mechanism, we studied biological behaviors of periodontal ligament stem cells under inflammatory microenvironment induced by different concentrations (0, 10, 20, 50, and 100 ng/mL) of tumor necrosis factor-α (TNF-α) and examined how different concentrations (0, 5, 10, 20, and 50 IU/mL) of erythropoietin changed biological behaviors of periodontal ligament stem cells. *Materials and Methods.* Cell Counting Kit-8 was used for cell proliferation assay. Annexin V-PI-FITC was used for cell apoptosis through flow cytometry. Matrigel plug was adopted to measure the angiogenic capacity *in vitro*. RNA sequencing was used to detect the downstream signaling pathway. Quantitative real-time polymerase chain reaction was conducted to examine mRNA expression level. Western blot and immunofluorescence were applied to testify the protein expression level. *Results.* Periodontal ligament stem cells upregulated apoptosis and suppressed autophagy and angiogenesis under inflammatory microenvironment. Erythropoietin could activate autophagy to rescue apoptosis and angiogenesis levels of periodontal ligament stem cells through the Akt/Erk1/2/BAD signaling pathway under inflammatory microenvironment. *Conclusions.* Erythropoietin could protect periodontal ligament stem cells from inflammatory microenvironment, which provided a novel theory for periodontal regeneration.

1. Introduction

Periodontitis, a commonly infectious oral disease, is deemed as the sixth disease of the globe, which would risk psychological and physical health [1]. Periodontitis is characterized as loss of periodontal tissues and detachment of teeth, which is caused by a series of microbiological and immune factors [2, 3]. Hitherto, there is still lack of effective therapy to reverse the periodontal loss [4, 5]. Many researchers have turned to odontogenic stem cells for novel strategies [6], such as periodontal ligament stem cells (PDLSCs) [7] and apical papilla stem cells (APSCs) [8]. PDLSCs have shown the great

ability of multidirectional differentiation, especially in osteogenesis and angiogenesis [9]. However, two crucial problems are waiting to be solved. Firstly, it is essential to reverse the differentiational capacity of PDLSCs, which is always undermined by inflammatory environment. Secondly, it is vital to regenerate vascularized bone in periodontal regeneration, which offers nutrition to the bone [10].

Tissue reconstruction also relies on the cytokines. Erythropoietin (EPO), a glycoprotein secreted by the kidney, is reported as a promising candidate cytokine for periodontal tissue engineering. EPO plays a great effect on osteogenic and angiogenic differentiation of mesenchymal stem cells (MSCs) [11, 12]. It is widely investigated that biomaterials loaded with EPO could promote osteogenesis and angiogenesis of bone marrow stem cells (BMSCs) and vein endothelial cells (VECs) through upregulating the EphB4/EphrinB2 signaling pathway [13–15]. Furthermore, EPO regulates Wnt/β-catenin and p38/MAPK signaling pathway to enhance osteogenesis of PDLSCs [16, 17]. EPO is also seen as an anti-inflammation factor, which provides a stable microenvironment for tissue engineering. Relative researches have proven that oxidative stress and cell apoptosis can be improved by EPO through reducing IL1β, iNOS, and CD68 expression [18, 19]. Collectively, EPO dually regulates multidirectional differentiation and anti-inflammation effects, which could be used for periodontal regeneration.

Cumulative studies have proved that autophagy is closely related to cell differentiation and apoptosis. Autophagy is considered as a helpful process for cell viability, which could enable cells to adapt to the change and pressure of circumstance [20]. Jiang et.al [21] explored the relationship between autophagy and Akt signaling pathway, which indicated that increasing LC3 expression could enhance the remodeling of alveolar bone. Autophagy decreased apoptosis and retained the osteogenic ability of PDLSCs and osteoblasts [22, 23]. Angiogenesis of PDLSCs could also be induced via upregulating autophagy [24]. Researchers also found that higher autophagy-related gene expression of LC3, Beclin1, Atg7, and Atg12 protected PDLSCs from apoptosis in inflammatory microenvironment [25]. It is evidenced that autophagy could be activated through overexpression of the tumor necrosis factor alpha-induced protein 3 (TNFAIP3) to diminish inflammation of periodontal ligament cells (PDLCs) induced by lipopolysaccharide (LPS) and nicotine [26].

The Akt signaling pathway always participates in autophagy, apoptosis, and differentiation. Akt-related autophagy maintains the stemness of mouse embryonic palatal mesenchymal stem cells, which could suppress cleft palate development [27]. It has been discussed that autophagy could be augmented by upregulating the Akt signaling pathway to regulate cell fate [28–30]. The Akt signaling pathway is also involved in the angiogenesis of BMSCs, VECs, and adipose-derived stem cells (ASCs) to promote fracture repair [31–34].

According to the existing literatures and our previous study, we aimed to investigate the antiapoptosis and angiogenesis of EPO under inflammatory microenvironment. We also explored the involvement of autophagy and Akt sig-

naling pathway in this process, wishing to find a novel approach for periodontal repair.

2. Methods and Materials

2.1. Isolation and Cultivation of PDLSCs.
With fully informed consent, we collected 50 healthy orthodontic teeth from adolescent patients (12-20 years old) under the approval of the Biomedical Ethics Committee of the Affiliated Stomatology Hospital of Southwest Medical University (Lot No. 2020112600). After collecting teeth, the periodontal ligaments were scraped from the tooth root and incubated reversely for 4 hours in a culture flask. The medium, mixture of α-MEM (Gibco, CA, USA), 10% fetal bovine serum (FBS) (EveryGreen, Shanghai, China), and 1% penicillin-streptomycin solution (Beyotime, Shanghai, China), was added into the flask to obtain periodontal ligament stem cells. The cells usually crawled out about 2 weeks later. The culturing incubator (Thermo Fisher, CA, USA) was set as 37°C and 5% CO_2.

2.2. Flow Cytometry Detection for Surface Marker.
After digesting and washing, the fourth-generation (p4) PDLSCs were used to detect specific surface markers under flow cytometry instrument (BD Biosciences, NJ, USA). Mesenchymal stem cell surface antibodies (CD90, CD44, and CD105) (BD Biosciences, NJ, USA) and hematopoietic stem cell surface antibodies (CD45, CD31) (BD Biosciences, NJ, USA) were selected to examine.

2.3. Osteogenic and Lipogenic Induction Assays.
Osteogenesis and lipogenesis induction were used to detect the multidirectional differentiation ability of PDLSCs. The osteogenic induction solution formulation consisted of D-MEM (Hyclone, USA), 10% FBS, 10 mmol/L sodium β-glycerate (Macklin, Shanghai, China), 0.1 μmol/L dexamethasone (Solarbio, Beijing, China), and 50 mg/L vitamin C (Solarbio, Beijing, China). Osteogenic induction solution was changed every 3 days and maintained for 28 days. Then, cells were fixed by paraformaldehyde and stained by alizarin red solution (Solarbio, Beijing, China). The lipogenic induction solution was formulated with D-MEM, 10% FBS, 10 μmol/L dexamethasone (Solarbio, Beijing, China), 200 μmol/L indomethacin (Solarbio, Beijing, China), 0.5 mmol/L 3-isobutyl-1-methylxanthine (IBMX) (Sigma, USA), and 10 mg/L insulin (Solarbio, Beijing, China). Cultured for 28 days, the cells were fixed and stained by oil red O solution (Solarbio, Beijing, China). Calcium nodules and lipid droplets were observed under a fluorescent inverted microscope (Olympus, Japan).

2.4. Cell Proliferation Assay.
Cell Counting Kit-8 (CCK8) (Dojindo, Japan) was used for cell proliferation assay. The p4 PDLSC was inoculated in 96-well plates at a density of 2000 cells per well, and the cells were divided into different treated groups. Detection was performed on days 1, 3, 5, and 7 after inoculation, respectively. Overall, 10 μL of CCK8 solution and 90 μL α-MEM were added to each well, incubated for one hour and then detected at 450 nm absorbance in an enzyme microplate reader (BioTek, USA).

2.5. Annexin V-FITC-PI Double-Staining Assay (Cell Apoptosis Assay). Annexin V-FITC-PI double-staining assay was performed under flow cytometry to detect cell apoptosis level. Cells were collected after incubating for 1 day and diffused in 400 μL binding buffer. Then, PDLSCs were stained with 2 μL Annexin V and 1 μL propidium iodide (PI) (BD Biosciences, NJ, USA) and incubated for 30 min.

2.6. Total RNA Extraction and Real-Time Quantitative Polymerase Chain Reaction (qPCR). Total RNA was extracted according to the instructions of the Total RNA Extraction Kit (TIANGEN, Beijing, China), and then, RNA was reverse transcribed to cDNA using the Takara Reverse Transcription Kit (TOYOBO, Tokyo, Japan) for subsequent experiment. We prepared a 20 μL amplification system using the SYBR FAST qPCR Master Mix Kit (TOYOBO, Tokyo, Japan) and then performed amplification in Bio-Rad/CFX96 fluorescence quantitative PCR instrument (Bio-Rad, USA). The specific conditions of denaturation, annealing, and extension were as follows: 95°C for 3 min, 95°C for 5 sec, 56°C for 10 sec, and 72°C for 25 sec in 40 cycles. The forward and reverse primer (BI, Shanghai, China) sequences used in the experiment are shown in Table 1. The relative expression of target genes was normalized to the expression of β-actin, and the changes in gene expression were calculated by the 2-$^{\triangle\triangle}$CT method.

2.7. Total Protein Extraction and Western Blot Assay. Total protein was extracted under the guidance of the kit (Solarbio, Beijing, China) instructions. The protein concentration of each group was determined using the BCA protein concentration assay kit (Solarbio, Beijing, China). SDS-PAGE gels were configured, and the proteins were electrophoresed vertically and transferred to PVDF membranes (Millipore, Germany). The membranes were blocked for 2 hours in blocking buffer (Solarbio, Beijing, China) at room temperature. Then, membranes were incubated with primary antibody at 4°C overnight. Washed in TBST solution for 3 times, membranes were incubated with anti-rabbit IgG, HRP-linked antibody (#7074, CST, USA) at room temperature for 1 hour. ECL developer (Absin, Shanghai, China) was added and photographed in a chemiluminescence imaging system (Tanon, Shanghai, China). The primary antibodies are listed in Table 2 (Supplementary Figure 1, raw data of western blot).

2.8. Matrigel Plug Assay. Melted matrix gel (Corning, USA) was evenly added in the volume of 50 μL to the precooled 96-well plate and placed in the incubator for 30 minutes. Pretreated PDLSCs were added to the wells at a density of 2000 cells per well. Tube formation in each well was observed after 6 hours and photographed under fluorescent inverted microscope.

2.9. RNA-Sequencing Assay. The transcriptome expression of PDLSCs in control groups (TNF-α treatment) and treated groups (TNF-α and EPO treatment) was examined through mRNA sequencing to discover downstream regulatory pathways of EPO. Each group had 3 biological replicates. RNA extraction, specific RNA library preparation, RNA sequencing, and bioinformatics analysis were done by OE biotech Co., Ltd. (Shanghai, China). The sequence raw data has been submitted to NCBI Sequence Read Archive (Accession number PRJNA824457). The sequence results have been validated by qPCR.

2.10. Immunofluorescence and Confocal Laser Microscope Observation. PDLSCs were treated under different conditions on the cell climbing sheets for 1 day. Fixed by paraformaldehyde, 1000 μL blocking buffer (0.2% Triton-100 and 5% donkey serum) was added onto each sheet. Then, the cells were incubated with the primary antibody (VEGF-a or LC3B) at 4°C overnight. After rewarming to room temperature, the cells were dealt with the secondary antibody, DyLight680 (Invitrogen, CA, USA) for 1 hour. DAPI and phalloidin (CoraLite488, Proteintech, Wuhan, China) were used to stain cell nucleus and cytoskeleton. Images of cells were observed and captured under Olympus SpinSR confocal laser microscope (Olympus, Tokyo, Japan).

2.11. Study Design. All experiments were all performed under p4 PDLSCs. Experiment groups of this research were mainly divided into 4 parts:

(1) Concentration gradient of TNF-α (treated for 3 days): 0, 10, 20, 50, and 100 ng/mL

(2) Concentration gradient of EPO (under inflammatory microenvironment induced by 20 ng/mL TNF-α) (treated for 3 days): 0, 5, 10, 20, and 50 IU/mL

(3) To explore the roles of the Akt/ERK1/2/BAD signaling pathway (treated for 1 day): ① TNF-α (50 ng/mL), ② TNF-α (50 ng/mL)+LY294002 (10 μM)+EPO (20 IU/mL), and ③ TNF-α (50 ng/mL)+EPO (20 IU/mL)

(4) To explore the roles of autophagy (treated for 1 day): ① TNF-α (50 ng/mL), ② TNF-α (50 ng/mL)+3-methyladenine (3-MA) (5 mM)+EPO (20 IU/mL), and ③ TNF-α (50 ng/mL)+EPO (20 IU/mL)

2.12. Statistical Analysis. Statistical calculation was completed at GraphPad Prism 9.0 software (GraphPad, CA, USA). Results were presented in the form of mean ± standard deviation (SD). Each experiment has been performed at least three times. One-way ANOVA was used to determine multiple-group comparisons. And Students' t-test was used to compare among two groups. It was considered as statistically significant when $P < 0.05$.

3. Results

3.1. Identification of PDLSCs and Establishment of Inflammatory Microenvironment. Cells were obtained from the periodontal ligament tissues (Figure 1(a)). Cells could differentiate into osteogenesis and adipogenesis under induction, which suggested the capacity of multidirectional differentiation (Figures 1(b) and 1(c)). Regarding the cell surface markers, cells highly expressed specific markers of MSCs (CD90, CD44, and CD105) but rarely expressed specific markers of HSCs (CD45, CD31) (Figure 1(d)). The mRNA expression level of the inflammatory cytokines (IL-

TABLE 1: Primer sequences of target genes for qPCR.

Target gene name (human)	Forward primer sequence	Reverse primer sequence
IL-1β	5′-ACAGATGAAGTGCTCCTTCCA-3′	5′-GTCGGAGATTCGTAGCTGGAT-3′
IL-8	5′-ATGACTTCCAAGCTGGCCGTGGCT-3′	5′-TCTCAGCCCTCTTCAAAAACTTCTC-3′
Bax	5′-GATGCGTCCACCAAGAAGCTGAG-3′	5′-CACGGCGGCAATCATCCTCTG-3′
Bcl2	5′-TGGACTGCCCCAGAAAAATA-3′	5′-TCTTGATTGAGCGAGCCTTT-3′
VEGF-a	5′-CATGCAGATTATGCGGATCAA-3′	5′-GCATTCACATTTGTTGTGCTGTAG-3′
FGF-2	5′-AAGAGCGACCCTCACATCAAG-3′	5′-GTTCGTTTCAGTGCCACATACC-3′
IGF-1	5′-TGTCCTCCTCGCATCTCTTCT-3′	5′-CCATACCCTGTGGGCTTGT-3′
Beclin1	5′-ATTCGAGAGCAGCATCC AAC-3′	5′-AACAGGAAGCTGCTTCTCAC-3′
LC3B	5′-GGGGCCTCGGAGCAAGTCCA-3′	5′-CCCCGGGAGCCTCGTTCAGGT-3′
DUSP4	5′-TACTCGGCGGTCATCGTCTACG-3′	5′-CGGAGGAAAACCTCTCATAGCC-3′
EREG	5′-GGACAGACTTCCAAGATGAGCC-3′	5′-CCACACTGCATTCATCAGGAGAG-3′
KDR	5′-GGAACCTCACTATCCGCAGAGT-3′	5′-CCAAGTTCGTCTTTTCCTGGGC-3′
ITGA10	5′-CCTTTGCTTCCAAGTGACCTCC-3′	5′-CAGAGCCATCAAATGCTGCACG-3′
CSF3	5′-TCCAGGAGAAGCTGGTGAGTGA-3′	5′-CGCTATGGAGTTGGCTCAAGCA-3′
PCK2	5′-TAGTGCCTGTGGCAAGACCAAC-3′	5′-GAAGCCGTTCTCAGGGTTGATG-3′
THBS4	5′-ACCGACAGTAGAGATGGCTTCC-3′	5′-CGTCACATCTGAAGCCAGGAGA-3′
β-Actin	5′-CCTGGCACCCAGCACAAT-3′	5′-GCCGATCCACACGGAGTA-3′

TABLE 2: Primary antibodies for western blot and immunofluorescence.

Primary antibody	Source	Diluted multiple
Anti-Bax	Abcam, ab182733	1 : 2000
Anti-Bcl2	Abcam, ab182858	1 : 2000
Anti-VEGF-a	Abcam, ab185238	1 : 00000
Anti-FGF-2	Abcam, ab208687	1 : 1000
Anti-IGF-1	Abcam, ab133542	1 : 1000
Anti-Beclin1	Abcam, ab210498	1 : 1000
Anti-LC3B	Abcam, ab192890	1 : 2000
Anti-Akt	CST, #4691	1 : 1000
Anti-p-Akt (Ser473)	Abcam, ab81283	1 : 5000
Anti-Erk1/2	CST, #4695	1 : 1000
Anti-p-Erk1/2 (Thr202/Tyr204)	CST, #4370	1 : 2000
Anti-BAD	CST, #9292	1 : 1000
Anti-p-BAD (Ser112)	Abcam, ab129192	1 : 5000
Anti-β-actin	CST, #4970	1 : 1000

1β, IL-8) significantly upregulated with the ascent of TNF-α concentration (Figure 1(e)).

3.2. PDLSCs Reduced Proliferation and Upregulated Apoptosis under Inflammatory Microenvironment. CCK8 results showed that PDLSCs gradually reduced proliferation under different concentrations of TNF-α on days 1, 3, 5, and 7 (Figure 2(a)). The mRNA expression of Bax/Bcl2 ratio was significantly upregulated with the raising of TNF-α concentration (Figure 2(b)). The protein expression trend was the same (Figure 2(c)). Annexin V-FITC-PI assay showed the enhancement of apoptosis rate, accompanying with the increasing TNF-α concentration (Figure 2(d)). In a short, TNF-α impaired cell viability and upregulated apoptosis of PDLSCs.
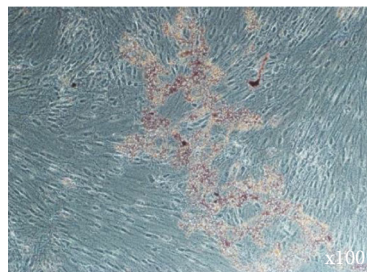
3.3. PDLSCs Repressed Autophagy and Angiogenic Capacity under Inflammatory Microenvironment. The mRNA and protein expression levels of autophagy-related cytokines (Beclin1, LC3B) indicated that TNF-α can significantly repress autophagy, especially in 20 and 50 ng/mL groups (Figures 3(a) and 3(b)). Additionally, the mRNA and protein expression levels of vascularization-related cytokines (VEGF-a, IGF-1, and FGF-2) descended when TNF-α concentration was enhanced, particularly in 20, 50, and 100 ng/mL groups (Figures 3(c) and 3(d)).

3.4. EPO Rescued Inflammation and Apoptosis Levels of PDLSCs under Inflammatory Microenvironment. Cell viability suggested that EPO could rescue the proliferation of inflammatory PDLSCs on days 3, 5, and 7, especially in 20 IU/mL groups (Figure 4(a)). The mRNA expression level of IL-1β

(a)

(b)

(c)

Figure 1: Continued.

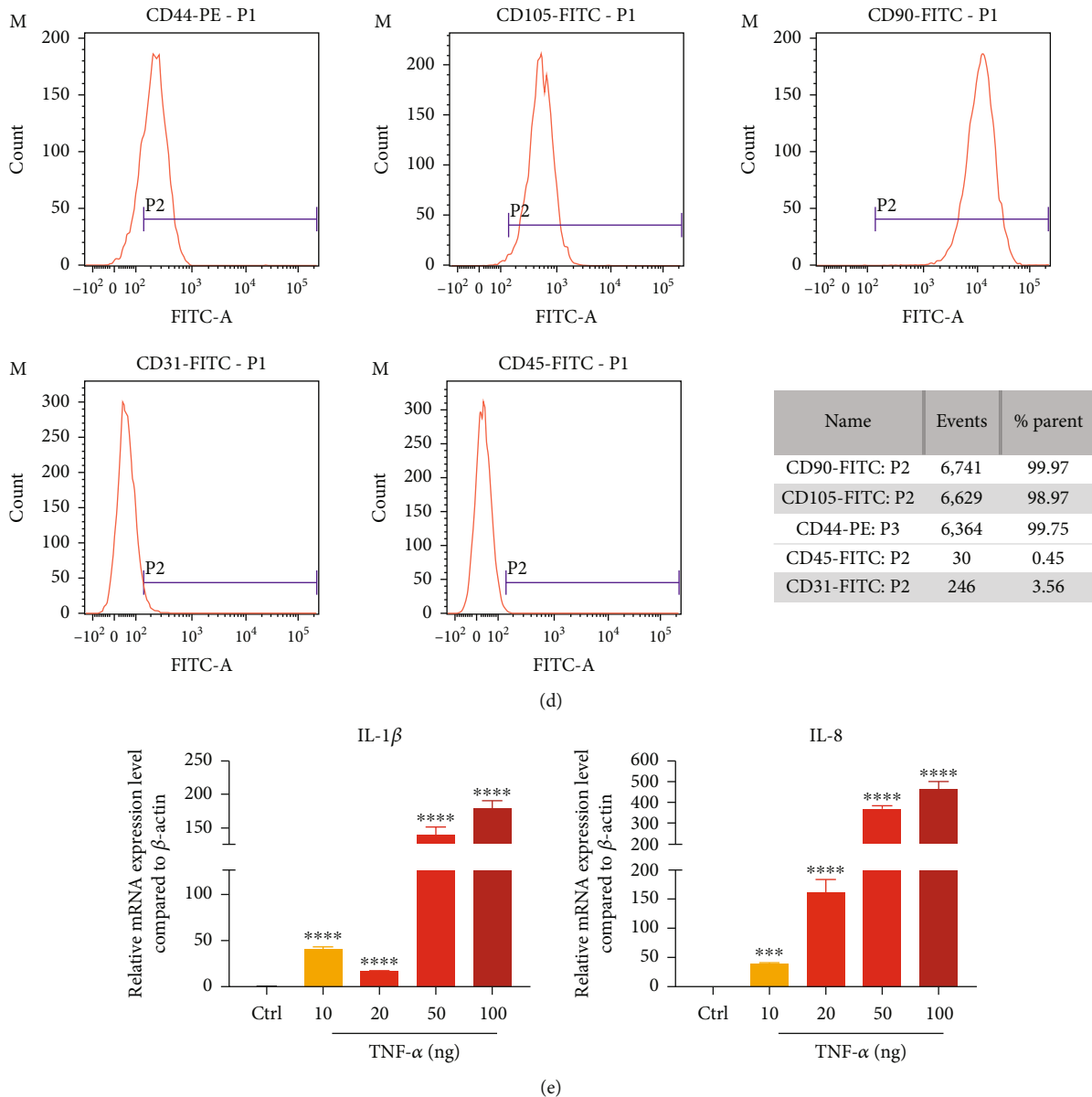| Name	Events	% parent
CD90-FITC: P2	6,741	99.97
CD105-FITC: P2	6,629	98.97
CD44-PE: P3	6,364	99.75
CD45-FITC: P2	30	0.45
CD31-FITC: P2	246	3.56

(d)

(e)
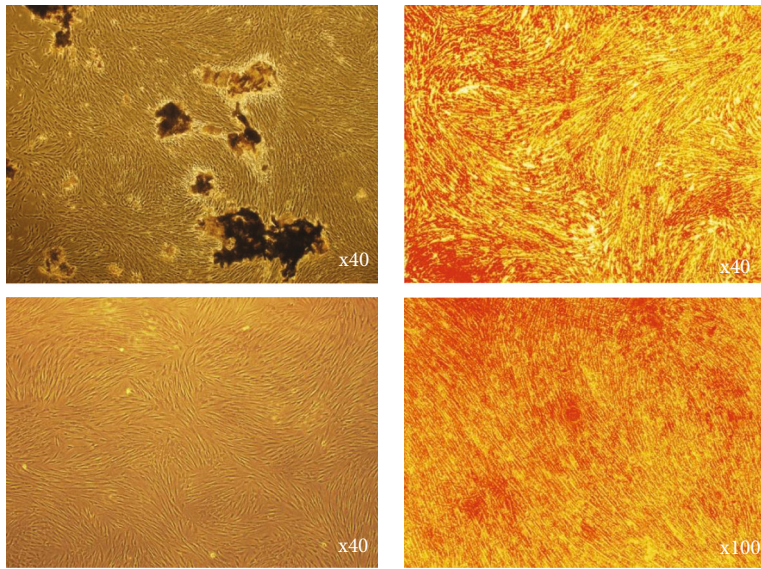
FIGURE 1: Identification of PDLSCs and establishment of inflammatory microenvironment. (a) Primary passage PDLSCs derived from periodontal ligament and the first passage PDLSCs digested from primary passage. (b) Observed osteogenic induction of PDLSCs under fluorescent inverted microscope. (c) Observed lipogenic induction of PDLSCs under fluorescent inverted microscope. (d) Flow cytometry detected cell surface marker (CD44, CD105, CD90, CD31, and CD45). (e) mRNA expression level of IL-1β and IL-8 compared to β-actin through qPCR. Data are presented as mean $\pm$ SD ($n = 3$); $^{*}P < 0.05$, $^{**}P < 0.01$, $^{***}P < 0.001$, and $^{****}P < 0.0001$.

and IL-8 downregulated under the treatment of EPO (Figure 4(b)).

Under EPO treatment, qPCR and western blot revealed that the Bax/Bcl2 ratio was downregulated, indicating a declining trend of cell apoptosis (Figures 4(c) and 4(d)). The declining trend could also be observed in cell apoptosis assay (Figure 4(e)). It was concluded that EPO attuned the inflammation and cell apoptosis raised by TNF-α.

3.5. EPO Promoted Autophagy and Angiogenesis of PDLSCs under Inflammatory Microenvironment. According to the mRNA/protein expression trend, EPO improved the expression of VEGF-a, IGF-1, and FGF-2 in a concentration-dependent manner (Figures 5(a) and 5(b)). Tube formation in vitro exhibited that EPO contributed to the angiogenic capacity of PDLSCs especially in 10, 20, and 50 IU/mL groups (Figure 5(c)).

Autophagy depressed by TNF-α was also promoted by EPO, based on the results of the mRNA/protein expression trend of Beclin1 and LC3B (Figures 5(d) and 5(e)).

3.6. EPO Regulated Autophagy, Apoptosis, and Angiogenesis of PDLSCs through the Akt/ERK1-2/BAD Signaling Pathway under Inflammatory Microenvironment. RNA sequencing was conducted to explore the signaling pathway aroused by EPO, recommending significant upregulation of
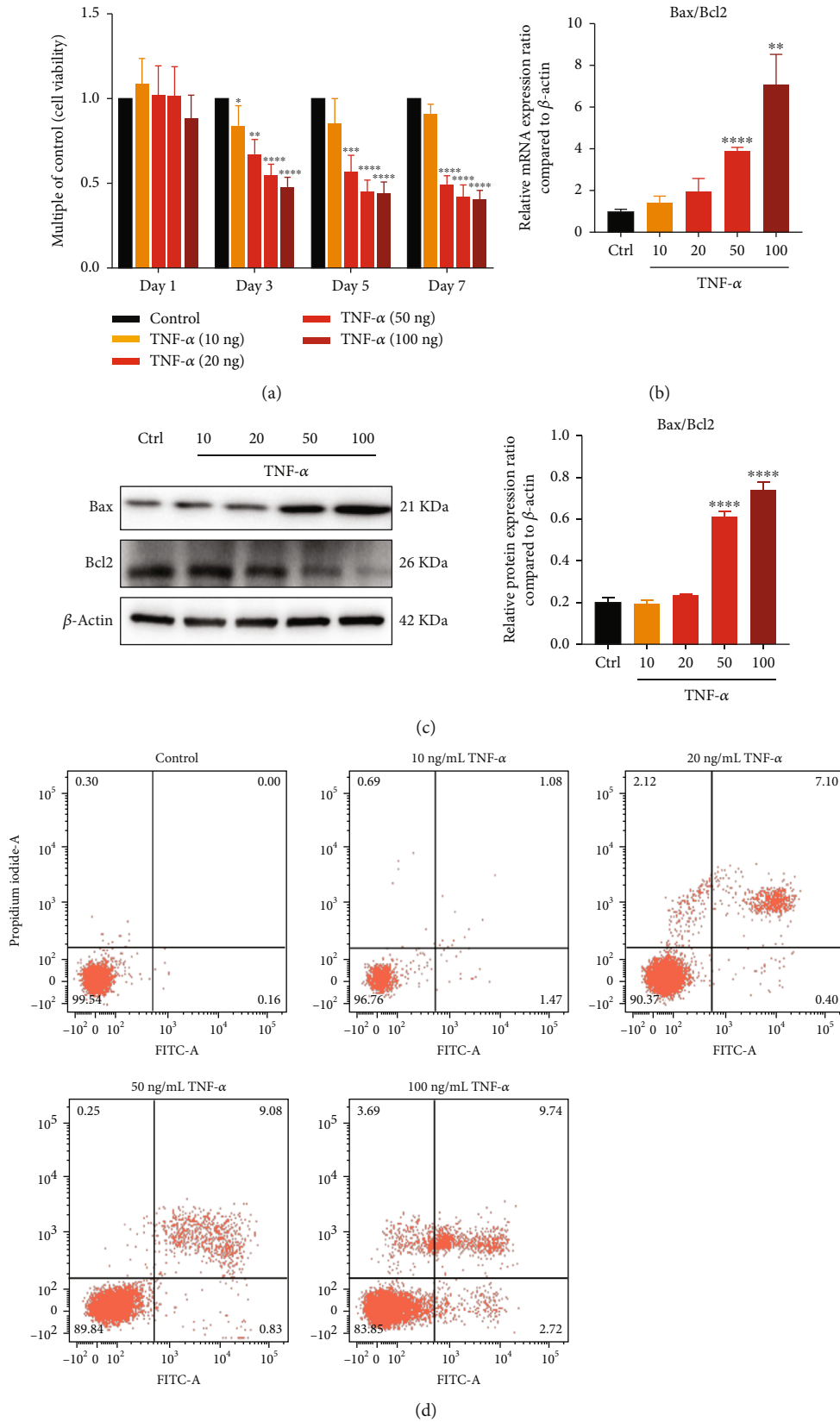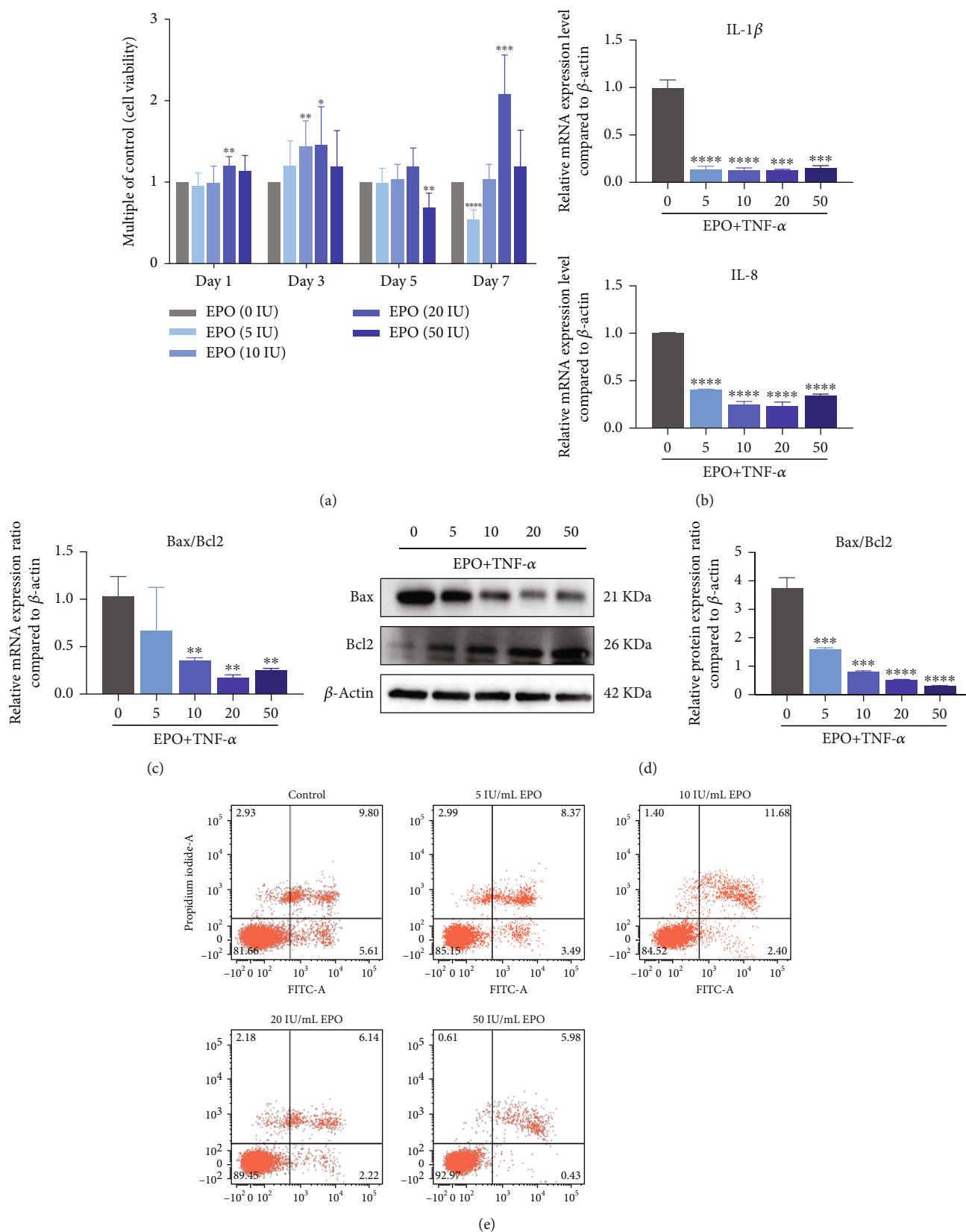
(a)

(b)

(c)

(d)

FIGURE 2: PDLSCs reduced proliferation and upregulated apoptosis under inflammatory microenvironment. (a) Cell viability of TNF-α treatment groups. (b) mRNA expression levels of Bax/Bcl2 ratio compared to β-actin through qPCR. (c) Protein expression levels of Bax/Bcl2 ratio compared to β-actin through western blot. (d) Cell apoptosis rate of TNF-α treatment groups. Data are presented as mean ± SD ($n = 3$); $^{*}P < 0.05$, $^{**}P < 0.01$, $^{***}P < 0.001$, and $^{****}P < 0.0001$.
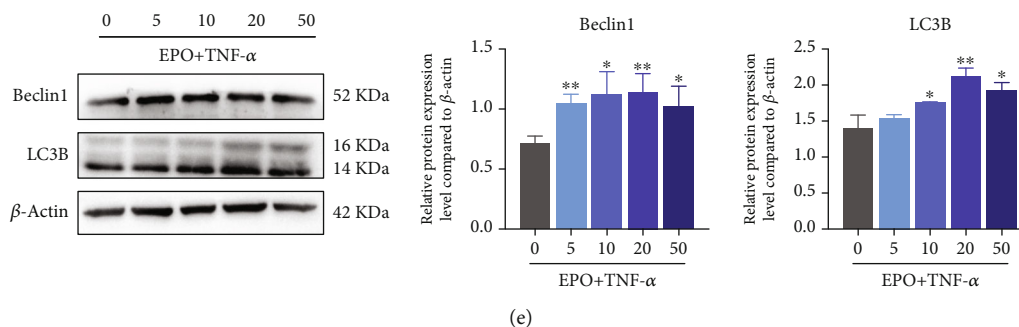
(a)

(b)

(c)

(d)
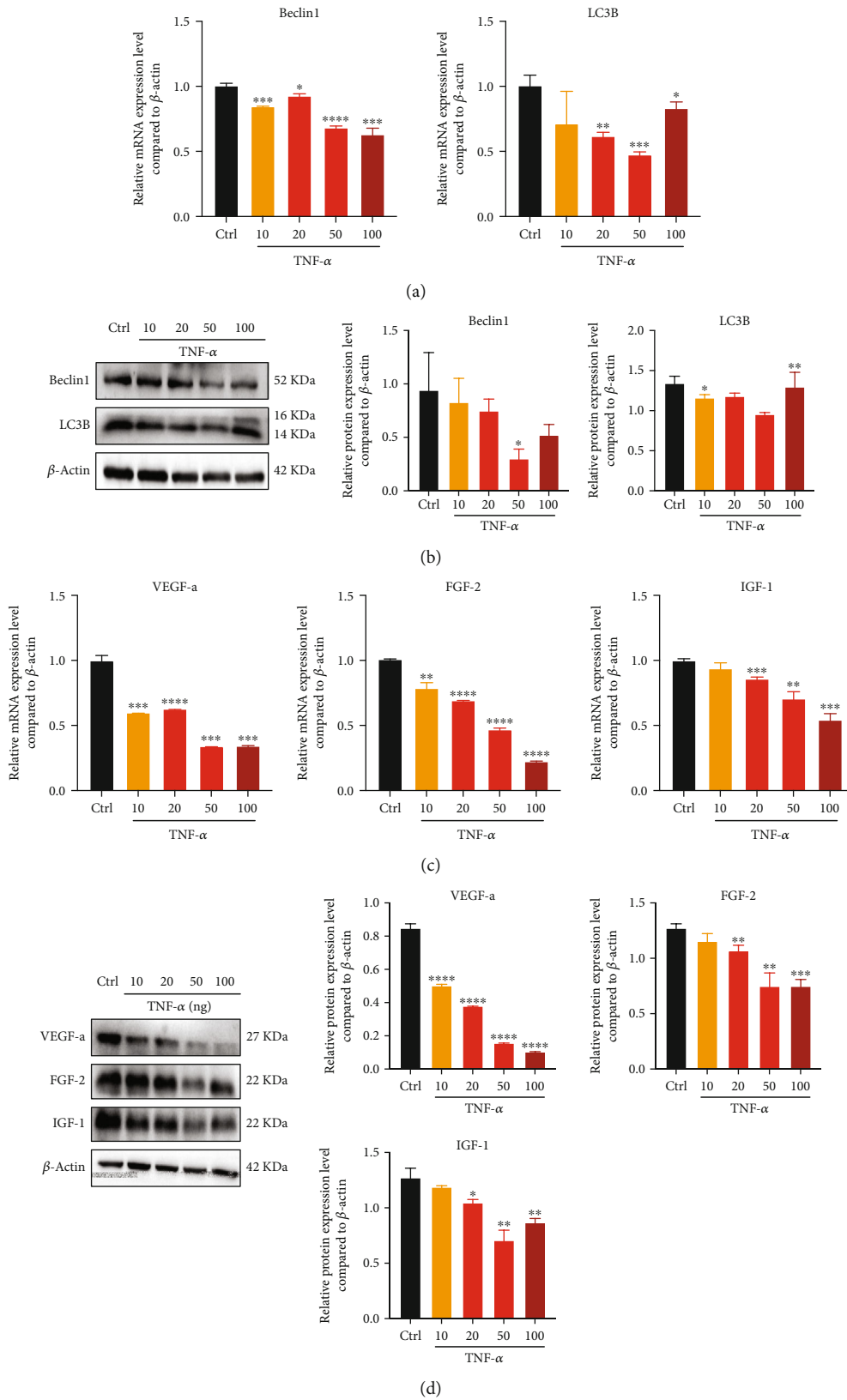
FIGURE 3: PDLSCs repressed autophagy and angiogenic capacity under inflammatory microenvironment. (a, b) mRNA and protein expression levels of Beclin1 and LC3B compared to β-actin through qPCR and western blot. (c, d) mRNA and protein expression levels of VEGF-a, FGF-2, and IGF-1 compared to β-actin through qPCR and western blot. Data are presented as mean ± SD ($n = 3$); $^{*}P < 0.05$, $^{**}P < 0.01$, $^{***}P < 0.001$, and $^{****}P < 0.0001$.

(a)

(b)

(c)

(d)

(e)

Figure 4: EPO rescued inflammation and apoptosis levels of PDLSCs under inflammatory microenvironment. (a) Cell viability of EPO treatment groups. (b) mRNA expression levels of IL-1β and IL-8 compared to β-actin through qPCR. (c, d) mRNA and protein expression levels of Bax/Bcl2 ratio compared to β-actin through qPCR and western blot. (e) Cell apoptosis rate of EPO treatment groups. Data are presented as mean ± SD ($n = 3$); $^{*}P < 0.05$, $^{**}P < 0.01$, $^{***}P < 0.001$, and $^{****}P < 0.0001$.

(a)

(b)

(c)

(d)

FIGURE 5: Continued.

(e)
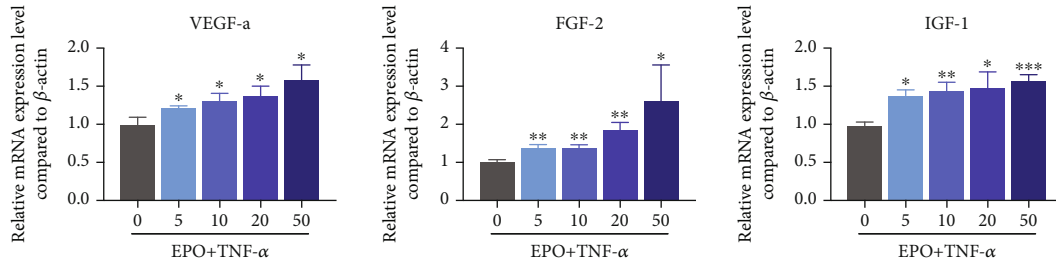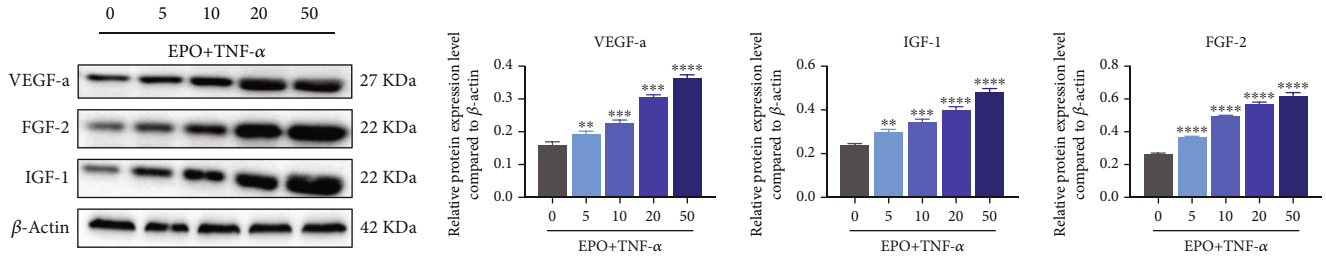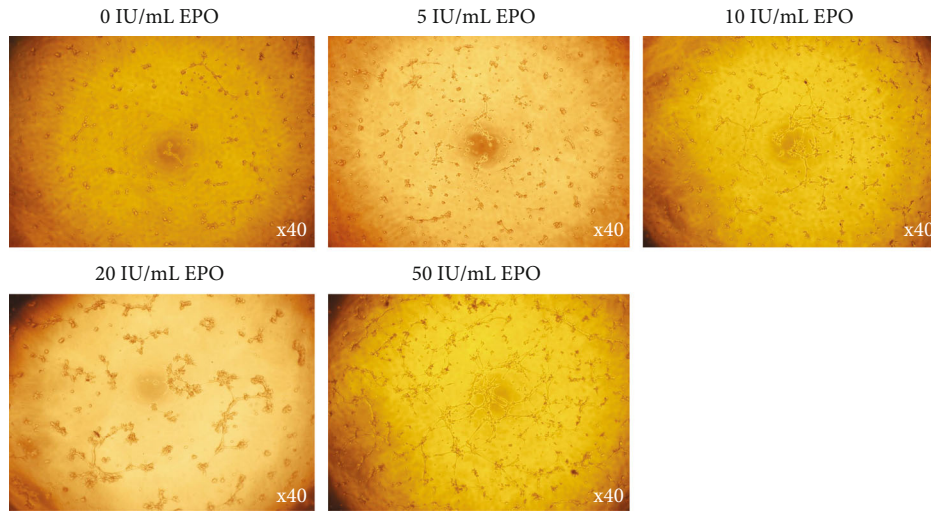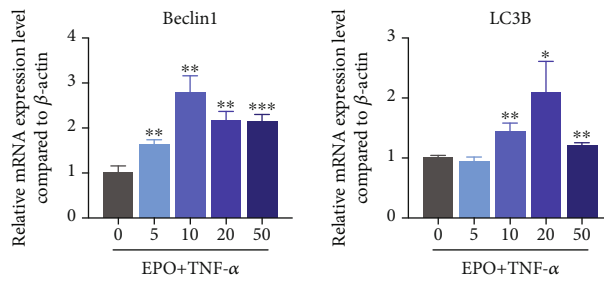
FIGURE 5: EPO promoted autophagy and angiogenesis of PDLSCs under inflammatory microenvironment. (a, b) mRNA and protein expression levels of VEGF-a, FGF-2, and IGF-1 compared to β-actin through qPCR and western blot. (c) Tube formation under EPO treatment. (d, e) mRNA and protein expression levels of Beclin1 and LC3B compared to β-actin through qPCR and western blot. Data are presented as mean $\pm$ SD ($n = 3$); $^*P < 0.05$, $^{**}P < 0.01$, $^{***}P < 0.001$, and $^{****}P < 0.0001$.

the Akt signaling pathway (Figure 6(a)). To test its validation and reliability, qPCR was used to compare mRNA changing trend, affirming the result of RNA sequencing (Figures 6(b) and 6(c)). Through searching for the KEGG maps, some crucial regulatory factors of the P13K/Akt signaling pathway (Akt, ERK1/2, and BAD) were focused and phosphorylation levels were measured by western blot (Figure 6(d)). And phosphorylation levels could be depleted by LY294002, a specific inhibitor of the P13K/Akt signaling pathway. qPCR and western blot demonstrated that LY294002 could decrease effects of EPO on cell autophagy, apoptosis, and angiogenesis (Figures 6(e) and 6(f)). Matrigel plug showed that tube numbers increased in the TNF-α+EPO group (Figure 6(g)). And cell apoptosis decreased mostly in the TNF-α+EPO group (Figure 6(h)). Images of immunofluorescence (VEGF-a, LC3B) were in accordance with the results of western blot (Figures 6(i) and 6(j)).

3.7. EPO Moderated Apoptosis and Angiogenesis of PDLSCs through Targeting Autophagy under Inflammatory Microenvironment. As an autophagy inhibitor, 3-MA was added to investigate how EPO regulated cell autophagy on apoptosis and angiogenesis. Both qPCR and western blot inferred that 3-MA could downregulate cell autophagy, further changing antiapoptosis and angiogenesis induced by EPO (Figures 7(a) and 7(b)). Matrigel plug showed that tube numbers increased in the TNF-α+EPO group (Figure 7(c)). And cell apoptosis decreased mostly in the TNF-α+EPO group (Figure 7(d)). Results of immunofluorescence (VEGF-a, LC3B) were in concord with western blot (Figures 7(e) and 7(f)).

4. Discussion

Periodontitis is always triggered by dental bacterial plaque and accelerated by local or wholesome factors. Regarding the pathological process, it involves the invasion of bacteria, activation of immune reaction, recession of junctional epithelium, and depredation of alveolar bone [35]. To defend harmful LPS originated from bacteria, TNF-α is excessively expressed in the process of periodontitis, which degrades periodontal tissue and fastens cell apoptosis [36, 37]. TNF-

α is the core inflammatory cytokine during periodontitis, which is suitable for establishment of inflammatory microenvironment [38–40]. Biological behaviors of PDLSCs were always undermined under such inflammatory microenvironment [41–44].

Here, we selected TNF-α to mock the microenvironment of periodontitis, and we established a TNF-α concentration gradient to explore biological behaviors of inflammatory PDLSCs. Coherent with existed literatures [41, 45, 46], TNF-α inhibited cell viability and increased expression of inflammatory genes *via* the NF-κB signaling pathway. Fang et al. [47] and Meng et al. [41] mentioned that TNF-α could also induce apoptosis and oxidative stress of PDLSCs, which was analogous to our study. In our research, TNF-α agitated the expression of IL-1β and IL-8, suppressed cell proliferation, and enforced Bax/Bcl2 expression ratio, especially in 50 ng/mL and 100 ng/mL groups. And other researchers also used 20 ng/mL or 50 ng/mL TNF-α to mimic the inflammatory microenvironment, which supported results. As the same, those also reckoned that proliferation rate was evidently suppressed and inflammatory cytokines expressed most on 72 hours [46, 48, 49].

Autophagy is reckoned as a double-edged sword for biological behaviors. In some views, autophagy played a harmful role in the pathogenesis, which indicated that autophagy was positively relevant to inflammatory level and apoptosis [50, 51], while some viewpoints displayed its potential therapeutic value, which could protect cells from apoptosis and promote vascularization [52]. It is controversial that TNF-α would decrease or increase cellular autophagy. Some researchers pointed that TNF-α contributed to autophagy to protect PDLSCs from apoptosis at an early stage, while attenuating autophagy in a long run [25]. Chen et.al [53] held that TNF-α often downregulated LC3B, Beclin1, and Atg7, resulting the osteogenic decline of PDLSCs. According to the results, the expression level of Beclin1 and LC3B was further diminished with the increasing concentration of TNF-α, which aggravated apoptosis. As the same, the secretions of VEGF-a, FGF-2, and IGF-1 were declined with the increasing concentration of TNF-α, which denoted the decreasing angiogenic level. Taken together, autophagy impaired by TNF-α was considered as a protective factor
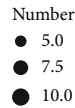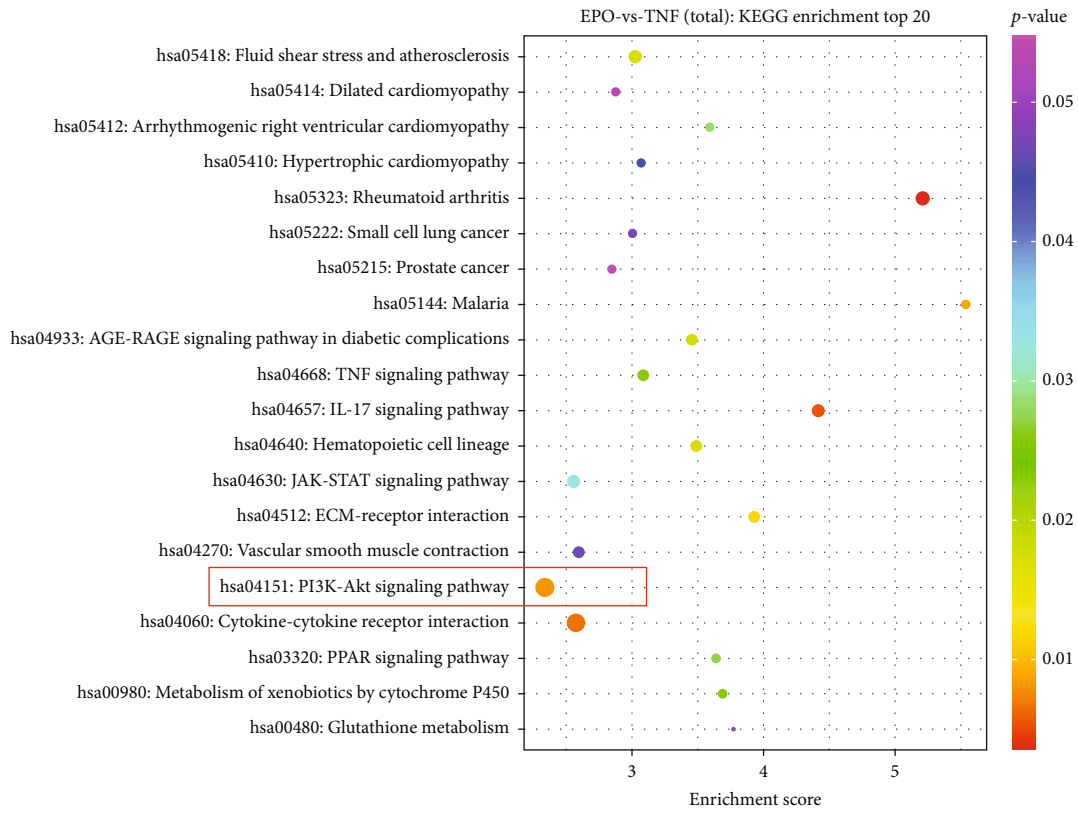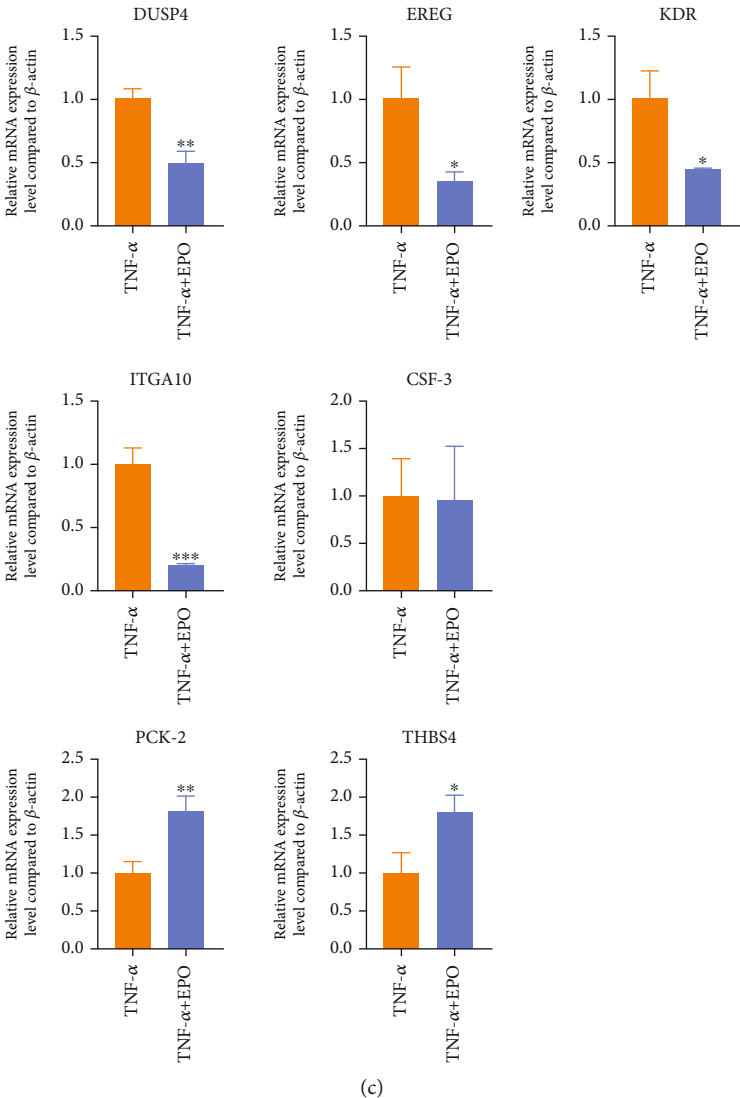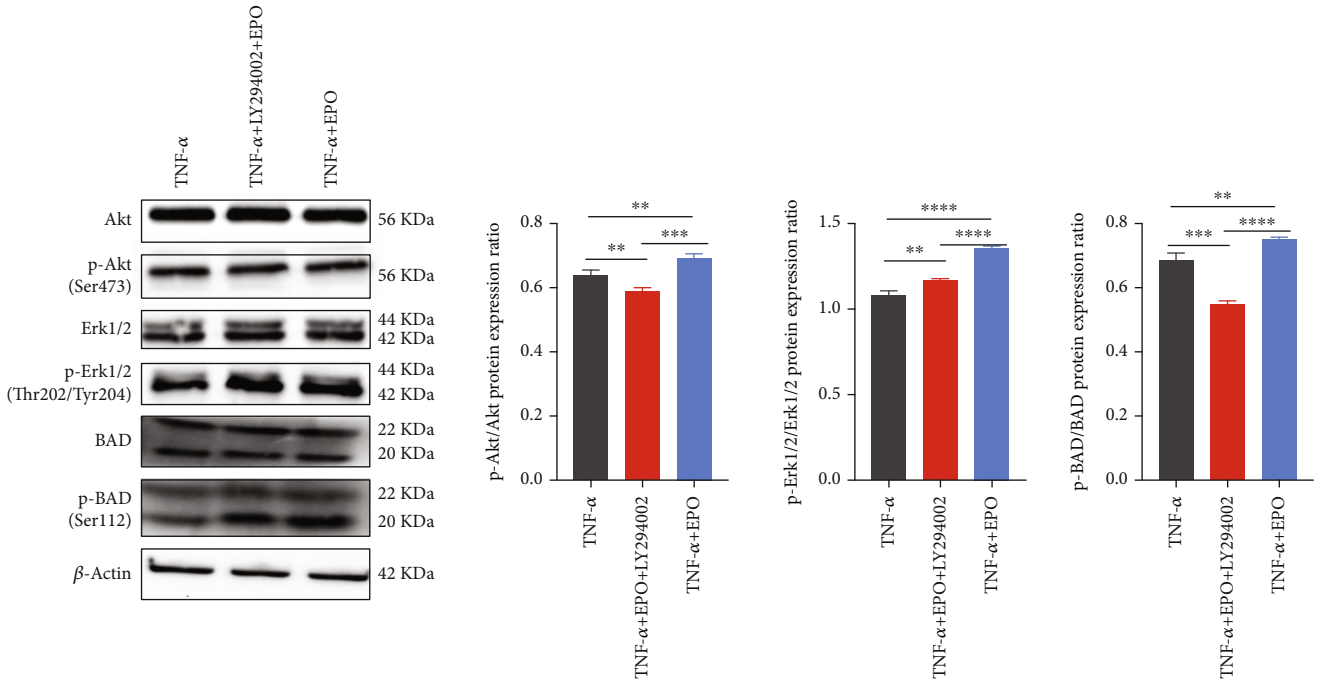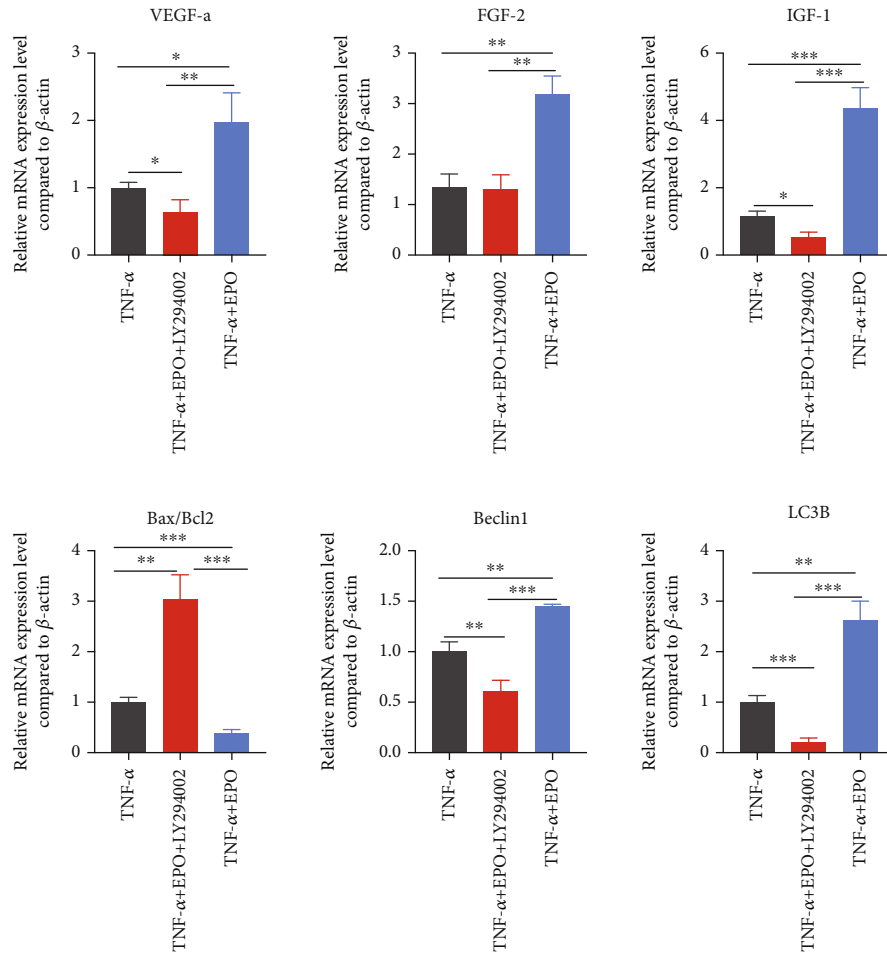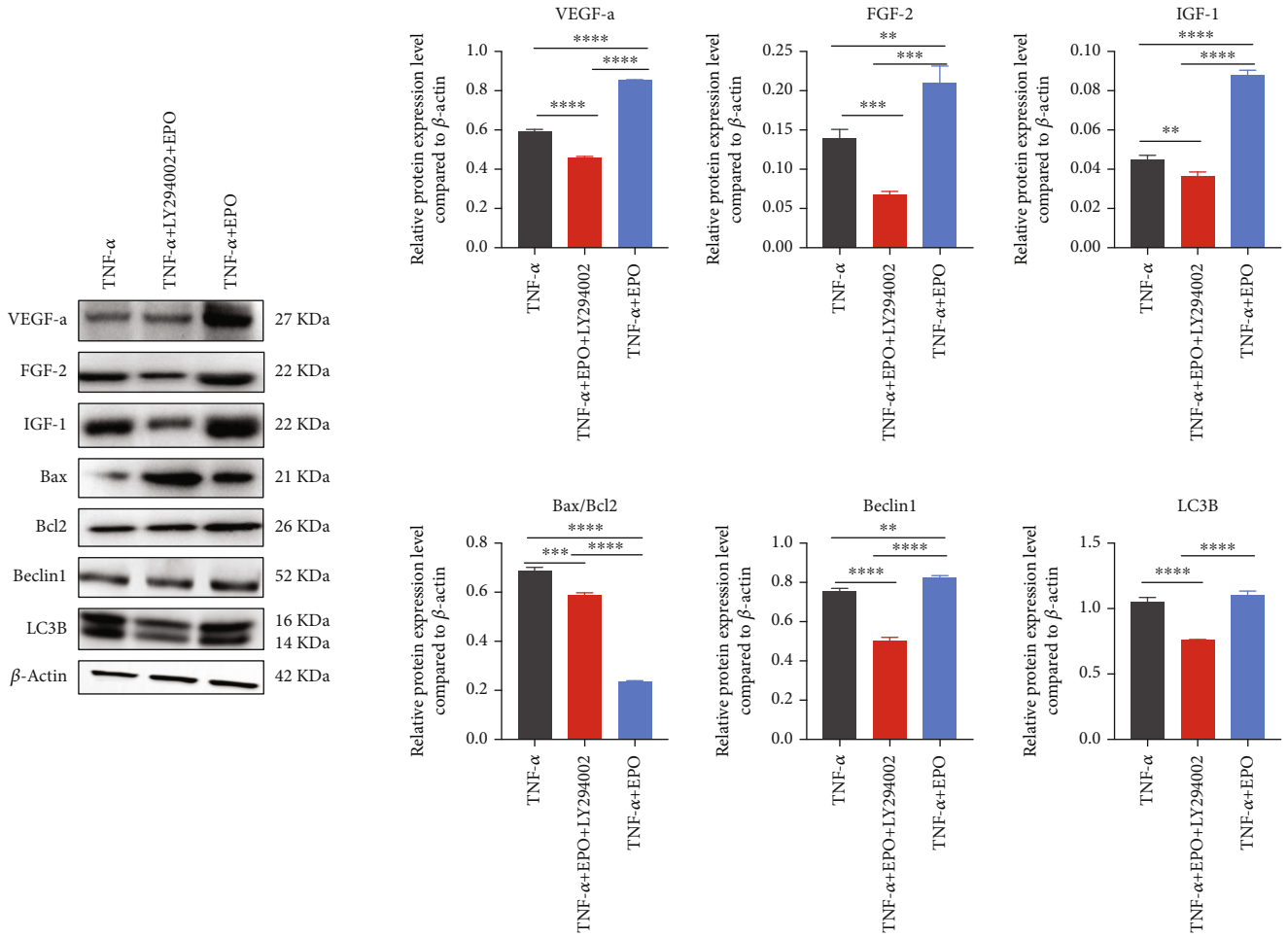
(a)
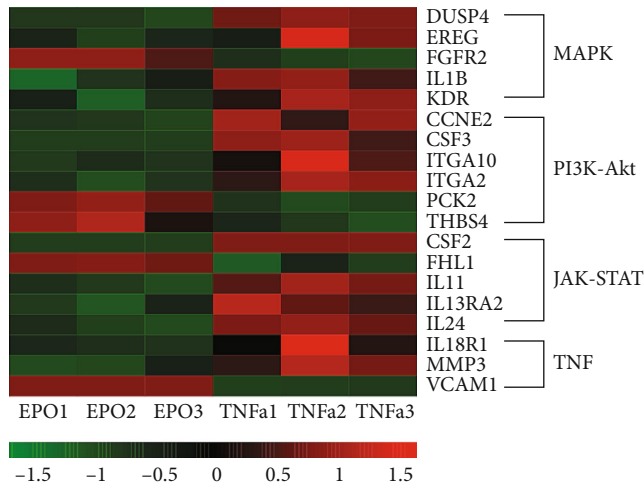
(b)

FIGURE 6: Continued.

(c)
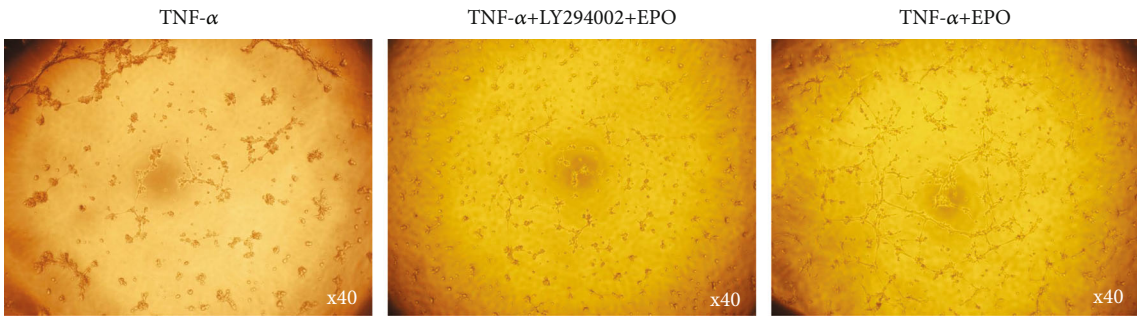
Figure 6: Continued.
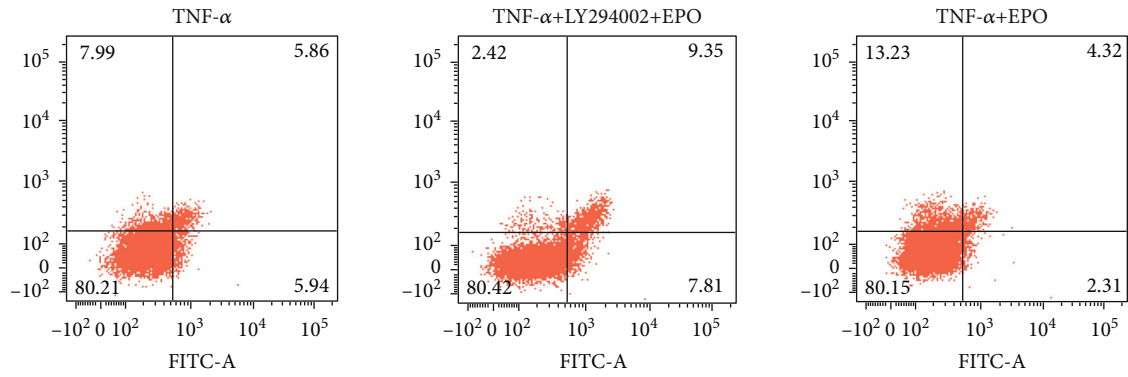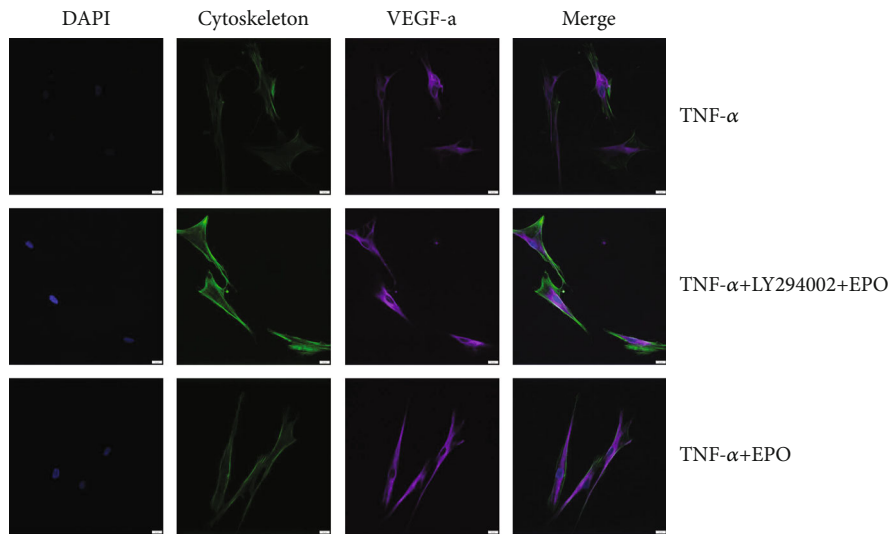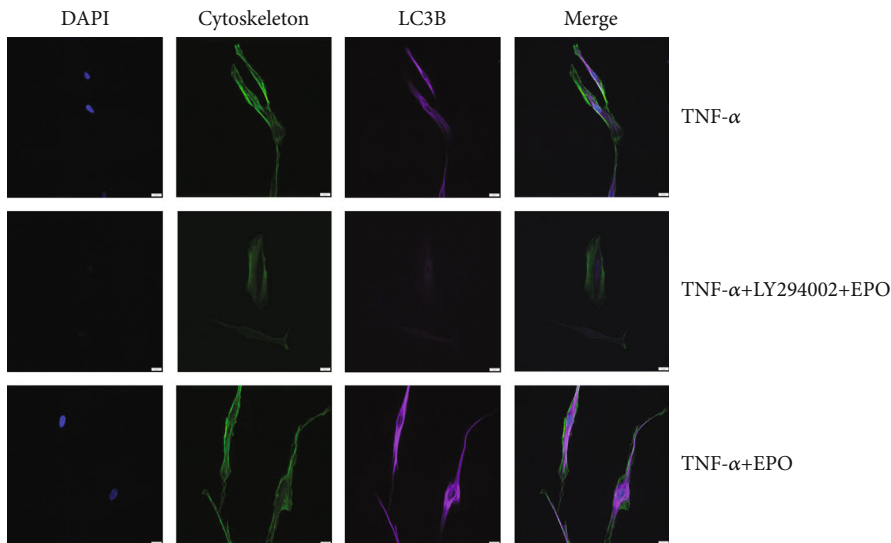
(d)

(e)

Figure 6: Continued.

(f)

(g)

Figure 6: Continued.

(h)

(i)

(j)

FIGURE 6: EPO regulated autophagy, apoptosis, and angiogenesis of PDLSCs through the Akt/ERK1-2/BAD signaling pathway under inflammatory microenvironment. (a) Bubble map of KEGG enrichment of RNA sequencing. (b, c) Heat map of enriched genes and qPCR validation (CSF3, ITGA10, PCK2, THBS4, DUSP4, ERGE, and KDR). (d) Protein expression levels of Akt, p-Akt, Erk1/2, p-Erk1/2, BAD, and p-BAD through western blot. (e, f) mRNA and protein expression levels of VEGF-a, FGF-2, IGF-1, Bax/Bcl2, Beclin1, and LC3B through qPCR and western blot. (g) Tube formation under different treatments. (h) Cell apoptosis rate under different treatments. (i, j) Immunofluorescence on DAPI, cytoskeleton, and VEGF-a/LC3B. Data are presented as mean ± SD ($n = 3$); $^{*}P < 0.05$, $^{**}P < 0.01$, $^{***}P < 0.001$, and $^{****}P < 0.0001$.

(a)

FIGURE 7: Continued.

(b)

(c)
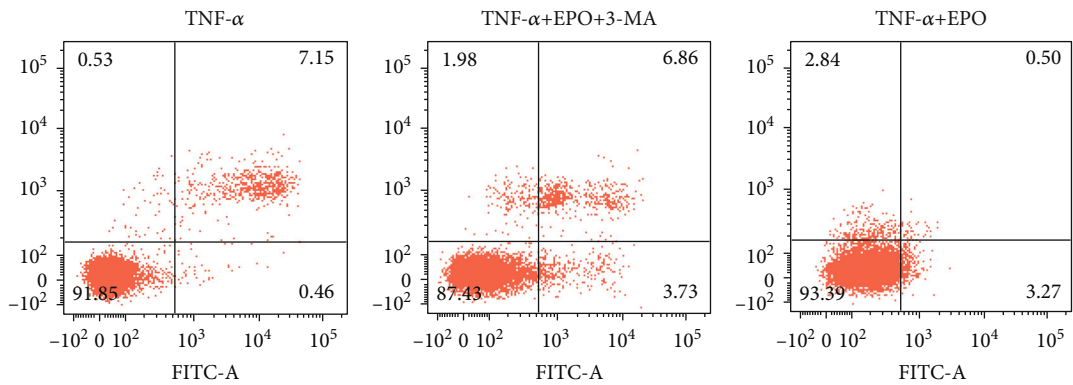
(d)

FIGURE 7: Continued.

(e)

(f)
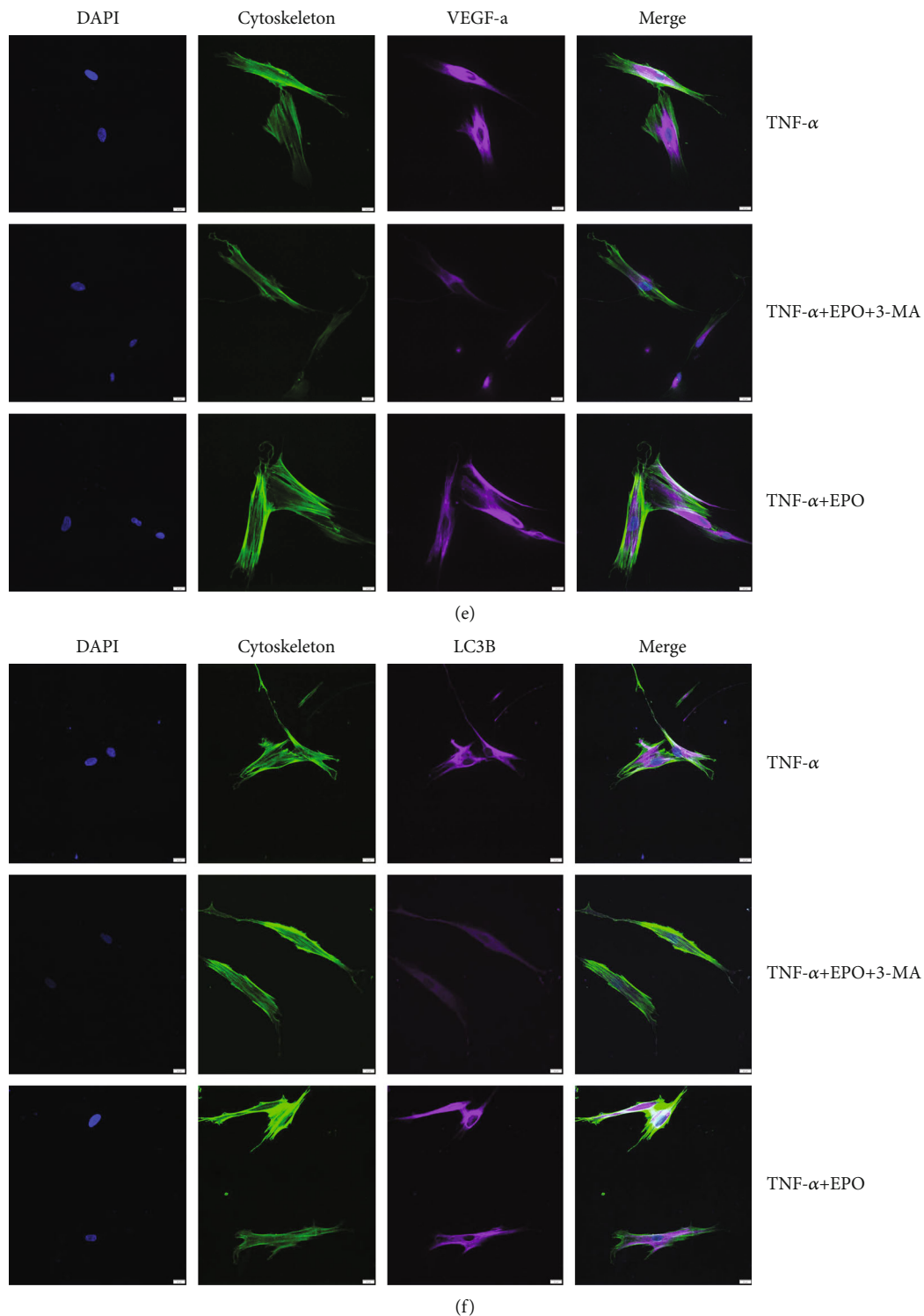
FIGURE 7: EPO moderated apoptosis and angiogenesis of PDLSCs through targeting autophagy under inflammatory microenvironment. (a, b) mRNA and protein expression levels of VEGF-a, FGF-2, IGF-1, Bax/Bcl2, Beclin1, and LC3B through qPCR and western blot. (c) Tube formation under different treatments. (d) Cell apoptosis rate under different treatments. (e, f) Immunofluorescence on DAPI, cytoskeleton, and VEGF-a/LC3B. Data are presented as mean ± SD ($n = 3$); $^*P < 0.05$, $^{**}P < 0.01$, $^{***}P < 0.001$, and $^{****}P < 0.0001$.
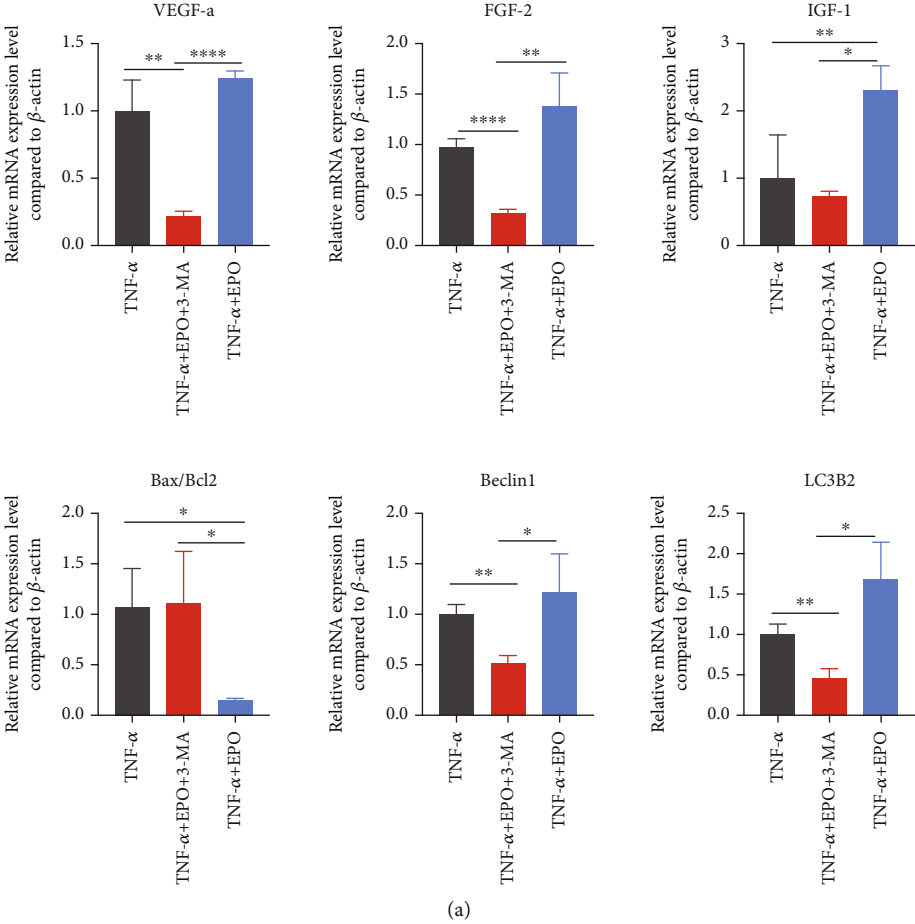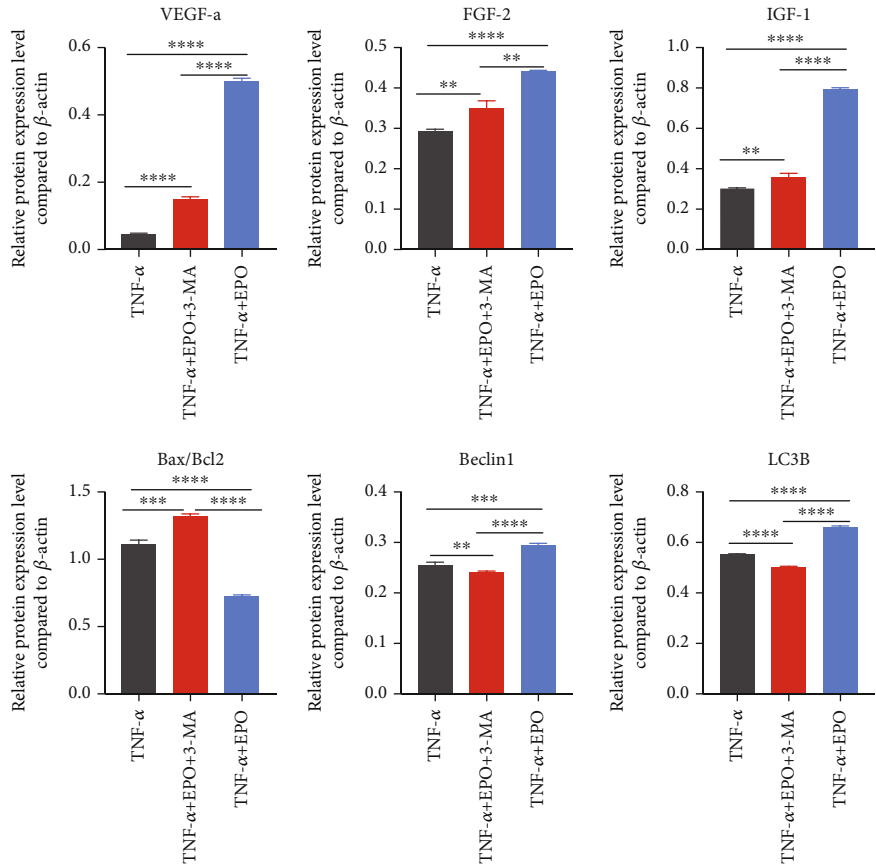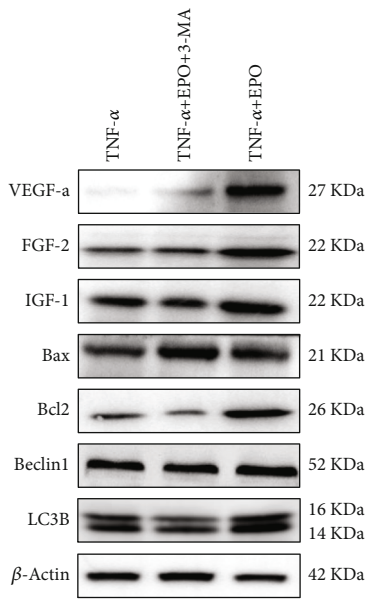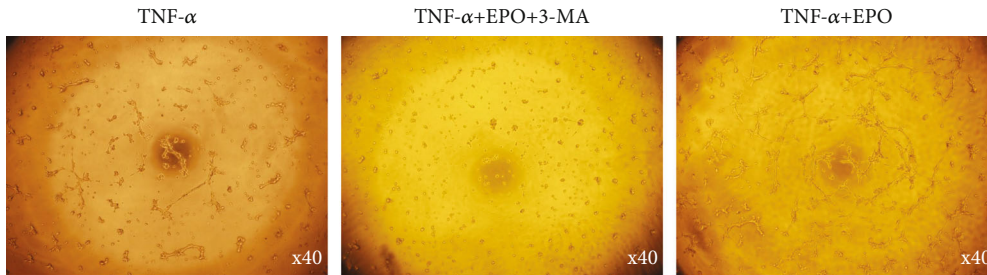
for PDLSCs in the inflammatory microenvironment. Collectively, 50 ng/mL TNF-α was picked for the continuing experiment.

EPO has been learned as a multifunctional cytokine/ drug for wound healing and bone regeneration, particularly in the realm of periodontology [54–56]. An avalanche of

researches argued that EPO attenuated inflammation, contributed to antiapoptosis, enhanced autophagy, and promoted angiogenesis [13, 18, 57–59]. Meanwhile, some researches [60–62] supported that EPO receptor (EPOR) was expressed in many CD105^{+}/CD90^{+}/CD44^{+} stem cells—such as PDLSCs, dental pulp stem cells, and bone marrow progenitor cells—which demonstrated that the EPO/EPOR signaling pathway played a crucial role in regulating biological behaviors of these cells. And PDLSCs were also characterized as CD105^{+}, CD90^{+}, and CD44^{+} mesenchymal stem cells. The expression of EPOR on CD105^{+}/CD90^{+}/CD44^{+} PDLSCs provided basics for EPO treatment. Therefore, we conducted experiments focusing on the protective effects of EPO for PDLSCs. In the inflammatory microenvironment, proliferation of PDLSCs was enhanced with the treatment of EPO, especially in the 20 IU/mL group. IL-1β and IL-8 were obviously resisted after the treatment of EPO. Likewise, a similar experiment showed that the inflammation level of PDLSCs could be attenuated by ascorbic acid, revealing that inflammation of PDLSCs was significantly related with the NF-κB signaling pathway and DNMT1, which could activate expression of proinflammatory cytokines [63]. The expression ratio of Bax/Bcl2 was also inhibited, which protected cells from early or late apoptosis. Additionally, the strengthening expression of VEGF-a, FGF-2, and IGF-1 could also be noted under the treatment of EPO, which indicated the upregulating angiogenesis of PDLSCs. Autophagy-related genes Beclin1 and LC3B were also heightened by EPO, especially in 10 IU/mL and 20 IU/mL groups. Above these data, it was speculated that EPO could preserve antiapoptosis, angiogenesis, and autophagy of PDLSCs under inflammatory microenvironment, which suggested its promising use for controlling periodontitis. Regarding its various effects on PDLSCs, therefore, 20 IU/mL EPO was the optimal group for subsequent experiments.

The Akt signaling pathway always participated in the regulation of apoptosis, autophagy, and angiogenesis [27, 29]. Akt was also the main target of EPO, bridging the downstream signal and interacting with autophagy and then stirring up biological activities and determining cell fate [58, 59, 64]. According to RNA-sequencing results, KEGG enrichment demonstrated that the P13K/Akt signaling pathway was significantly upregulated in EPO treatment groups. Through analyzing the KEGG map, Akt, Erk1/2, and BAD were taken into measurement. According to the existing references, LY294002, an inhibitor for the PI3K/Akt signaling pathway, has been confirmed that could also inhibit the phosphorylation of Akt, ERK1/2, and BAD in human or rat cells [65–67]. Phosphorylated Akt, Erk1/2, and BAD protein were raised by EPO and suppressed by TNF-α or PI3K/Akt specific inhibitor—LY294002, denoting that the Akt/Erk1/2/BAD signaling pathway was activated through phosphorylation. p-Erk1/2 and p-BAD changed following the change of phosphorylated Akt. VEGF-a, FGF-2, and IGF-1 levels may be regulated by p-Erk1/2 [68]; Bax/Bcl2 ratio may be relevant to p-BAD [69]; Beclin1 and LC3B may be targeted by Akt [70]. Additionally, some researchers also found that expression of LC3 and Erk/p-Erk played a vital role in the regulation of dental pulp stem cell inflammation,

suggesting that the prompt LC3 and p-Erk rescued autophagy, which was consistent with our results [71]. LY294002 could reverse tube numbers induced by EPO and also aggravate cell apoptosis attenuated by EPO. Collectively, EPO could enhance antiapoptosis, angiogenesis, and autophagy of PDLSCs via the Akt/Erk1/2/BAD signaling pathway under inflammatory microenvironment, which would be blocked by LY294002.

Autophagy also dually moderates apoptosis and angiogenesis [24, 25]. In one viewpoint, autophagy maintains cell survivability through blocking the Akt signaling pathway [72, 73]. Contradictorily, another view argued that autophagy was reserved by activating the Akt signaling pathway [28, 30]. Our data has revealed that autophagy could be regulated by the Akt/Erk1/2/BAD signaling pathway. Wondering whether autophagy increased by EPO could regulate apoptosis and angiogenesis, autophagy inhibitor 3-methyladenine (3-MA) was used to verify its effects. When 3-MA was added, Beclin1, LC3B, VEGF-a, FGF-2, and IGF-1 levels decreased compared to the TNF-α+EPO group; Bax/Bcl2 ratio increased compared to the TNF-α+EPO group. Noticeably, 3-MA reduced tube numbers enhanced by EPO and augmented cell apoptosis rescued by EPO. Comprehensively, autophagy lifted by EPO could also moderate apoptosis and angiogenesis of PDLSCs under inflammatory microenvironment.

However, there still exists drawback, such as lack of animal experiments. A step further, *in vivo* experiments would be conducted to testify its *in vivo* effects. Due to the limitations of fundamental experiment, clinical performance was not certain, requiring further research.

Above all, EPO attenuated inflammation, reduced apoptosis, rescued autophagy, and augmented angiogenesis of PDLSCs under inflammatory microenvironment. And its potential mechanism was also conducted. EPO activated autophagy to moderate apoptosis and angiogenesis via the Akt/Erk1/2/BAD signaling pathway (Supplementary Figure 2, graphical abstract). Our research provided a novel strategy for curing periodontal inflammation and accomplishing angiogenic tissue engineering.

5. Conclusion

It could be demonstrated that EPO could protect biological behaviors of PDLSCs from inflammatory microenvironment and promote angiogenic tissue regeneration, which brought a brand-new sight for periodontal tissue engineering.

Abbreviations

EPO:	Erythropoietin
PDLSCs:	Periodontal ligament stem cells
TNF-α:	Tumor necrosis factor-α
APSCs:	Apical papilla stem cells
MSCs:	Mesenchymal stem cells
BMSCs:	Bone marrow stem cells
VECs:	Vein endothelial cells
TNFAIP3:	Tumor necrosis factor alpha-induced protein 3
PDLCs:	Periodontal ligament cells

LPS: Lipopolysaccharide
ASCs: Adipose-derived stem cells
FBS: Fetal bovine serum
CCK-8: Cell Counting Kit-8
qPCR: Real-time quantitative polymerase chain reaction.

Data Availability

All the research data used to support the findings of this study are available from the corresponding author upon request.

Conflicts of Interest

The authors declare that there are no conflicts of interest regarding the publication of this paper.

Authors' Contributions

Denghao Huang was responsible for investigation, methodology, and roles/writing—original draft. Jie Lei was responsible for roles/writing—original draft, investigation, and methodology. Xingrui Li was responsible for investigation and data curation. Zhonghao Jiang was responsible for methodology and data curation. Maoxuan Luo was responsible for writing—review and editing and supervision. Yao Xiao was responsible for supervision, project administration, and funding acquisition. Denghao Huang and Jie Lei contributed equally to this work as co-first authors.

Acknowledgments

Supplementary Materials

Supplementary 1. Supplementary Figure 1: results of western blot assay have been replicated for three times and blots are included in the file.

Supplementary 2. Supplementary Figure 2: EPO attenuated inflammation, reduced apoptosis, rescued autophagy, and augmented angiogenesis of PDLSCs under inflammatory microenvironment. EPO activated autophagy to moderate apoptosis and angiogenesis via the Akt/Erk1/2/BAD signaling pathway.

References

[1] P. I. Eke, B. A. Dye, L. Wei et al., "Update on prevalence of periodontitis in adults in the United States: NHANES 2009 to 2012," *Journal of Periodontology*, vol. 86, no. 5, pp. 611–622, 2015.

[2] N. Silva, L. Abusleme, D. Bravo et al., "Host response mechanisms in periodontal diseases," *Journal of Applied Oral Science*, vol. 23, no. 3, pp. 329–355, 2015.

[3] M. Costalonga and M. C. Herzberg, "The oral microbiome and the immunobiology of periodontal disease and caries," *Immunology Letters*, vol. 162, no. 2, pp. 22–38, 2014.

[4] M. C. Bottino, V. Thomas, G. Schmidt et al., "Recent advances in the development of GTR/GBR membranes for periodontal regeneration–a materials perspective," *Dental Materials*, vol. 28, no. 7, pp. 703–721, 2012.

[5] F. M. Chen and Y. Jin, "Periodontal tissue engineering and regeneration: current approaches and expanding opportunities," *Tissue Engineering. Part B, Reviews*, vol. 16, no. 2, pp. 219–255, 2010.

[6] S. Hemmat, D. M. Lieberman, and S. P. Most, "An introduction to stem cell biology," *Facial Plastic Surgery*, vol. 26, no. 5, pp. 343–349, 2010.

[7] B. M. Seo, M. Miura, S. Gronthos et al., "Investigation of multipotent postnatal stem cells from human periodontal ligament," *The Lancet*, vol. 364, no. 9429, pp. 149–155, 2004.

[8] J. Kang, W. Fan, Q. Deng, H. He, and F. Huang, "Stem cells from the apical papilla: a promising source for stem cell-based therapy," *BioMed Research International*, vol. 2019, Article ID 6104738, 8 pages, 2019.

[9] A. Tomokiyo, N. Wada, and H. Maeda, "Periodontal ligament stem cells: regenerative potency in periodontium," *Stem Cells and Development*, vol. 28, no. 15, pp. 974–985, 2019.

[10] Á. E. Mercado-Pagán, A. M. Stahl, Y. Shanjani, and Y. Yang, "Vascularization in bone tissue engineering constructs," *Annals of Biomedical Engineering*, vol. 43, no. 3, pp. 718–729, 2015.

[11] M. Pandya, M. Saxon, J. Bozanich, C. Tillberg, X. Luan, and T. G. H. Diekwisch, "The glycoprotein/cytokine erythropoietin promotes rapid alveolar ridge regeneration in vivo by promoting new bone extracellular matrix deposition in conjunction with coupled angiogenesis/osteogenesis," *International Journal of Molecular Sciences*, vol. 22, no. 6, p. 2788, 2021.

[12] Q. Gong, J. Zeng, X. Zhang et al., "Effect of erythropoietin on angiogenic potential of dental pulp cells," *Experimental and Therapeutic Medicine*, vol. 22, no. 4, p. 1079, 2021.

[13] Y. Wang, P. Wang, Q. Wu et al., "Loading of erythropoietin on biphasic calcium phosphate bioceramics promotes osteogenesis and angiogenesis by regulating EphB4/EphrinB2 molecules," *Journal of Materials Science. Materials in Medicine*, vol. 33, no. 2, p. 19, 2022.

[14] D. Li, L. Deng, X. Xie, Z. Yang, and P. Kang, "Evaluation of the osteogenesis and angiogenesis effects of erythropoietin and the efficacy of deproteinized bovine bone/recombinant human erythropoietin scaffold on bone defect repair," *Journal of Materials Science. Materials in Medicine*, vol. 27, no. 6, 2016.

[15] A. S. Tsiftsoglou, "Erythropoietin (EPO) as a key regulator of erythropoiesis, bone remodeling and endothelial transdifferentiation of multipotent mesenchymal stem cells (MSCs): implications in regenerative medicine," *Cell*, vol. 10, no. 8, p. 2140, 2021.

[16] D. H. Zheng, X. X. Wang, D. Ma, L. N. Zhang, Q. F. Qiao, and J. Zhang, "Erythropoietin enhances osteogenic differentiation of human periodontal ligament stem cells via Wnt/β-catenin signaling pathway," *Drug Design, Development and Therapy*, vol. 13, pp. 2543–2552, 2019.

[17] L. Wang, F. Wu, Y. Song, Y. Duan, and Z. Jin, "Erythropoietin induces the osteogenesis of periodontal mesenchymal stem cells from healthy and periodontitis sources via activation of the p38 MAPK pathway," *International Journal of Molecular Medicine*, vol. 41, no. 2, pp. 829–835, 2017.

[18] D. H. Zheng, Z. Q. Han, X. X. Wang, D. Ma, and J. Zhang, "Erythropoietin attenuates high glucose-induced oxidative stress and inhibition of osteogenic differentiation in periodontal ligament stem cell (PDLSCs)," *Chemico-Biological Interactions*, vol. 305, pp. 40–47, 2019.

[19] P. K. Govindappa and J. C. Elfar, "Erythropoietin promotes M2 macrophage phagocytosis of Schwann cells in peripheral nerve injury," *Cell Death & Disease*, vol. 13, no. 3, p. 245, 2022.

[20] Y. Wang, Y. Mo, M. Peng et al., "The influence of circular RNAs on autophagy and disease progression," *Autophagy*, vol. 18, no. 2, pp. 240–253, 2022.

[21] N. Jiang, D. He, Y. Ma et al., "Force-induced autophagy in periodontal ligament stem cells modulates M1 macrophage polarization via AKT signaling," *Frontiers in Cell and Development Biology*, vol. 9, 2021.

[22] K. Zhang, F. Liu, D. Jin et al., "Autophagy preserves the osteogenic ability of periodontal ligament stem cells under high glucose conditions in rats," *Archives of Oral Biology*, vol. 101, pp. 172–179, 2019.

[23] T. Chen, F. Gao, D. Luo et al., "Cistanoside A promotes osteogenesis of primary osteoblasts by alleviating apoptosis and activating autophagy through involvement of the Wnt/β-catenin signal pathway," *Annals of Translational Medicine*, vol. 10, no. 2, p. 64, 2022.

[24] W. Wei, Y. An, Y. An, D. Fei, and Q. Wang, "Activation of autophagy in periodontal ligament mesenchymal stem cells promotes angiogenesis in periodontitis," *Journal of Periodontology*, vol. 89, no. 6, pp. 718–727, 2018.

[25] Y. An, W. Liu, P. Xue, Y. Zhang, Q. Wang, and Y. Jin, "Increased autophagy is required to protect periodontal ligament stem cells from apoptosis in inflammatory microenvironment," *Journal of Clinical Periodontology*, vol. 43, no. 7, pp. 618–625, 2016.

[26] H. Tang, Y. Ye, L. Li et al., "A20 alleviated caspase-1-mediated pyroptosis and inflammation stimulated by Porphyromonas gingivalis lipopolysaccharide and nicotine through autophagy enhancement," *Human Cell*, vol. 35, no. 3, pp. 803–816, 2022.

[27] L. Shi, B. Li, B. Zhang, C. Zhen, J. Zhou, and S. Tang, "Mouse embryonic palatal mesenchymal cells maintain stemness through the PTEN-Akt-mTOR autophagic pathway," *Stem Cell Research & Therapy*, vol. 10, no. 1, p. 217, 2019.

[28] W. Liu, L. Xu, X. Wang et al., "PRDX1 activates autophagy via the PTEN-AKT signaling pathway to protect against cisplatin-induced spiral ganglion neuron damage," *Autophagy*, vol. 17, no. 12, pp. 4159–4181, 2021.

[29] B. Zhao, Q. Peng, E. H. L. Poon et al., "Leonurine promotes the osteoblast differentiation of rat BMSCs by activation of autophagy via the PI3K/Akt/mTOR pathway," *Frontiers in Bioengineering and Biotechnology*, vol. 9, 2021.

[30] L. Qu, C. Chen, W. He et al., "Glycyrrhizic acid ameliorates LPS-induced acute lung injury by regulating autophagy through the PI3K/AKT/mTOR pathway," *American Journal of Translational Research*, vol. 11, no. 4, pp. 2042–2055, 2019.

[31] J. Yang, J. Gao, F. Gao et al., "Extracellular vesicles-encapsulated microRNA-29b-3p from bone marrow-derived mesenchymal stem cells promotes fracture healing via modulation of the PTEN/PI3K/AKT axis," *Experimental Cell Research*, vol. 412, no. 2, 2022.

[32] Y. Sun, Y. Li, Y. Zhang, T. Wang, K. Lin, and J. Liu, "A polydopamine-assisted strontium-substituted apatite coating for titanium promotes osteogenesis and angiogenesis via FAK/MAPK and PI3K/AKT signaling pathways," *Materials Science & Engineering. C, Materials for Biological Applications*, vol. 131, p. 112482, 2021.

[33] Y. Yi, M. Wu, X. Zhou et al., "Ascorbic acid 2-glucoside pre-conditioning enhances the ability of bone marrow mesenchymal stem cells in promoting wound healing," *Stem Cell Research & Therapy*, vol. 13, no. 1, p. 119, 2022.

[34] Z. Zhu, L. Guo, N. Yeltai, H. Xu, and Y. Zhang, "Chemokine (C-C motif) ligand 2-enhanced adipogenesis and angiogenesis of human adipose-derived stem cell and human umbilical vein endothelial cell co-culture system in adipose tissue engineering," *Journal of Tissue Engineering and Regenerative Medicine*, vol. 16, no. 2, pp. 163–176, 2022.

[35] K. Chatzivasileiou, K. Kriebel, G. Steinhoff, B. Kreikemeyer, and H. Lang, "Do oral bacteria alter the regenerative potential of stem cells? A concise review," *Journal of Cellular and Molecular Medicine*, vol. 19, no. 9, pp. 2067–2074, 2015.

[36] H. Kato, Y. Taguchi, K. Tominaga, M. Umeda, and A. Tanaka, "Porphyromonas gingivalis LPS inhibits osteoblastic differentiation and promotes pro-inflammatory cytokine production in human periodontal ligament stem cells," *Archives of Oral Biology*, vol. 59, no. 2, pp. 167–175, 2014.

[37] E. Schilling, R. Weiss, A. Grahnert, M. Bitar, U. Sack, and S. Hauschildt, "Molecular mechanism of LPS-induced TNF-α biosynthesis in polarized human macrophages," *Molecular Immunology*, vol. 93, pp. 206–215, 2018.

[38] O. S. Kim, K. J. Park, H. M. Jin et al., "Activation and increased production of interleukin-17 and tumour necrosis factor-α of mucosal-associated invariant T cells in patients with periodontitis," *Journal of Clinical Periodontology*, vol. 49, no. 7, pp. 706–716, 2022.

[39] K. K. Y. Pereira, C. M. Jara, G. L. Antunes et al., "Effects of periodontitis and periodontal treatment on systemic inflammatory markers and metabolic profile in obese and non-obese rats," *Journal of Periodontology*, 2022.

[40] X. Liu and H. Li, "A systematic review and meta-analysis on multiple cytokine gene polymorphisms in the pathogenesis of periodontitis," *Frontiers in Immunology*, vol. 12, 2021.

[41] T. Meng, Y. Zhou, J. Li et al., "Azithromycin promotes the osteogenic differentiation of human periodontal ligament stem cells after stimulation with TNF-α," *Stem Cells International*, vol. 2018, Article ID 7961962, 11 pages, 2018.

[42] N. Yang, Y. Li, G. Wang, Y. Ding, Y. Jin, and Y. Xu, "Tumor necrosis factor-α suppresses adipogenic and osteogenic differentiation of human periodontal ligament stem cell by inhibiting miR-21/Spry1 functional axis," *Differentiation*, vol. 97, pp. 33–43, 2017.

[43] X. Liu, G. R. Tan, M. Yu et al., "The effect of tumour necrosis factor-α on periodontal ligament stem cell differentiation and the related signaling pathways," *Current Stem Cell Research & Therapy*, vol. 11, no. 7, pp. 593–602, 2016.

[44] Y. J. Wang, P. Zhao, B. D. Sui et al., "Resveratrol enhances the functionality and improves the regeneration of mesenchymal stem cell aggregates," *Experimental & Molecular Medicine*, vol. 50, no. 6, pp. 1–15, 2018.

[45] W. Zhu, Q. Qiu, H. Luo et al., "High glucose exacerbates TNF-α-induced proliferative inhibition in human periodontal ligament stem cells through upregulation and activation of TNF receptor 1," *Stem Cells International*, vol. 2020, Article ID 4910767, 17 pages, 2020.

[46] H. Luo, W. Zhu, W. Mo, and M. Liang, "High-glucose concentration aggravates TNF-alpha-induced cell viability reduction in human CD146-positive periodontal ligament cells via TNFR-1 gene demethylation," *Cell Biology International*, vol. 44, no. 12, pp. 2383–2394, 2020.

[47] H. Fang, K. Yang, P. Tang et al., "Glycosylation end products mediate damage and apoptosis of periodontal ligament stem cells induced by the JNK-mitochondrial pathway," *Aging*, vol. 12, no. 13, pp. 12850–12868, 2020.

[48] B. Zhao, W. Zhang, Y. Xiong, Y. Zhang, L. Jia, and X. Xu, "Rutin protects human periodontal ligament stem cells from TNF-α induced damage to osteogenic differentiation through suppressing mTOR signaling pathway in inflammatory environment," *Archives of Oral Biology*, vol. 109, p. 104584, 2020.

[49] T. Dong, X. Sun, and H. Jin, "Role of YAP1 gene in proliferation, osteogenic differentiation, and apoptosis of human periodontal ligament stem cells induced by TNF-α," *Journal of Periodontology*, vol. 92, no. 8, pp. 1192–1200, 2021.

[50] J. Zhang, X. Dong, Q. Yan et al., "Galectin-1 inhibited LPS-induced autophagy and apoptosis of human periodontal ligament stem cells," *Inflammation*, vol. 44, no. 4, pp. 1302–1314, 2021.

[51] Y. M. Mei, L. Li, X. Q. Wang et al., "AGEs induces apoptosis and autophagy via reactive oxygen species in human periodontal ligament cells," *Journal of Cellular Biochemistry*, vol. 121, no. 8-9, pp. 3764–3779, 2020.

[52] Y. Yang, Y. Huang, and W. Li, "Autophagy and its significance in periodontal disease," *Journal of Periodontal Research*, vol. 56, no. 1, pp. 18–26, 2021.

[53] L. Chen, J. Bao, Y. Yang et al., "Autophagy was involved in tumor necrosis factor-α-inhibited osteogenic differentiation of murine calvarial osteoblasts through Wnt/β-catenin pathway," *Tissue & Cell*, vol. 67, p. 101401, 2020.

[54] H. Aslroosta, S. Yaghobee, S. Akbari, and N. Kanounisabet, "The effects of topical erythropoietin on non-surgical treatment of periodontitis: a preliminary study," *BMC Oral Health*, vol. 21, no. 1, p. 240, 2021.

[55] S. Yaghobee, N. Rouzmeh, M. Taheri et al., "Evaluation of topical erythropoietin application on the healing outcome of gingival graft recipient site; a randomized controlled clinical trial," *BMC Oral Health*, vol. 21, no. 1, p. 578, 2021.

[56] Y. Yu, L. Ma, H. Zhang et al., "EPO could be regulated by HIF-1 and promote osteogenesis and accelerate bone repair," *Artif Cells Nanomed Biotechnol*, vol. 48, no. 1, pp. 206–217, 2020.

[57] G. Hu, T. Wang, and C. Ma, "EPO activates PI3K-IKKα-CDK1 signaling pathway to promote the proliferation of Glial Cells under hypoxia environment," *Genetics and Molecular Biology*, vol. 45, no. 1, article e20210249, 2022.

[58] L. Zhong, H. Zhang, Z. F. Ding et al., "Erythropoietin-induced autophagy protects against spinal cord injury and improves neurological function via the extracellular-regulated protein kinase signaling pathway," *Molecular Neurobiology*, vol. 57, no. 10, pp. 3993–4006, 2020.

[59] M. A. Senousy, M. E. Hanafy, N. Shehata, and S. M. Rizk, "Erythropoietin and Bacillus Calmette-Guérin vaccination mitigate 3-nitropropionic acid-induced Huntington-like disease in rats by modulating the PI3K/Akt/mTOR/P70S6K pathway and enhancing the autophagy," *ACS Chemical Neuroscience*, vol. 13, no. 6, pp. 721–732, 2022.

[60] K. Anam and T. A. Davis, "Comparative analysis of gene transcripts for cell signaling receptors in bone marrow-derived hematopoietic stem/progenitor cell and mesenchymal stromal cell populations," *Stem Cell Research & Therapy*, vol. 4, no. 5, p. 112, 2013.

[61] Q. Gong, H. Jiang, X. Wei, J. Ling, and J. Wang, "Expression of erythropoietin and erythropoietin receptor in human dental pulp," *Journal of Endodontia*, vol. 36, no. 12, pp. 1972–1977, 2010.

[62] J. Kim, Y. Jung, H. Sun et al., "Erythropoietin mediated bone formation is regulated by mTOR signaling," *Journal of Cellular Biochemistry*, vol. 113, no. 1, pp. 220–228, 2012.

[63] G. D. Marconi, L. Fonticoli, S. Guarnieri et al., "Ascorbic acid: a new player of epigenetic regulation in LPS-*gingivalis* treated human periodontal ligament stem cells," *Oxidative Medicine and Cellular Longevity*, vol. 2021, Article ID 6679708, 13 pages, 2021.

[64] Z. Tóthová, M. Šemeláková, Z. Solárová, J. Tomc, N. Debeljak, and P. Solár, "The role of PI3K/AKT and MAPK signaling pathways in erythropoietin signalization," *International Journal of Molecular Sciences*, vol. 22, no. 14, p. 7682, 2021.

[65] G. S. Nam, K. S. Lee, and K. S. Nam, "Anti-platelet activity of mineral-balanced deep sea water is mediated via the regulation of Akt and ERK pathway crosstalk," *International Journal of Molecular Medicine*, vol. 45, no. 2, pp. 658–668, 2020.

[66] J. Z. Li, X. X. Zhou, W. Y. Wu et al., "Concanavalin a promotes angiogenesis and proliferation in endothelial cells through the Akt/ERK/cyclin D1 axis," *Pharmaceutical Biology*, vol. 60, no. 1, pp. 65–74, 2022.

[67] X. S. Zhang, X. Zhang, Q. Wu et al., "Astaxanthin alleviates early brain injury following subarachnoid hemorrhage in rats: possible involvement of Akt/bad signaling," *Marine Drugs*, vol. 12, no. 8, pp. 4291–4310, 2014.

[68] J. Pizzicannella, S. D. Pierdomenico, A. Piattelli et al., "3D human periodontal stem cells and endothelial cells promote bone development in bovine pericardium-based tissue biomaterial," *Materials*, vol. 12, no. 13, p. 2157, 2019.

[69] C. M. Simbulan-Rosenthal, Y. Haribabu, S. Vakili et al., "Employing CRISPR-Cas9 to generate CD133 synthetic lethal melanoma stem cells," *International Journal of Molecular Sciences*, vol. 23, no. 4, p. 2333, 2022.

[70] R. Zhang, L. Xie, F. Wu et al., "ALG-bFGF hydrogel inhibiting autophagy contributes to protection of blood-spinal cord barrier integrity *via* PI3K/Akt/FOXO1/KLF4 pathway after SCI," *Frontiers in Pharmacology*, vol. 13, 2022.

[71] F. Diomede, D. Tripodi, O. Trubiani, and J. Pizzicannella, "HEMA effects on autophagy mechanism in human dental pulp stem cells," *Materials*, vol. 12, no. 14, p. 2285, 2019.

[72] Q. Yang, S. Li, Z. Zhou et al., "Trimetazidine mitigates high glucose-induced retinal endothelial dysfunction by inhibiting PI3K/Akt/mTOR pathway-mediated autophagy," *Bioengineered*, vol. 13, no. 3, pp. 7515–7527, 2022.

[73] X. J. Mi, H. S. Choi, H. Perumalsamy et al., "Biosynthesis and cytotoxic effect of silymarin-functionalized selenium nanoparticles induced autophagy mediated cellular apoptosis via downregulation of PI3K/Akt/mTOR pathway in gastric cancer," *Phytomedicine*, vol. 99, p. 154014, 2022.

Hindawi

Research Article

Endometrial Regenerative Cell-Derived Exosomes Attenuate Experimental Colitis through Downregulation of Intestine Ferroptosis

Yanglin Zhu [1,2] **Hong Qin,**[1,2] **Chenglu Sun** [1,2] **Bo Shao,**[1,2] **Guangming Li,**[1,2] **Yafei Qin,**[1,2] **Dejun Kong** [3] **Shaohua Ren** [1,2] **Hongda Wang,**[1,2] **Zhaobo Wang,**[4] **Jingyi Zhang,**[1,2] **and Hao Wang** [1,2]

[1]*Department of General Surgery, Tianjin Medical University General Hospital, Tianjin 300052, China*
[2]*Tianjin General Surgery Institute, Tianjin Medical University General Hospital, Tianjin 300052, China*
[3]*Nankai University, School of Medicine, Tianjin 300071, China*
[4]*School of Basic Medical Sciences, Tianjin Medical University, Tianjin 300052, China*

Correspondence should be addressed to Hao Wang; hwangca272@hotmail.com

Background. Endometrial regenerative cells (ERCs) have been identified to ameliorate colitis in mice; however, whether exosomes derived from ERCs (ERC-exos) own similar effects on colitis remains unclear. Ferroptosis, an iron-dependent cell programmed death form, has been reported to promote inflammation in UC. Thus, in this study, whether ERC-exos can treat colitis and regulate intestine ferroptosis will be explored. *Methods.* In this study, iron, malondialdehyde (MDA) production, glutathione (GSH) synthesis, and acyl-CoA synthetase long-chain family member (ACSL) 4 and glutathione peroxidase 4 (GPX4) expressions were measured in colon samples from healthy people and UC patients to explore the effects of ferroptosis. *In vitro*, ERC-exos were cocultured with ferroptosis inducer erastin-treated NCM460 human intestinal epithelial cell line, and ferroptotic parameters were measured. *In vivo*, colitis was induced by 3% dextran sulfate sodium (DSS) in BALB/c mice, and animals were randomly assigned to normal, untreated, and ERC-exos-treated groups. The Disease Activity Index (DAI) score, histological features, tissue iron, MDA, GSH, ACSL4, and GPX4 were measured to verify the role of ERC-exos in attenuating UC. *Results.* Compared with healthy people, UC samples exhibited higher levels of iron, MDA, and ACSL4, while less levels of GSH and GPX4. *In vitro*, the CCK-8 assay showed that ERC-exos rescued erastin-induced cell death, and ERC-exos treatment significantly increased the levels of GSH and expression of GPX4, while markedly decreasing the levels of iron, MDA, and expression of ACSL4. *In vivo*, ERC-exos treatment effectively reduced DAI score, ameliorated colon pathological damage, and improved disease symptoms. Moreover, ERC-exos treatment further enhanced the levels of GSH and the expression of GPX4 but reduced the levels of iron, MDA, and expression of ACSL4 in the colon of colitis mice. *Conclusions.* Ferroptosis was involved in the pathogenesis of UC, and ERC-exos attenuated DSS-induced colitis through downregulating intestine ferroptosis. This study may provide a novel insight into treating UC in the future.

1. Introduction

Ulcerative colitis (UC) is a chronic nonspecific inflammatory disease, which mainly affects the colon and rectum [1]. Occurring with rapid socioeconomic development, the prevalence of UC is increasing which continues to challenge the healthcare system all over the world [2]. At present, the pathogenesis of UC may involve imbalanced immune homeostasis, disordered intestinal flora, and inappropriate survival environment [3–5]. Although drugs for UC are various including hormones [6], biological agents [7], and immunosuppressants [8], during the application of these drugs, side effects such as renal impairment [9], severe infection [10], and venous thromboembolism [11] cannot be

ignored. Hence, exploring novel available strategies for treating UC is urgently required.

It has been proved that based on mesenchymal stem cell- (MSC-) mediated therapy on UC is effective and promising. Endometrial regenerative cells (ERCs) are a novel source of adult stem cells [12], which are collected from menstrual blood and own similar properties to MSCs [13]. Surprisingly, compared with MSCs, ERCs have unique advantages of abundant sources, noninvasive acquisition [14, 15], and so on. In addition, studies showed that ERCs amplifies twice as fast as bone marrow-MSCs (BM-MSCs) [14] and the yield is 2-4-fold higher than that of BM-MSCs [16]. ERCs have been identified to exert therapeutic effects on experimental colitis [17], acute immune-mediated hepatitis [18], myocardial injury [19], and cardiac allograft rejection [20], etc. by our team and others. As known, the way MSCs exert therapeutic effects is mainly through paracrine mechanism, including cytokines, free mitochondria, and exosomes [21]. Exosomes are biological nanovesicles with a diameter of 30-150 nm containing diverse biomolecules, such as lipids, proteins, and nucleic acids [22], which can function as a unidirectional carrier to transfer signals among cells [23]. Superior to MSCs, MSC-derived exosomes (MSC-exos) have higher chemical stability, longer distance intercellular communication, and stronger autonomous targeting capabilities [24]. Previous studies have demonstrated that MSC-exos can attenuate experimental colitis *via* regulating immune cells [25]. Our previous study has revealed ERC-derived condition medium can treat colitis, which may involve ERC-exos' participation [26].

Ferroptosis is an iron-dependent programmed cell death, which was coined fairly in 2012 [27]. In 2018, the Nomenclature Committee on Cell Death defined ferroptosis as a form of regulated cell death initiated by intracellular oxidative perturbations, which is under constitutive control by GPX4 and can be inhibited by iron chelators and lipophilic antioxidants [28]. Studies have verified that ferroptosis was involved in the pathogenesis of various disease, including cancers [29], ischemia/reperfusion injuries (IRI) [30], cardiovascular disease [31], stroke [32], and inflammatory diseases [33]. Xu et al. have revealed that ferroptosis participated in UC [34] and Dong et al. and Wang et al. have demonstrated that inhibiting ferroptosis could alleviate UC [35, 36]. Therefore, focusing on regulating ferroptosis may provide a novel insight into the treatment of UC.

Given the promising therapeutic effects of ERC-exos and inspired by previous studies of ferroptosis, the current study was designed to investigate whether ERC-exos can attenuate experimental colitis through regulating intestine ferroptosis.

2. Materials and Methods

2.1. Clinical Samples. Colon samples of UC patients ($n = 10$) and healthy control ($n = 10$) were collected from the Department of General Surgery, Tianjin Medical University General Hospital. Control colon samples were taken from normal intestinal tissue removed during surgery in patients with colorectal cancer. All samples used in this study were approved by the Ethical Committee of Tianjin Medical Uni-

versity General Hospital (Ethic No. IRB2022-WZ-031). Samples soaked in formalin were used to make paraffin sections for detecting the expression of GPX4, and frozen tissues were used to assess the levels of iron, GSH, and MDA. In addition, proteins extracted from samples were used to measure the expressions of GPX4 and ACSL4.

2.2. Animals. Male BALB/c mice, aging 6-8 weeks and weighing 22-25 g, were purchased from China Food and Drug Inspection Institute (Beijing, China). All animals were housed in a conventional experimental environment with enough food and water following the guidelines of the China Association for the Production of Animals and the protocol was approved by the Animal Ethical and Welfare Committee of Tianjin Medical University General Hospital (ethic no. IRB2022-DW-07).

2.3. Experimental Groups. Colitis was induced by feeding with water containing 3% DSS (Yeasen, Shanghai, China). All animals were randomly assigned to three groups ($n = 6$ per group): the normal control group, untreated group, and ERC-exos-treated group. The mice in normal control group were fed with free water for 10 days while the other two groups were fed with water containing 3% DSS for 7 days and then administered water for 3 days as described previously [17]. ERC-exos-treated mice were injected with ERC-exos (100 μg total protein in 200 μL volume) *via* the tail veins on days 2, 5, and 8 of DSS administration. On day 10, mice were killed for the collection of colon samples which were excised from the ileocecal junction to the anus.

2.4. Preparations of ERCs and ERC-exos. The menstrual blood of healthy woman volunteers were collected on the second day of the menstrual cycle (20-30 years old). ERC harvest and culture were followed as described in the previous study [37]. In brief, the mononuclear cells were isolated via a standard Ficoll method and then were cultured in Dulbecco's modified Eagle's medium supplemented with 10% fetal bovine serum and 1% penicillin/streptomycin. At passage 3, the morphology and the surface markers CD105, CD44, CD45, CD73, CD79a, and HLA-DR of ERCs were examined by microscopy and flow cytometry.

When ERCs reached 60-70% confluency, aspirating the medium and rinsing ERCs three times with sterile PBS were done. After adding a fresh serum-free culture medium (Umibio, Shanghai, China) to incubate cells for 48 h, the conditioned medium were collected and then acquired exosomes by ultracentrifugation. Briefly, the conditioned medium were centrifuged for 10 min at 300 g, 20 min at 2000 g, and 30 min at 10,000 g to remove cell debris. Then, the supernatant was transferred to fresh tubes and centrifuged for 70 min at 110,000 g twice to harvest pure ERC-exos.

2.5. Exosome Identification. The exosome from ERC supernatants were verified by nanoparticle, morphology, and surface markers. The size distribution of the precipitated particles was measured by nanoparticle tracking analysis. The size of the particles was analyzed using Zetasizer Software. Results are presented in a particle size distribution
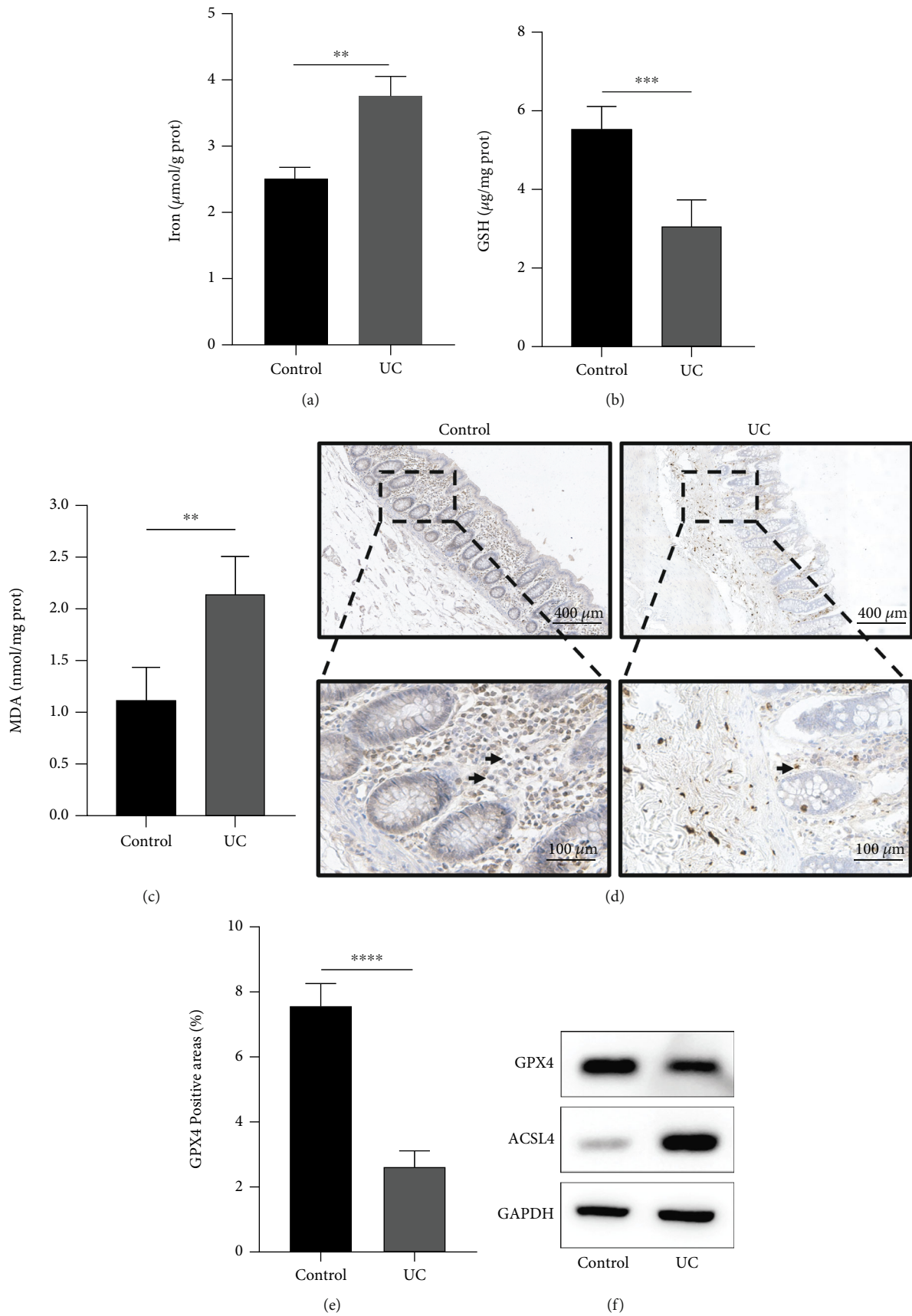
(a)

(b)

(c)

(d)
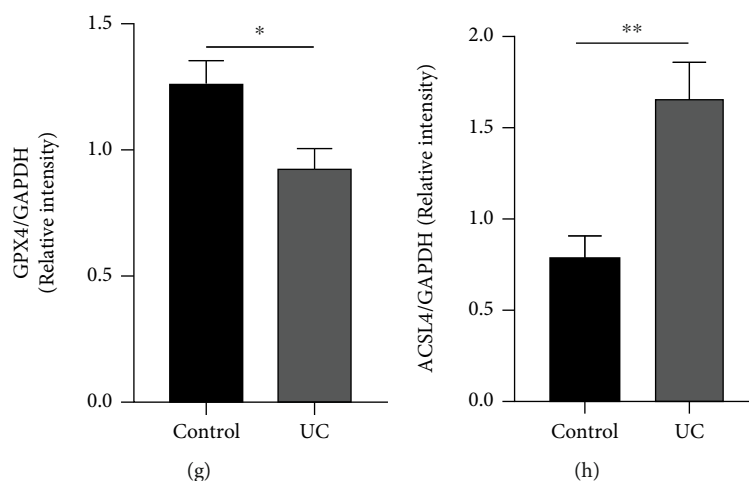

(e)

(f)

Figure 1: Continued.

(g)

(h)

Figure 1: Ferroptosis was involved in the pathogenesis of UC. (a) Iron, (b) GSH levels, and (c) MDA levels were detected in colon samples from the healthy people and UC patients, respectively. (d) Representative images of immunohistochemical analysis measuring GPX4 levels in human colon samples, and (e) quantitative data of cell counts are shown. (f–h) Western blotting analysis of GPX4 and ACSL4. GAPDH was used as the loading control. The p value was determined by unpaired t-test. $^*p < 0.05$, $^{**}p < 0.01$, $^{***}p < 0.001$, and $^{****}p < 0.0001$.

graph. The morphology of exosomes was observed by transmission electron microscopy. Briefly, isolated exosomes were resuspended in PBS, and then, exosomes were suspended in 2% glutaraldehyde and loaded onto copper grids, after which they were negatively stained with 3% (w/v) aqueous phosphotungstic acid for 1 min. Finally, exosomes were observed by transmission electron microscope. ERC-exos protein concentration was determined using a BCA kit (Solarbio, Beijing, China). CD9, CD63, and Alix were used as markers of exosomes in immunoblot assays.

2.6. Cell Lines and Treatment.
The human normal colonic epithelial cell line NCM460 were used *in vitro*. In the erastin-treated group, ferroptosis inducer $20 \mu M$ erastin (MCE, HY-15763) was added to the culture medium after culturing NCM460 for 24 h. And in the ERC-exos-treated group, $20 \mu M$ erastin and $15 \mu g$ ERC-exos were added to NCM460 at the same time and cocultured for 24 h.

2.7. Cell Viability.
Cell Counting Kit-8 reagent (CCK-8, Solarbio, Beijing, China) was used to determine the cell viability according to the manufacturer's instructions. Briefly, NCM460 were seeded onto a 96-well plate at a density of 5×10^3 cells/well and treated with vehicle control (DMSO solvent), erastin, and erastin plus ERC-exos. $10 \mu L$ CCK-8 was added per well and cultured for 1 h. The absorbance at 450 nm was measured in a multimode microplate reader for cell viability assessment.

2.8. Iron, GSH, and MDA Analyses.
Protein samples were collected from colon tissues or NCM460 cells to measure the levels of iron, GSH, and MDA. An iron assay kit (TC1015, Leagene, Beijing, China), a GSH assay kit (BC1175, Solarbio, Beijing, China), and an MDA assay kit (A020-2, Jian Cheng, Nanjing, China) were used to determine the levels of iron, GSH, and MDA.

2.9. Histology and Immunohistochemistry.
All colon samples were fixed in 10% formalin, embedded in paraffin, and then sectioned into $5 \mu m$ slices. Hematoxylin and eosin staining was used for examination of histopathological changes. To evaluate ferroptosis in colitis, immunohistochemistry was performed for GPX4. After deparaffinization and rehydration, sections were incubated with 3% H_2O_2 to eliminate endogenous peroxides and then heated in the microwave for antigen retrieval. 10% goat serum was used to block nonspecific antigens and sections were finally incubated with rabbit anti-mouse GPX4 antibody (Abcam, ab125066) overnight at 4°C. The next day, horseradish peroxidase-conjugated avidin and brown-colored 3,3′-diaminobenzidine were used to develop the signal and the sections were stained with hematoxylin and then were recorded for analysis.

2.10. Western Blot Analysis.
Proteins from cell samples and colon tissues were extracted using RIPA lysis mixed with PMSF (Solarbio, Beijing, China) and quantified using a BCA assay kit (Solarbio, Beijing, China). Then, the total protein was separated by sodium dodecyl sulfate polyacrylamide gel electrophoresis and transferred to PVDF membranes. After blocking with 5% skim milk, PVDF membranes were incubated with anti-GPX4 antibody (dilution at 1 : 1000, Abcam, Cambridge, UK), anti-ACSL4 antibody (dilution at 1 : 1000, Abclonal, Wuhan, China), and anti-GAPDH antibody (dilution at 1 : 1000, Sevicebio, Wuhan, China) at 4°C overnight. On the other day, the membranes were incubated with anti-mouse secondary antibody (dilution at 1 : 1000, Servicebio, Wuhan, China) or anti-rabbit secondary antibody (dilution at 1 : 1000, CST, Boston, USA) for 50 min at room temperature. Finally, signals were detected with electrochemiluminescence solution (ECL, Millipore, Massachusetts, USA) using a ChemiScope exposure machine (Clinx Science Instruments Co., Ltd., Shanghai, China) and images were analyzed by ImageJ software.
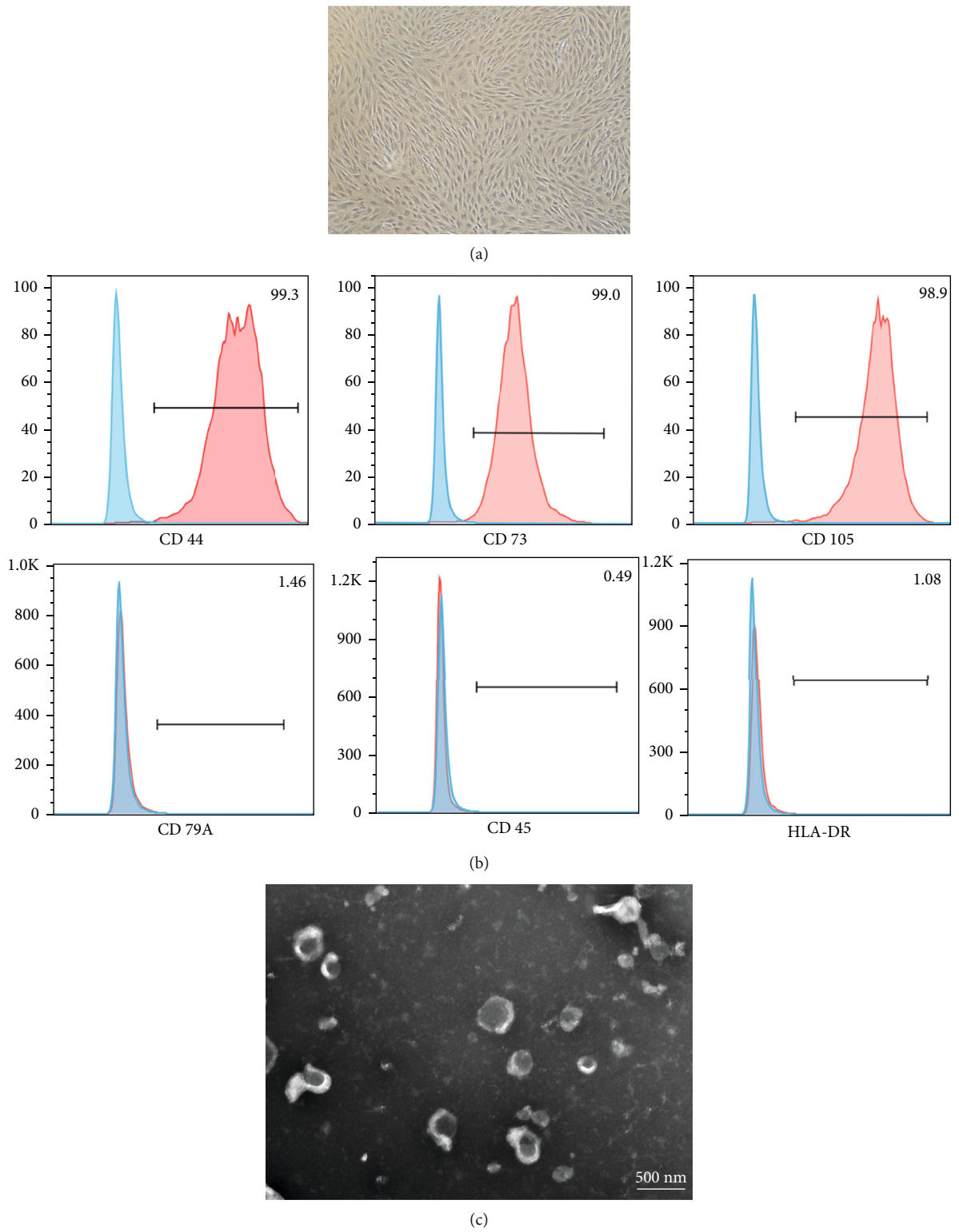
(a)
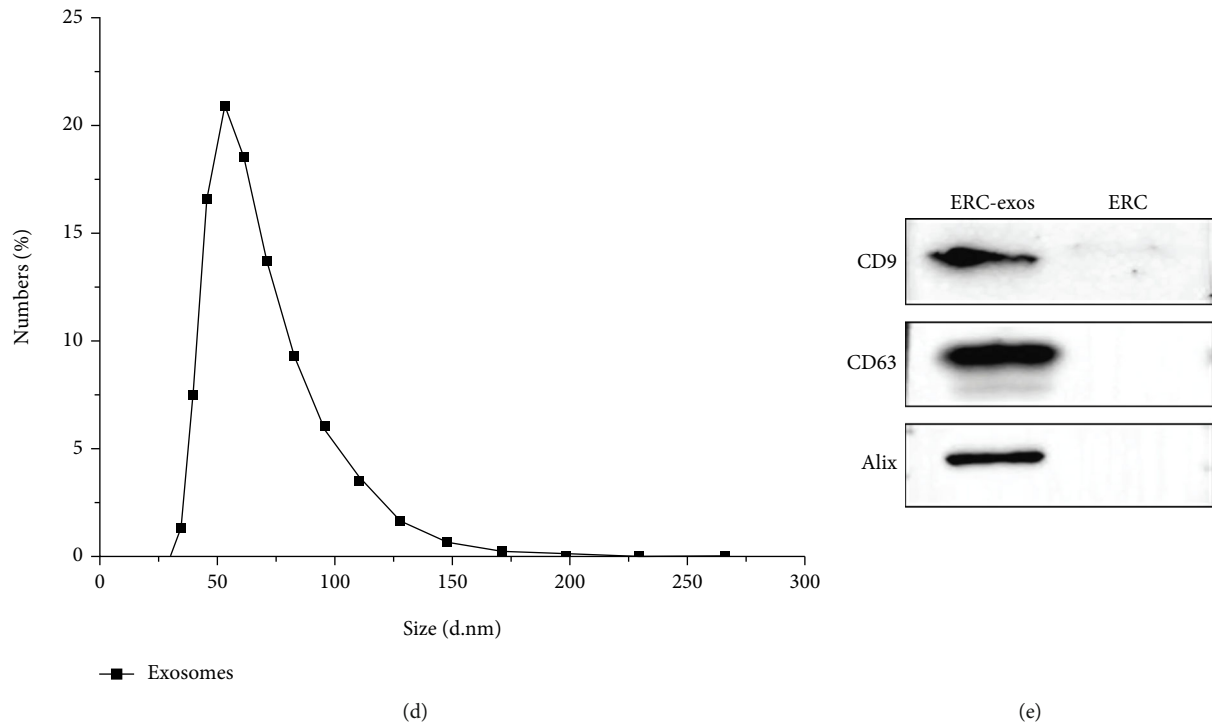

(b)

(c)

Figure 2: Continued.

(d)

(e)

FIGURE 2: Identification of ERCs and ERC-exos. (a) Morphology of ERCs at P3. (b) Flow cytometry analysis of surface markers of ERCs. (c) Representative image of exosomes. (d) Particle size distribution of exosomes. (e) Immunoblot of exosome markers (CD9, CD63, and Alix).

2.11. Statistical Analysis. All data were expressed as mean ± standard deviation (SD). The differences among groups were analyzed by using unpaired t-test (groups = 2) or ANOVA analysis (groups ≥ 3). p value < 0.05 was considered statistically significant.

3. Results

3.1. Ferroptosis Was Involved in the Pathogenesis of UC Patients. To verify the presence of ferroptosis in the colon of UC patients, samples were collected from ten UC patients and ten healthy people, respectively, for the measurement. The results showed that the iron was significantly increased in UC compared with the healthy control (Figure 1(a), the control group vs. UC group, $p < 0.01$). The lipid peroxidation product MDA was increased (Figure 1(c), the control group vs. UC group, $p \leq 0.01$), while GSH synthesis was markedly inhibited in colitis samples (Figure 1(b), the control group vs. UC group, $p \leq 0.001$). In addition, the levels of GPX4 which directly reduces peroxidized phospholipids as an antioxidant enzyme in colonic specimens were measured by immunohistochemistry and western blot, and results showed a significantly lower expression of GPX4 in UC patients (IHC: Figures 1(d) and 1(e), the control group vs. UC group, $p < 0.0001$; western blot: Figures 1(f) and 1(g), the control group vs. UC group, $p < 0.05$). ACSL4 expression was also increased in the UC patients (Figures 1(f) and 1(h), the control group $vs.$ UC group, $p < 0.01$). All these results indicated that ferroptosis was involved in the UC.

3.2. Characterization of ERCs and ERC-exos. As shown in Figure 2(a), ERCs exhibited spindle-shaped and fibroblast-like morphology. Flow cytometry analysis showed that ERCs positively expressed CD44, CD105, and CD73, and negatively expressed CD45, CD79a, and HLA-DR (Figure 2(b)). Exosomes from the conditioned medium derived from ERCs exhibited typical lipid bilayer membrane encapsulation (Figure 2(c)) and the particle size distribution ranged from 30 to 150 nm (Figure 2(d)). In addition, the western blot showed that CD63, CD9, and Alix were expressed on exosomes (Figure 2(e)). Taken together, the properties of ERC-exos in this study met the typical criteria for exosomes.

3.3. ERC-exos Downregulated NCM460 Ferroptosis In Vitro. In order to investigate whether ERC-exos could regulate ferroptosis in the UC, $in vitro$ NCM460 cell line was used to mimic the intestine. Erastin was added to culture systems prior to ERC-exos. Cell viability assay revealed that erastin reduced cell viability (Figure 3(a), the erastin group vs. control group, $p < 0.0001$), while ERC-exos obviously increased cell viability (Figure 3(a), the ERC-exos group vs. erastin group, $p < 0.0001$). In addition, cells induced by erastin had higher levels of iron and MDA (Figures 3(b) and 3(d), the iron, erastin group vs. control group, $p < 0.0001$; the MDA, erastin group vs. control group, $p < 0.0001$), as well as inhibiting GSH synthesis (Figure 3(c), the erastin group vs. control group, $p < 0.01$), while the treatment of ERC-exos reversed ferroptosis in cells (Figures 3(b)–3(d),the iron : ERC-exos group vs. erastin group, $p < 0.0001$; the GSH : ERC-exos group vs. erastin group, $p < 0.05$; the MDA : ERC-exos group vs. erastin group, $p < 0.001$). Moreover,
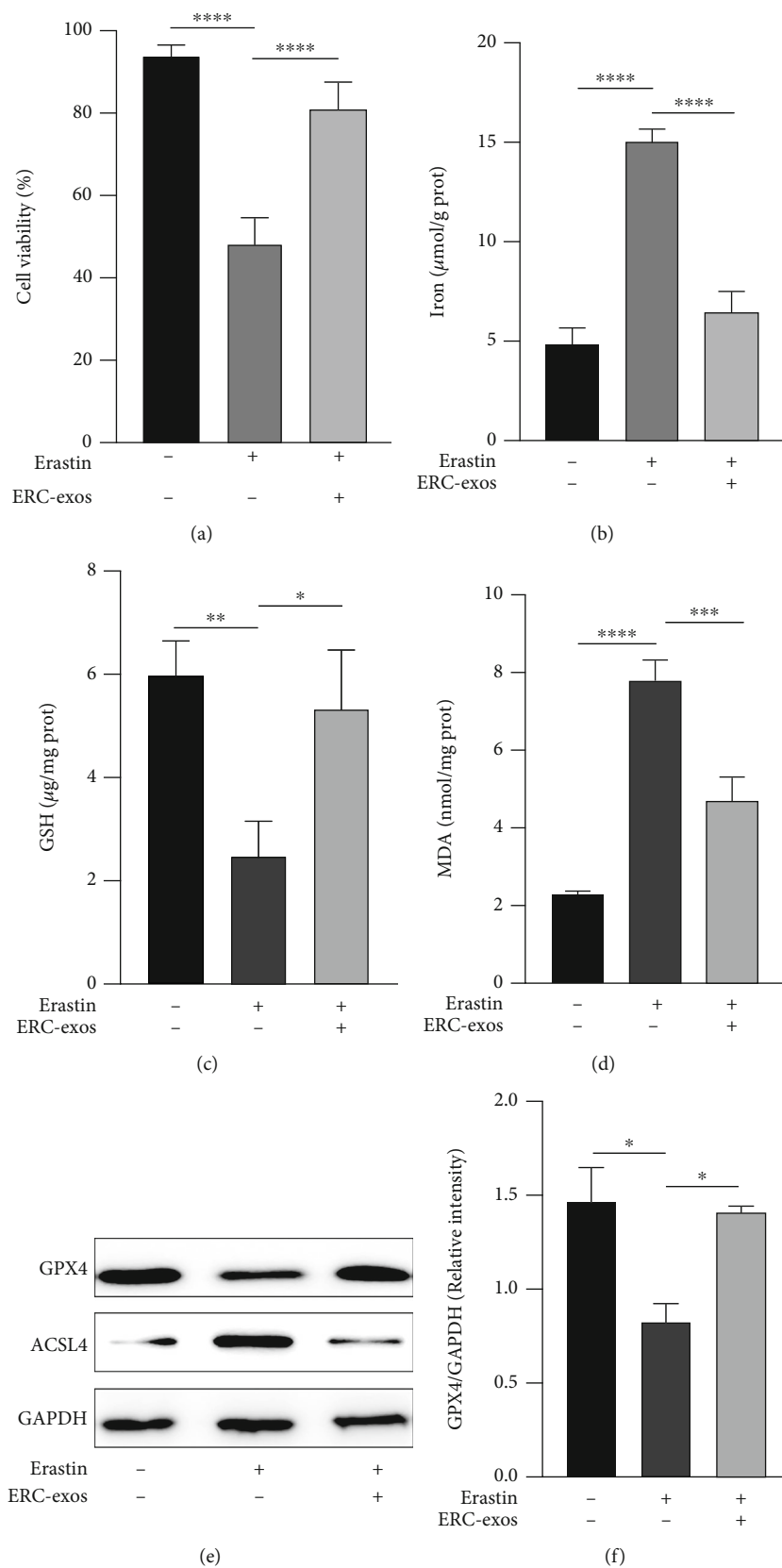
(a)

(b)

(c)
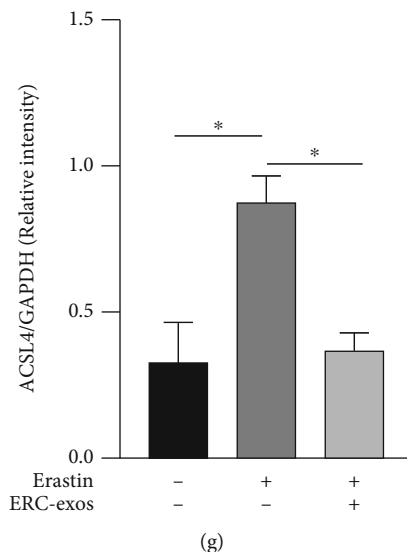
(d)

(e)

(f)

FIGURE 3: Continued.

(g)

Figure 3: ERC-exos downregulated ferroptosis induced by erastin in NCM460. (a) Relative vitality in erastin-induced NCM460 was measured by CCK-8 kit. The levels of (b) iron, (c) GSH, and (d) MDA in NCM460 treated with erastin or ERC-exos. (e–g) The GPX4 and ACSL4 protein expressions in NCM460 measured by western blot. The p value was calculated by one-way ANOVA. $^*p < 0.05$, $^{**}p < 0.01$, $^{***}p < 0.001$, and $^{****}p < 0.0001$.

treatment of ERC-exos led to decreased level of ACSL4 but an increased level of GPX4 (Figures 3(e)–3(g), the GPX4 : ERC-exos group vs. erastin group, $p < 0.05$; ACSL4 : ERC-exos group vs. erastin group, $p < 0.05$). Collectively, these data suggested that ERC-exos downregulated ferroptosis in erastin-treated NCM460 *in vitro*.

3.4. ERC-exos Alleviated DSS-Induced Colitis Symptoms in Mice. To further confirm the effects of ERC-exos in colitis, after 3% DSS induction for seven days, the clinical symptoms were evaluated. Mice in the untreated group exhibited colitis with severe bloody stool and weight loss, while ERC-exos-treated mice showed improved symptoms (Figures 4(a) and 4(b)). The Disease Activity Index (DAI) score further reflected the therapeutic effects of ERC-exos (Figure 4(c)). In addition, the shortened colon caused by continuous DSS administration was improved by ERC-exos treatment (Figures 4(d) and 4(e), the untreated group vs. control group, $p < 0.001$; the ERC-exos group *vs.* untreated group, $p < 0.01$). Colon slices from the untreated group showed massive inflammatory cell infiltration, goblet cell depletion, and damaged crypt structure and epithelium cells, whereas ERC-exos ameliorated the pathological changes (Figures 4(f) and 4(g), the untreated group vs. control group, $p < 0.0001$; the ERC-exos group vs. untreated group, $p < 0.0001$). Through the above results, it has been confirmed that ERC-exos relieved experimental colitis.

3.5. ERC-exos Could Regulate Ferroptosis in DSS-Induced Colitis. To thoroughly verify whether ERC-exos could alleviate colitis through regulation of ferroptosis, iron, GSH, MDA, GPX4, and ACSL4 were measured. Evidence demonstrated that ERC-exos could decrease levels of iron and MDA but increase GSH synthesis (Figures 5(a)–5(c), the iron : ERC-exos group vs. untreated group, $P < 0.01$; the

GSH : ERC-exos group vs. untreated group, $p < 0.01$; the MDA : ERC-exos group vs. untreated group, $p < 0.0001$). Immunohistochemistry analysis and western blot further confirmed that ERC-exos effectively promote the GPX4 expression (Figures 5(d)–5(g), the IHC : ERC-exos group vs. untreated group, $p < 0.001$; the WB : ERC-exos group vs. untreated group, $p < 0.05$). In addition, ERC-exos treatment decreased ACSL4 expression in colons (Figures 5(f) and 5(h), the ERC-exos group vs. untreated group, $p < 0.05$). Taken together, these results indicated that ERC-exos could alleviate colitis through downregulating ferroptosis.

4. Discussion

UC is a complex disease in which the interaction of genetic, environmental, psychiatric factors, and microbial factors drive chronic intestinal inflammation. In this study, indicators related to ferroptosis were detected in colons from healthy people and UC patients and found that there was a significant increase in ferroptotic parameters in UC patients. *In vitro*, erastin was used to induced ferroptosis in NCM460, whereas ERC-exos treatment markedly downregulated ferroptosis in this cell line. *In vivo*, DSS-induced mice were treated with ERC-exos *via* tail vein injection. Symptoms such as colon length, bloody stool, and weight loss were significantly attenuated in the ERC-exos-treated group. Intestinal pathological results showed that colons in the ERC-exos-treated group presented an improved structure of epithelium and crypts, with abundant goblet cells. All results suggested that ERC-exos attenuated experimental colitis in mice. In addition, by measuring ferroptosis-related indicators we confirmed that ERC-exos downregulate intestine ferroptosis.

Iron is an essential element of the body and a component of many enzymes and immune system compounds; however, it can produce harmful oxygen radicals through the
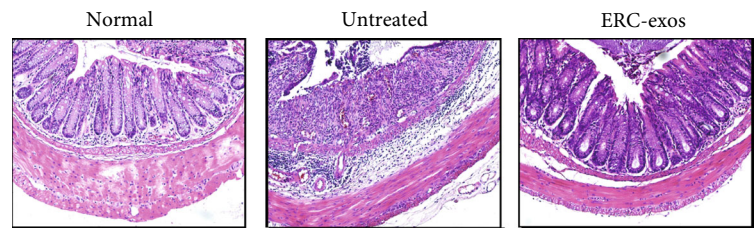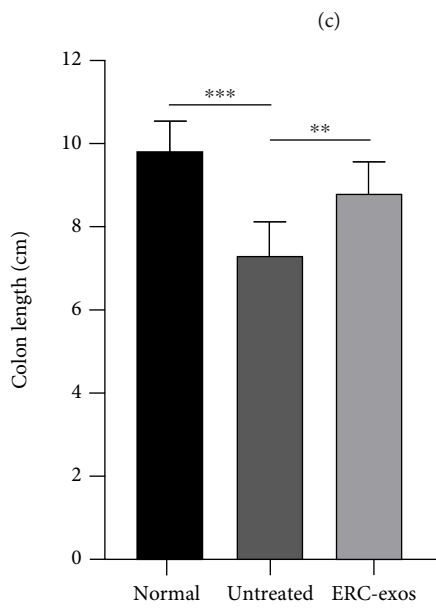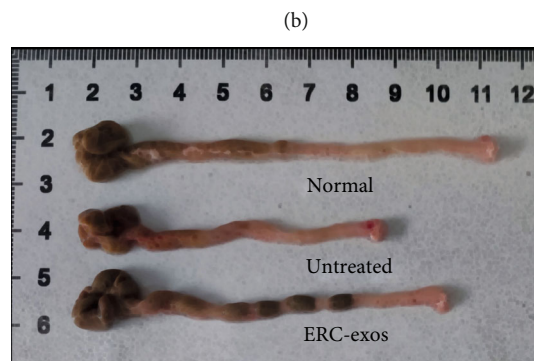
(a)

(b)

(c)
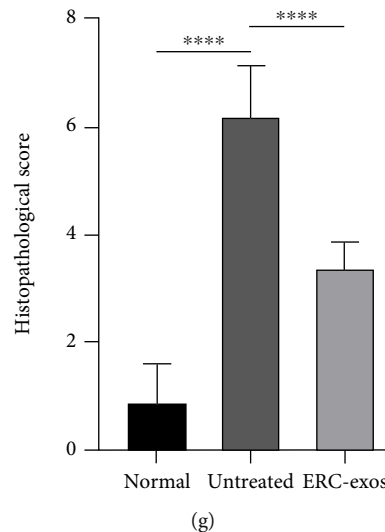
(d)

(e)

(f)

Figure 4: Continued.

(g)
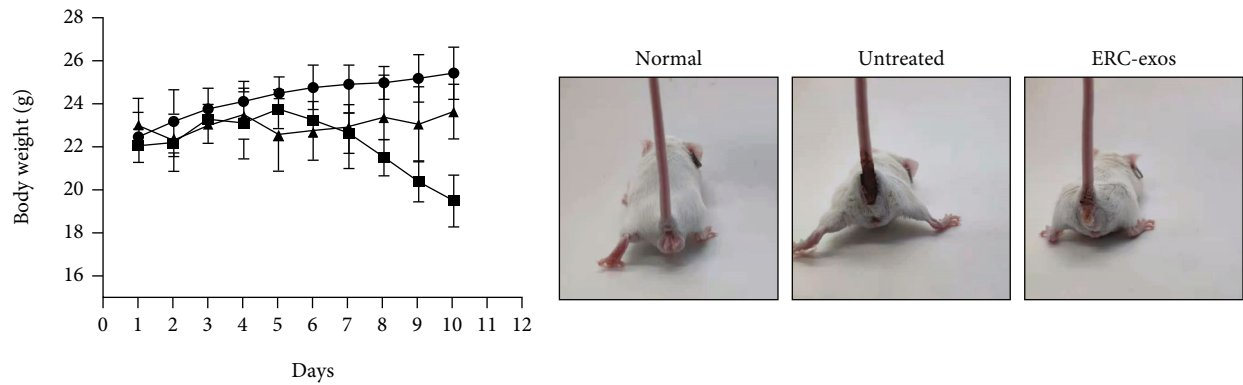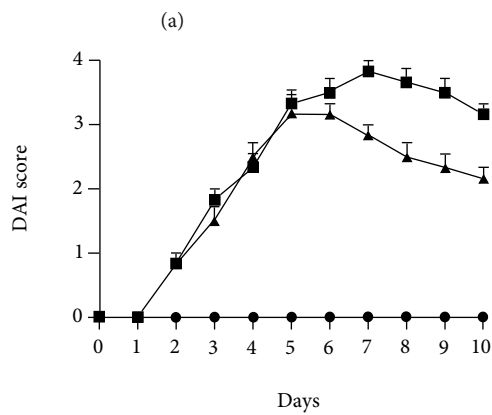
FIGURE 4: ERC-exos attenuated experimental colitis in mice. (a) Body weight changes of mice from each group. (b) Representative pictures showing bloody stool indifferent groups. (c) DAI score was used to assess the colitis activity. (d, e) The length of colons was measured and analyzed. (f) Representative images of colon tissues in each group (H&E staining). (g) Histopathology scores were evaluated and calculated. The p value was determined by one-way ANOVA. $^{*}p < 0.05$, $^{**}p < 0.01$, $^{***}p < 0.001$, and $^{****}p < 0.0001$.

Fenton reaction leading to increased tissue damage and inflammation [38]. One of the pathogenesis of colitis is iron-derived oxidant activity [39]. It has been reported that high dietary iron intake increased the risk of UC [40], iron overload led to dysregulated reactive oxygen species (ROS) generation, and interference with intestinal bacteria thus aggravated UC, while iron chelation therapy is effective in the treatment of colitis [41]. Since lipid peroxidation product such as MDA causes changes in the fluidity and permeability of cell membranes, ultimately leading to changes in cell structure and function [32], lipid peroxidation is considered another main molecular mechanism of toxicity process leading to cell death. Lipid peroxidation depends on the formation of free polyunsaturated fatty acids and the synthesis of free fatty acids requires the involvement of ACSL4 [42]. GPX4 and its cofactor GSH are the main pathways for the elimination of lipid peroxidation products which can reduce lipid hydroperoxides to nontoxic lipid alcohols, thereby limiting the propagation of lipid peroxidation within the membrane [43]. It has been found that lipid peroxidation occurs and ferroptosis is induced, when excess iron in the intestine produces ROS via the Fenton reaction which destroyed the intestinal epithelial cells and damaged the intestinal mucosal barrier resulting in UC [44, 45]. Therefore, in this study, the intestinal iron was used to respond to the level of iron metabolism, and MDA, GSH, GPX4, and ACSL4 were used to reflect the level of lipid peroxidation. In addition, significant downregulation and upregulation of ferroptosis-associated genes highlight the close relationship between ferroptosis and UC. Yang et al. found that the upregulation of NRF2 could inhibit ferroptosis and attenuate colitis-related mucosal damage and colonic inflammation [46]. In addition, Wang et al. clarified the vital role of GPX4 in negatively regulating ferroptosis in UC [36]. In this experiment, increased iron, MDA, and ACSL4 and decreased GPX4 and GSH in patients with UC also demonstrated the presence of ferroptosis, which is consistent with the conclusion of other studies [34, 35].

Researches on ERCs are now well mature, and it is well known that ERCs highly express MSC surface markers such as CD44, CD73, and CD105 and lowly express CD45, CD79a, and HLA-DR. In addition, studies demonstrated that ERCs can exert therapeutic effects through regulating immune response [47], promoting damage recovery [48], and differentiating into targeted cells [19, 49], and so on. Moreover, ERCs' clinical curative effects have been confirmed, Ichim et al. revealed that ERCs could improve heart function of patient suffering from dilated cardiomyopathy [50], and Xu et al. showed that ERC infusion could improve severe and critical COVID-19 [51]. ERC-exos are virtually unaffected by biological barriers [52] and safer to the host compared with ERCs [53], which could serve as a convincing novel type of cell-free treatment. Current researches indicated that MSC-exos act by following mechanisms. The wide repertoire of miRNAs in MSC-exos could provide a miRNA-based mechanism for the therapeutic effects of MSC-exos. Wang et al. revealed that exosomal miR-223 contributed to MSC-mediated cardioprotection in sepsis [54], and Xin et al. demonstrated that miR-17-92 in MSC-exos enhanced neurological [55]. Notably, lncRNA and circRNA also play an important role in the function of MSC-exos [56, 57]. In addition, proteins in MSC-exos have the potential to modulate the biological processes of diseases including myocardial ischemia/reperfusion injury [58], cystinosis [59], renal injury [60], and hyperoxic lung injury [61]. Apart from RNA species and protein, the effect of exosomal DNA cannot be ignored [62]. Kitai et al. confirmed that exosomes acted by packaging and transferring their mitochondrial DNA to targeted cells [63]. Ferroptosis is involved in the progression of numerous diseases, and it has been proved that MSC-exos could attenuate diseases through inhibiting ferroptosis. Studies have found that MSC-exos could deliver its miRNA and proteins that act on genes participating in iron metabolism and lipid peroxide process to regulate
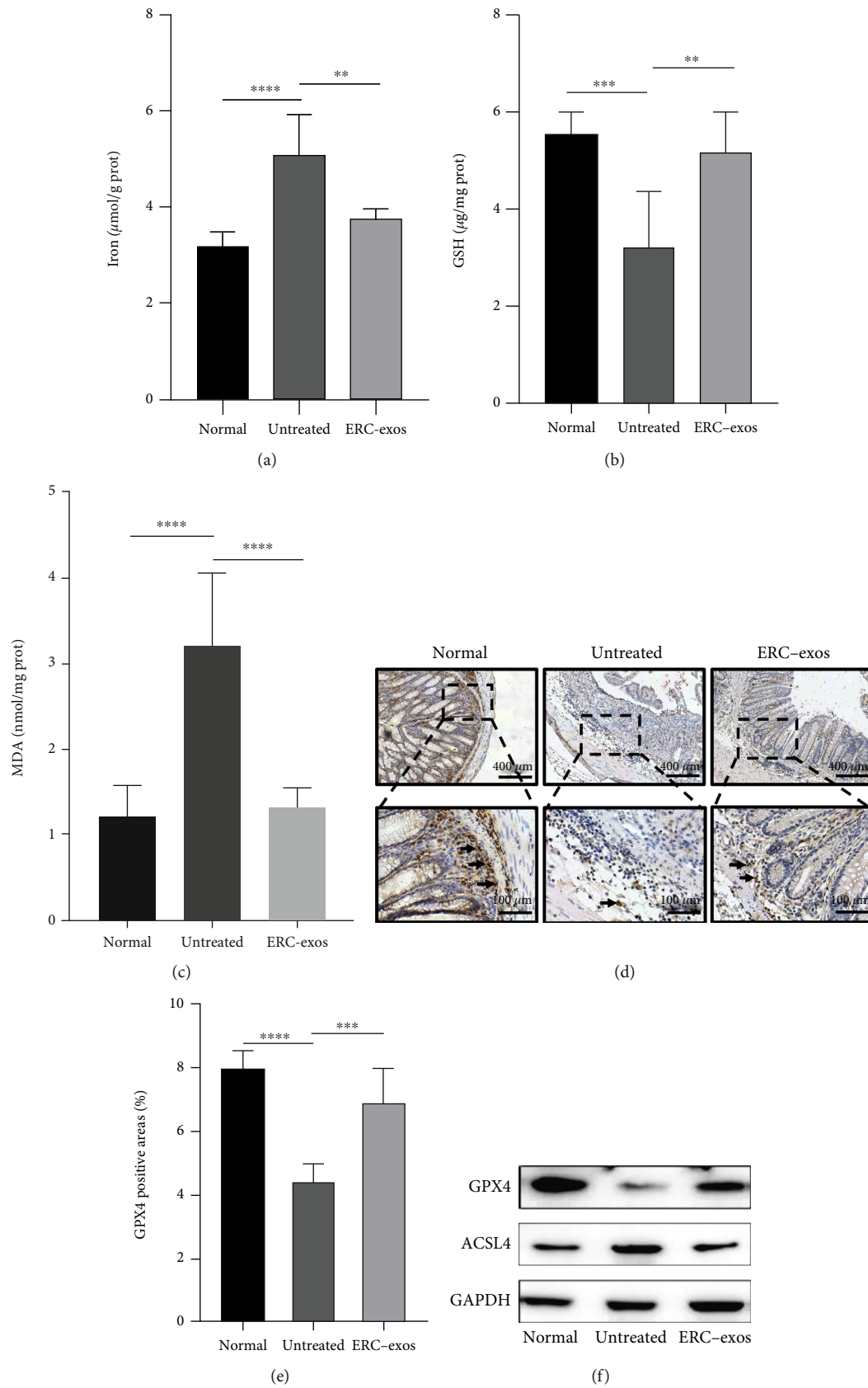
(a)

(b)

(c)

(d)
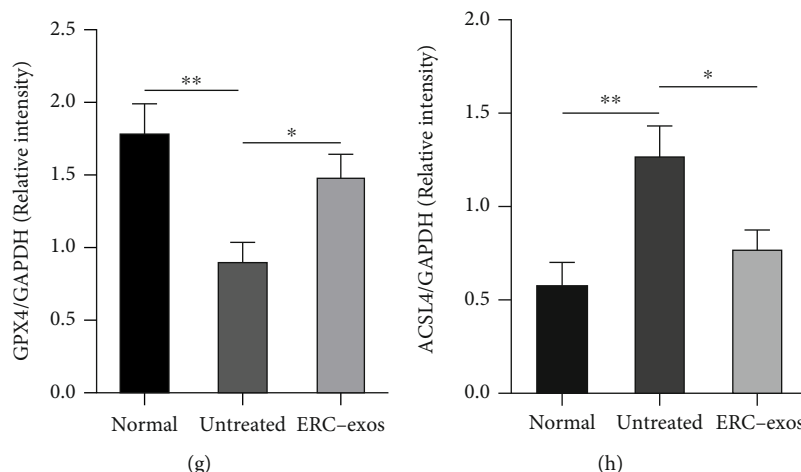

(e)

(f)

FIGURE 5: Continued.

(g)

(h)

Figure 5: ERC-exos downregulated ferroptosis in mouse colitis model. The levels of (a) iron, (b) GSH, and (c) MDA of colon samples from different groups were measured. (d, e) Representative images of immunohistochemical analysis measuring GPX4 levels in colons from mice. (f–h) Western blot analysis measuring GPX4 and ACSL4 expression levels in mouse colon samples from different groups. GAPDH was used as the loading control. The p value was counted by one-way ANOVA. $^{*}p < 0.05$, $^{**}p < 0.01$, $^{***}p < 0.001$, and $^{****}p < 0.0001$.

ferroptosis. Song et al. revealed that divalent metal transporter 1 is a target gene of miR-23a-3p carried by MSC-exos, and miR-23a-3p could suppress divalent metal transporter 1 expression to inhibit ferroptosis [64]. BECN1 is a biofactor of ferroptosis delivered by MSC-exo. Tan et al. proved that MSC-exos may promote xCT/GPX4-mediated activated hepatic stellate cells ferroptosis through the delivery of BECN1 [65]. Lin et al. also concluded that MSC-exos might alleviate ferroptosis via the CD44 and OTUB1-mediated stabilization of SLC7A11 [66]. Therefore, we speculated that ERC-exos regulates ferroptosis primarily through delivering its rich proteins and miRNA. In the coming period, we will further explore the role of proteins of ERC-exos in ferroptosis in UC. Studies have showed that ERC-exos can improve liver function [67], protect myocardial tissue [68], inhibit tumor cell growth [69], and improve the regenerative capacity of β islets [70]. To validate the role of ERC-exos on UC, the DSS-induced experimental colitis model was used, and pathology, DAI, and weight changes of mice were assessed. For further revealing the effect of ERC-exos on ferroptosis, in an vitro experiment, the erastin-induced group were compared with the ERC-exos-treated group. The results showed that the use of ERC-exos significantly downregulated ferroptosis in NCM460. Furthermore, the effects of ERC-exos on ferroptosis were confirmed in an *in vivo* model. Consistent with the advanced results, GPX4 expression and GSH synthesis were increased in the ERC-exos-treated group, while iron, MDA, and the expression of ACSL4 were decreased in the DSS-induced group, which suggested that ERC-exos can downregulated ferroptosis in colitis.

Programmed cell death such as apoptosis and pyroptosis are essential parts in the process of the disease. It has been proved that the inhibition of intestinal epithelial cell apoptosis and macrophage pyroptosis facilitate remission of colitis [71, 72]. Ferroptosis is a new form of programmed cell death characterized by increased iron and lipid peroxidation. In this study, we have confirmed that ferroptosis was involved in the pathogenesis of UC and ERC-exos did improve

ferroptosis-related factors and thus alleviate the symptoms of UC. However, our study has some experimental limitations, the underlined specific mechanisms towards regulation of ferroptosis were not explored, and the comparison with ferroptosis inhibitors was not performed. Therefore, it is necessary to explore the detailed mechanisms of ERC-exos-mediated therapeutic effects in the future.

5. Conclusion

In conclusion, the results in this study have demonstrated that ferroptosis is involved in the pathogenesis of UC and ERC-exos can attenuate colitis in mice through downregulation of ferroptosis, which can provide a novel insight for the UC treatment.

Abbreviations

ACSL4:   Acyl-CoA synthetase long-chain family member 4
BM-MSCs: Bone marrow cell derived exosomes
CCK-8:   The Cell Counting Kit-8
DAI: The disease activity
DSS: Dextran sulfate sodium
ERCs: Endometrial regenerative cells
ERC-exos: Endometrial regenerative cell-derived exosomes
GPX4:   Glutathione peroxidase 4
GSH: Glutathione
IBD: Inflammatory bowel disease
MDA: Malondialdehyde
MSCs: Mesenchymal stem cells
MSC-exos: Mesenchymal stem cell-derived exosomes
ROS: Reactive oxygen species
UC: Ulcerative colitis.

Data Availability

All data included in this manuscript can be available.

Conflicts of Interest

The authors declare that they have no conflict of interests.

Authors' Contributions

Yanglin Zhu, Hong Qin, and Chenglu Sun designed and carried out the research, analyzed the data, and drafted the manuscript. Bo Shao, Guangming Li, Yafei Qin, Dejun Kong, Shaohua Ren, Hongda Wang, Zhaobo Wang, and Jingyi Zhang performed the research. Hao Wang conceived and designed the research, provided administrative and financial support, and helped in revising the manuscript. Yanglin Zhu, Hong Qin, and Chenglu Sun are co-first authors on this paper.

Acknowledgments

References

[1] H. S. de Souza and C. Fiocchi, "Immunopathogenesis of IBD: current state of the art," *Nature Reviews. Gastroenterology & Hepatology*, vol. 13, no. 1, pp. 13–27, 2016.

[2] S. C. Ng, H. Y. Shi, N. Hamidi et al., "Worldwide incidence and prevalence of inflammatory bowel disease in the 21st century: a systematic review of population-based studies," *Lancet*, vol. 390, no. 10114, pp. 2769–2778, 2017.

[3] A. Ponder and M. D. Long, "A clinical review of recent findings in the epidemiology of inflammatory bowel disease," *Clinical Epidemiology*, vol. 5, pp. 237–247, 2013.

[4] G. Ray and M. S. Longworth, "Epigenetics, DNA organization, and inflammatory bowel disease," *Inflammatory Bowel Diseases*, vol. 25, no. 2, pp. 235–247, 2019.

[5] D. Piovani, S. Danese, L. Peyrin-Biroulet, G. K. Nikolopoulos, T. Lytras, and S. Bonovas, "Environmental risk factors for inflammatory bowel diseases: an umbrella review of meta-analyses," *Gastroenterology*, vol. 157, no. 3, pp. 647–659.e4, 2019.

[6] H. P. Sham, M. Bazett, M. Bosiljcic et al., "Immune stimulation using a gut microbe-based immunotherapy reduces disease pathology and improves barrier function in ulcerative colitis," *Frontiers in Immunology*, vol. 9, p. 2211, 2018.

[7] J. P. Segal, J. F. LeBlanc, and A. L. Hart, "Ulcerative colitis: an update," *Clinical Medicine*, vol. 21, no. 2, pp. 135–139, 2021.

[8] B. G. Feagan, P. Rutgeerts, B. E. Sands et al., "Vedolizumab as induction and maintenance therapy for ulcerative colitis," *The New England Journal of Medicine*, vol. 369, no. 8, pp. 699–710, 2013.

[9] C. A. Lamb, N. A. Kennedy, T. Raine et al., "British Society of Gastroenterology consensus guidelines on the management of inflammatory bowel disease in adults," *Gut*, vol. 68, Suppl 3, pp. s1–s106, 2019.

[10] A. C. Ford and L. Peyrin-Biroulet, "Opportunistic infections with anti-tumor necrosis factor-α therapy in inflammatory bowel disease: meta-analysis of randomized controlled trials," *The American Journal of Gastroenterology*, vol. 108, no. 8, pp. 1268–1276, 2013.

[11] W. J. Sandborn, J. Panés, B. E. Sands et al., "Venous thromboembolic events in the tofacitinib ulcerative colitis clinical development programme," *Alimentary Pharmacology & Therapeutics*, vol. 50, no. 10, pp. 1068–1076, 2019.

[12] M. P. Murphy, H. Wang, A. N. Patel et al., "Allogeneic endometrial regenerative cells: an "off the shelf solution" for critical limb ischemia?," *Journal of Translational Medicine*, vol. 6, no. 1, p. 45, 2008.

[13] S. Darzi, J. A. Werkmeister, J. A. Deane, and C. E. Gargett, "Identification and characterization of human endometrial mesenchymal stem/stromal cells and their potential for cellular therapy," *Stem Cells Translational Medicine*, vol. 5, no. 9, pp. 1127–1132, 2016.

[14] X. Meng, T. E. Ichim, J. Zhong et al., "Endometrial regenerative cells: a novel stem cell population," *Journal of Translational Medicine*, vol. 5, no. 1, p. 57, 2007.

[15] X. Zhu, B. Péault, G. Yan, H. Sun, Y. Hu, and L. Ding, "Stem cells and endometrial regeneration: from basic research to clinical trial," *Current Stem Cell Research & Therapy*, vol. 14, no. 4, pp. 293–304, 2019.

[16] F. Alcayaga-Miranda, J. Cuenca, P. Luz-Crawford et al., "Characterization of menstrual stem cells: angiogenic effect, migration and hematopoietic stem cell support in comparison with bone marrow mesenchymal stem cells," *Stem Cell Research & Therapy*, vol. 6, no. 1, p. 32, 2015.

[17] Y. Lv, X. Xu, B. Zhang et al., "Endometrial regenerative cells as a novel cell therapy attenuate experimental colitis in mice," *Journal of Translational Medicine*, vol. 12, no. 1, p. 344, 2014.

[18] H. Wang, Y. Zhao, B. Ren et al., "Endometrial regenerative cells with galectin-9 high-expression attenuate experimental autoimmune hepatitis," *Stem Cell Research & Therapy*, vol. 12, no. 1, p. 541, 2021.

[19] N. Hida, N. Nishiyama, S. Miyoshi et al., "Novel cardiac precursor-like cells from human menstrual blood-derived mesenchymal cells," *Stem Cells*, vol. 26, no. 7, pp. 1695–1704, 2008.

[20] Y. Zhao, X. Li, D. Yu et al., "Galectin-9 is required for endometrial regenerative cells to induce long-term cardiac allograft survival in mice," *Stem Cell Research & Therapy*, vol. 11, no. 1, p. 471, 2020.

[21] L. M. A. Murray and A. D. Krasnodembskaya, "Concise review: intercellular communication via organelle transfer in the biology and therapeutic applications of stem cells," *Stem Cells*, vol. 37, no. 1, pp. 14–25, 2019.

[22] S. Mathivanan, H. Ji, and R. J. Simpson, "Exosomes: extracellular organelles important in intercellular communication," *Journal of Proteomics*, vol. 73, no. 10, pp. 1907–1920, 2010.

[23] Y. Tang, Y. Zhou, and H. J. Li, "Advances in mesenchymal stem cell exosomes: a review," *Stem Cell Research & Therapy*, vol. 12, no. 1, p. 71, 2021.

[24] W. Wei, Q. Ao, X. Wang et al., "Mesenchymal stem cell-derived exosomes: a promising biological tool in nanomedicine," *Frontiers in Pharmacology*, vol. 11, article 590470, 2020.

[25] H. Liu, Z. Liang, F. Wang et al., "Exosomes from mesenchymal stromal cells reduce murine colonic inflammation via a macrophage-dependent mechanism," *JCI Insight*, vol. 4, no. 24, 2019.

[26] C. Sun, J. Hao, H. Qin et al., "Endometrial regenerative cell-derived conditioned medium alleviates experimental colitis," *Stem Cells International*, vol. 2022, Article ID 7842296, 13 pages, 2022.

[27] S. J. Dixon, K. M. Lemberg, M. R. Lamprecht et al., "Ferroptosis: an iron-dependent form of nonapoptotic cell death," *Cell*, vol. 149, no. 5, pp. 1060–1072, 2012.

[28] L. Galluzzi, I. Vitale, S. A. Aaronson et al., "Molecular mechanisms of cell death: recommendations of the Nomenclature Committee on Cell Death 2018," *Cell Death and Differentiation*, vol. 25, no. 3, pp. 486–541, 2018.

[29] V. S. Viswanathan, M. J. Ryan, H. D. Dhruv et al., "Dependency of a therapy-resistant state of cancer cells on a lipid peroxidase pathway," *Nature*, vol. 547, no. 7664, pp. 453–457, 2017.

[30] J. P. Friedmann Angeli, M. Schneider, B. Proneth et al., "Inactivation of the ferroptosis regulator Gpx4 triggers acute renal failure in mice," *Nature Cell Biology*, vol. 16, no. 12, pp. 1180–1191, 2014.

[31] Y. Leng, X. Luo, J. Yu, H. Jia, and B. Yu, "Ferroptosis: a potential target in cardiovascular disease," *Frontiers in Cell and Development Biology*, vol. 9, article 813668, 2021.

[32] B. R. Stockwell, J. P. Friedmann Angeli, H. Bayir et al., "Ferroptosis: a regulated cell death nexus linking metabolism, redox biology, and disease," *Cell*, vol. 171, no. 2, pp. 273–285, 2017.

[33] Y. Sun, P. Chen, B. Zhai et al., "The emerging role of ferroptosis in inflammation," *Biomedicine & Pharmacotherapy*, vol. 127, article 110108, 2020.

[34] M. Xu, J. Tao, Y. Yang et al., "Ferroptosis involves in intestinal epithelial cell death in ulcerative colitis," *Cell Death & Disease*, vol. 11, no. 2, p. 86, 2020.

[35] S. Dong, Y. Lu, G. Peng et al., "Furin inhibits epithelial cell injury and alleviates experimental colitis by activating the Nrf2-Gpx4 signaling pathway," *Digestive and Liver Disease*, vol. 53, no. 10, pp. 1276–1285, 2021.

[36] S. Wang, W. Liu, J. Wang, and X. Bai, "Curculigoside inhibits ferroptosis in ulcerative colitis through the induction of GPX4," *Life Sciences*, vol. 259, article 118356, 2020.

[37] K. Ye, X. Lan, G. Wang et al., "B7-H1 expression is required for human endometrial regenerative cells in the prevention of transplant vasculopathy in mice," *Stem Cells International*, vol. 2018, Article ID 2405698, 12 pages, 2018.

[38] C. Loguercio, G. D'Argenio, M. D. Cave et al., "Direct evidence of oxidative damage in acute and chronic phases of experimental colitis in rats," *Digestive Diseases and Sciences*, vol. 41, no. 6, pp. 1204–1211, 1996.

[39] A. D. Millar, D. S. Rampton, and D. R. Blake, "Effects of iron and iron chelation In Vitro on mucosal oxidant activity in ulcerative colitis," *Alimentary Pharmacology & Therapeutics*, vol. 14, no. 9, pp. 1163–1168, 2000.

[40] Y. Kobayashi, S. Ohfuji, K. Kondo et al., "Association between dietary iron and zinc intake and development of ulcerative colitis: A case–control study in Japan," *Journal of Gastroenterology and Hepatology*, vol. 34, no. 10, pp. 1703–1710, 2019.

[41] M. Minaiyan, E. Mostaghel, and P. Mahzouni, "Preventive therapy of experimental colitis with selected iron chelators and anti-oxidants," *International Journal of Preventive Medicine*, vol. 3, Suppl 1, pp. S162–S169, 2012.

[42] S. Doll, B. Proneth, Y. Y. Tyurina et al., "ACSL4 dictates ferroptosis sensitivity by shaping cellular lipid composition," *Nature Chemical Biology*, vol. 13, no. 1, pp. 91–98, 2017.

[43] H. Imai, M. Matsuoka, T. Kumagai, T. Sakamoto, and T. Koumura, "Lipid peroxidation-dependent cell death regulated by GPx4 and ferroptosis," *Current Topics in Microbiology and Immunology*, vol. 403, pp. 143–170, 2017.

[44] T. Werner, S. J. Wagner, I. Martinez et al., "Depletion of luminal iron alters the gut microbiota and prevents Crohn's disease-like ileitis," *Gut*, vol. 60, no. 3, pp. 325–333, 2011.

[45] J. C. Carrier, E. Aghdassi, K. Jeejeebhoy, and J. P. Allard, "Exacerbation of dextran sulfate sodium-induced colitis by dietary iron supplementation: role of NF-kappaB," *International Journal of Colorectal Disease*, vol. 21, no. 4, pp. 381–387, 2006.

[46] Y. Yang, X. Cai, J. Yang et al., "Chemoprevention of dietary digitoflavone on colitis-associated colon tumorigenesis through inducing Nrf2 signaling pathway and inhibition of inflammation," *Molecular Cancer*, vol. 13, no. 1, p. 48, 2014.

[47] T. L. Spitzer, A. Rojas, Z. Zelenko et al., "Perivascular human endometrial mesenchymal stem cells express pathways relevant to self-renewal, lineage specification, and functional phenotype1," *Biology of Reproduction*, vol. 86, no. 2, p. 58, 2012.

[48] B. Xiang, L. Chen, X. Wang, Y. Zhao, Y. Wang, and C. Xiang, "Transplantation of menstrual blood-derived mesenchymal stem cells promotes the repair of LPS-induced acute lung injury," *International Journal of Molecular Sciences*, vol. 18, no. 4, p. 689, 2017.

[49] E. F. Wolff, X. B. Gao, K. V. Yao et al., "Endometrial stem cell transplantation restores dopamine production in a Parkinson's disease model," *Journal of Cellular and Molecular Medicine*, vol. 15, no. 4, pp. 747–755, 2011.

[50] T. E. Ichim, F. Solano, F. Lara et al., "Combination stem cell therapy for heart failure," *International Archives of Medicine*, vol. 3, no. 1, p. 5, 2010.

[51] X. Xu, W. Jiang, L. Chen et al., "Evaluation of the safety and efficacy of using human menstrual blood-derived mesenchymal stromal cells in treating severe and critically ill COVID-19 patients: an exploratory clinical trial," *Clinical and Translational Medicine*, vol. 11, no. 2, article e297, 2021.

[52] L. R. Galieva, V. James, Y. O. Mukhamedshina, and A. A. Rizvanov, "Therapeutic potential of extracellular vesicles for the treatment of nerve disorders," *Frontiers in Neuroscience*, vol. 13, p. 163, 2019.

[53] K. S. Park, E. Bandeira, G. V. Shelke, C. Lässer, and J. Lötvall, "Enhancement of therapeutic potential of mesenchymal stem cell-derived extracellular vesicles," *Stem Cell Research & Therapy*, vol. 10, no. 1, p. 288, 2019.

[54] X. Wang, H. Gu, D. Qin et al., "Exosomal miR-223 contributes to mesenchymal stem cell-elicited cardioprotection in polymicrobial sepsis," *Scientific Reports*, vol. 5, no. 1, article 13721, 2015.

[55] H. Xin, M. Katakowski, F. Wang et al., "MicroRNA-17–92 cluster in exosomes enhance neuroplasticity and functional recovery after stroke in rats," *Stroke*, vol. 48, no. 3, pp. 747–753, 2017.

[56] G. Mao, Y. Xu, D. Long et al., "Exosome-transported circRNA_0001236 enhances chondrogenesis and suppress cartilage degradation via the miR-3677-3p/Sox9 axis," *Stem Cell Research & Therapy*, vol. 12, no. 1, p. 389, 2021.

[57] Y. Liu, L. Lin, R. Zou, C. Wen, Z. Wang, and F. Lin, "MSC-derived exosomes promote proliferation and inhibit apoptosis of chondrocytes via lncRNA-KLF3-AS1/miR-206/GIT1 axis in osteoarthritis," *Cell Cycle*, vol. 17, no. 21-22, pp. 2411–2422, 2018.

[58] F. Arslan, R. C. Lai, M. B. Smeets et al., "Mesenchymal stem cell-derived exosomes increase ATP levels, decrease oxidative stress and activate PI3K/Akt pathway to enhance myocardial viability and prevent adverse remodeling after myocardial ischemia/reperfusion injury," *Stem Cell Research*, vol. 10, no. 3, pp. 301–312, 2013.

[59] D. M. Iglesias, R. el-Kares, A. Taranta et al., "Stem cell microvesicles transfer cystinosin to human cystinotic cells and reduce cystine accumulation in vitro," *PLoS One*, vol. 7, no. 8, article e42840, 2012.

[60] B. Shen, J. Liu, F. Zhang et al., "CCR2 positive exosome released by mesenchymal stem cells suppresses macrophage functions and alleviates ischemia/reperfusion-induced renal injury," *Stem Cells International*, vol. 2016, Article ID 1240301, 9 pages, 2016.

[61] S. Y. Ahn, W. S. Park, Y. E. Kim et al., "Vascular endothelial growth factor mediates the therapeutic efficacy of mesenchymal stem cell-derived extracellular vesicles against neonatal hyperoxic lung injury," *Experimental & Molecular Medicine*, vol. 50, no. 4, pp. 1–12, 2018.

[62] S. Fischer, K. Cornils, T. Speiseder et al., "Indication of horizontal DNA gene transfer by extracellular vesicles," *PLoS One*, vol. 11, no. 9, article e0163665, 2016.

[63] Y. Kitai, T. Kawasaki, T. Sueyoshi et al., "DNA-containing exosomes derived from cancer cells treated with topotecan activate a STING-dependent pathway and reinforce antitumor immunity," *Journal of Immunology*, vol. 198, no. 4, pp. 1649–1659, 2017.

[64] Y. Song, B. Wang, X. Zhu et al., "Human umbilical cord blood-derived MSCs exosome attenuate myocardial injury by inhibiting ferroptosis in acute myocardial infarction mice," *Cell Biology and Toxicology*, vol. 37, no. 1, pp. 51–64, 2021.

[65] Y. Tan, Y. Huang, R. Mei et al., "HucMSC-derived exosomes delivered BECN1 induces ferroptosis of hepatic stellate cells via regulating the xCT/GPX4 axis," *Cell Death & Disease*, vol. 13, no. 4, p. 319, 2022.

[66] F. Lin, W. Chen, J. Zhou et al., "Mesenchymal stem cells protect against ferroptosis via exosome-mediated stabilization of SLC7A11 in acute liver injury," *Cell Death & Disease*, vol. 13, no. 3, p. 271, 2022.

[67] L. Chen, B. Xiang, X. Wang, and C. Xiang, "Exosomes derived from human menstrual blood-derived stem cells alleviate fulminant hepatic failure," *Stem Cell Research & Therapy*, vol. 8, no. 1, p. 9, 2017.

[68] K. Wang, Z. Jiang, K. A. Webster et al., "Enhanced cardioprotection by human endometrium mesenchymal stem cells driven by exosomal microRNA-21," *Stem Cells Translational Medicine*, vol. 6, no. 1, pp. 209–222, 2017.

[69] L. Rosenberger, M. Ezquer, F. Lillo-Vera et al., "Stem cell exosomes inhibit angiogenesis and tumor growth of oral squamous cell carcinoma," *Scientific Reports*, vol. 9, no. 1, p. 663, 2019.

[70] E. Mahdipour, Z. Salmasi, and N. Sabeti, "Potential of stem cell-derived exosomes to regenerate β islets through Pdx-1 dependent mechanism in a rat model of type 1 diabetes," *Journal of Cellular Physiology*, vol. 234, no. 11, pp. 20310–20321, 2019.

[71] X. Cai, Z. Y. Zhang, J. T. Yuan et al., "hucMSC-derived exosomes attenuate colitis by regulating macrophage pyroptosis via the miR-378a-5p/NLRP3 axis," *Stem Cell Research & Therapy*, vol. 12, no. 1, p. 416, 2021.

[72] C. L. Chang, C. H. Chen, J. Y. Chiang et al., "Synergistic effect of combined melatonin and adipose-derived mesenchymal stem cell (ADMSC)-derived exosomes on amelioration of dextran sulfate sodium (DSS)-induced acute colitis," *American Journal of Translational Research*, vol. 11, no. 5, pp. 2706–2724, 2019.